

CLINICAL DIAGNOSIS, ULTRASTRUCTURAL STUDY AND ANTIGENIC CHARACTERIZATION  
OF PLATYNOSOMUM FASTOSUM IN CATS



A Dissertation Submitted in Partial Fulfillment of the Requirements  
for the Degree of Doctor of Philosophy in Veterinary Science and technology

Common Course

FACULTY OF VETERINARY SCIENCE

Chulalongkorn University

Academic Year 2020

Copyright of Chulalongkorn University

การวินิจฉัยทางคลินิก การศึกษาโครงสร้างเชิงลึก  
และการจำแนกคุณสมบัติการเป็นแอนติเจนของพยาธิ แพลททีโนโซมม ฟาสโตซุม ในแมว



วิทยานิพนธ์นี้เป็นส่วนหนึ่งของการศึกษาตามหลักสูตรปริญญาวิทยาศาสตรดุษฎีบัณฑิต  
สาขาวิชาวิทยาศาสตร์ทางการสัตวแพทย์และเทคโนโลยี ไม่สังกัดภาควิชา/เทียบเท่า  
คณะสัตวแพทยศาสตร์ จุฬาลงกรณ์มหาวิทยาลัย  
ปีการศึกษา 2563  
ลิขสิทธิ์ของจุฬาลงกรณ์มหาวิทยาลัย



บาบิ คโย โซ : การวินิจฉัยทางคลินิก การศึกษาโครงสร้างเชิงลึก  
และการจำแนกคุณสมบัติการเป็นแอนติเจนของพยาธิ แพลททีโนโซมูม ฟาสโตซุม  
ในแมว. ( CLINICAL DIAGNOSIS, ULTRASTRUCTURAL STUDY AND ANTIGENIC  
CHARACTERIZATION OF PLATYNOSOMUM FASTOSUM IN CATS)

อ.ที่ปรึกษาหลัก : วรพร สุขุมวาสิ, อ.ที่ปรึกษาร่วม : ภูมิ อติศักดิ์วัฒนา

แ พ ล ท ที โ น โซ มู ม ฟ า ส โ ต ซู ม  
เป็นพยาธิใบไม้ในตับที่เป็นสาเหตุของโรคตับและท่อน้ำดีในแมว  
เพื่อประเมินตัวชี้วัดในการสนับสนุนดัชนีการสงสัยสำหรับการตรวจวินิจฉัยโรคในช่วงแรกของการติด  
เชื้อแบบไม่แสดงอาการ ค่าทางชีวเคมีที่ประกอบด้วยค่าเอนไซม์ของตับ ตับอ่อน  
และสารบ่งชี้มะเร็งจึงได้ถูกศึกษาในแมวที่ติดเชื้อ *P. fastosum* ในธรรมชาติจำนวน 14 ตัว  
พบว่าค่า ALT และ GGT มีค่าสูงกว่าปกติคิดเป็นร้อยละ 57.8 (8/14) ของแมวที่ติดเชื้อ  
สำหรับการใช้เทคนิคภาพวินิจฉัย พบร้อยละ 85.7 (12/14) ของแมวที่ติดเชื้อมีตะกอนในถุงน้ำดี  
เนื่องจากจำนวนของไข่พยาธิที่พบในน้ำดีมีจำนวนมากกว่าที่พบในมูลแมวอย่างมีนัยสำคัญ  
( $p=$  0 . 0 0 1 )  
เทคนิคการเจาะถุงน้ำดีผ่านผิวหนังโดยใช้เครื่องคลื่นเสียงความถี่สูงจึงเป็นวิธีที่มีความเป็นไปได้เพื่อ  
นำมาช่วยวินิจฉัยยืนยัน เนื่องจากปัจจุบันยังไม่มียาที่มีประสิทธิภาพ  
ข้อมูลพื้นฐานในด้านโครงสร้างเชิงลึกของตัวเต็มวัยและไข่ของ *P. fastosum*  
จึงมีความจำเป็นสำหรับการทดสอบทางยาในอนาคต  
การใช้กล้องจุลทรรศน์อิเล็กตรอนแบบส่องกราดจึงถูกใช้เพื่อศึกษาพื้นผิวของผนังตัวพยาธิ  
โดยพบว่าถูกปกคลุมด้วยเนื้อเยื่อเยื่อมีลักษณะคล้ายนิ้วมีอัดกันแน่นและมีปุ่มบนผิว  
เมื่อใช้กล้องจุลทรรศน์อิเล็กตรอนแบบส่องผ่าน พบว่ามีเซลล์ผนังของพยาธิอย่างน้อย 1  
ชนิดที่สามารถผลิตเม็ดเล็ก ๆ ออกมา 2 ชนิดอยู่ภายในชั้นผนังของพยาธิ  
สำหรับการพัฒนาวิธีวินิจฉัยทางซีรัมวิทยา องค์ประกอบของแอนติเจนของ *P. fastosum*  
จึงได้ถูกจำแนกชนิด โดยพบโปรตีนของพยาธิจำนวน 3 ชนิด (ขนาด 70 kDa 53 kDa และ 13  
kDa) ที่ทำให้ภูมิคุ้มกันตอบสนองได้ และได้รับการระบุชนิดและลำดับของโปรตีน

สาขาวิชา วิทยาศาสตร์ทางการสัตวแพทย์ ลายมือชื่อนิสิต .....

และเทคโนโลยี

ปีการศึกษา 2563

ลายมือชื่อ อ.ที่ปรึกษาหลัก .....

ลายมือชื่อ อ.ที่ปรึกษาร่วม .....



## ACKNOWLEDGEMENTS

This research was partially funded to WS by the Chulalongkorn University Research Unit for Feline Infectious Disease and Health for Excellence, the Chulalongkorn University Research Unit for Microbial Food Safety and Antimicrobial Resistance, the Chulalongkorn University Research Unit (GRU 6203331007-1). This research was also funded to WS and Babi Kyi Soe by the 90th Anniversary of Chulalongkorn University Fund (Ratchadaphiseksomphot Endowment Fund). In addition, I would like to thank to CU-ASEAN and Non-ASEAN Scholarship for financial support of Doctoral Scholarship. It is genuine pleasure to express my gratitude to my main advisor Asst. Prof. Dr. Woraporn Sukhumavasi for her guidance and kindness support to get through everything in my Ph.D. study. I am also thankful to my co-advisor Assoc. Prof. Dr. Poom Adisakwattana for his valuable inputs, technical guidance and suggestions throughout this project. I have benefited greatly from his wealth of knowledge. I would like to thank to my thesis committee members; Prof. Dr. Somporn Techangamsuwan, Assoc. Prof. Dr. Nopadon Pirarat, Assoc. Prof. Dr. Sonthaya Tiawsirisup, Prof. Dr. Panat Anuracpreeda for their valuable suggestions and comments. My sincere thanks also go to Dr. Arin Ngamniyom and Dr. Vachira Hunprasit for their guidance. Immense gratitude also go to undergraduate students for their kind participating during sample collection and laboratory diagnosis. I am indebted to all the staff and graduate students from Parasitology Unit, Department of Pathology, Faculty of Veterinary Science, Chulalongkorn University for their encouragement.

Most of all, my father Kyi Soe deserves endless gratitude for his support, it was no exception. I would like to express my special appreciation and love to my beloved husband, Dr. Toe Win Naing and my lovely son, Kaung Zay Han for all their sacrifices they have made for me to pursue this study. Last but not least, I would like to thank my best friend, Dr. Aung Myo Thant for always being there for me to encourage.

Babi Kyi Soe



จุฬาลงกรณ์มหาวิทยาลัย  
**CHULALONGKORN UNIVERSITY**

## TABLE OF CONTENTS

	Page
ABSTRACT (THAI).....	iii
ABSTRACT (ENGLISH).....	iv
ACKNOWLEDGEMENTS .....	v
TABLE OF CONTENTS .....	vii
LIST OF TABLES.....	xiii
LIST OF FIGURES .....	xv
Importance and Rationale .....	17
Objectives.....	22
Hypotheses .....	24
Advantages of study.....	26
Chapter 1.....	27
1. Literature reviews .....	27
1.1 Epidemiology.....	27
1.2 Life cycle.....	28
1.2.1 General proposed life cycle.....	28
1.2.2 Experimental life cycle .....	29
1.3 Morphology.....	30
1.3.1 General morphology.....	30
1.3.1.1 Adult worm .....	30
1.3.1.2 Eggs .....	30
1.3.1.3 Developmental stages .....	31



1.3.1.4 Scanning electron microscopy and transmission electron microscopy.....	31
1.4 Diagnosis .....	32
1.4.1 Clinical signs.....	32
1.4.2 Imaging techniques .....	33
1.4.3 Blood biochemistry.....	34
1.4.4 Gross and histopathology .....	35
1.4.5 Fecal examination.....	35
1.5 Antigen detection for serodiagnosis of parasitic infection .....	36
1.6 Mass spectrometry- based parasitic proteomics.....	37
1.7 Treatment.....	38
Chapter 2.....	40
1. Introduction .....	43
2. Materials and methods.....	45
2.1 Sample size calculation and sample collection procedure.....	45
2.2 Blood sample collection.....	45
2.3 Sedation, general anesthesia, imaging and bile collection using PUC .....	46
2.4 Bile sample collection.....	47
2.5 Fecal sample collection.....	48
2.6 Kinetic egg shedding .....	48
2.7 Data analysis.....	48
3. Results.....	49
3.1 History taking.....	49
3.2 Fecal and bile microscopic examination.....	50

3.3 Hematology .....	52
3.4 Liver, pancreas biochemical profile and tumor markers .....	53
3.5 Alteration by imaging.....	55
3.6 Giemsa staining and bacterial culture.....	57
3.7 Egg shedding pattern .....	58
4. Discussion .....	61
5. Conclusion.....	69
REFERENCES .....	71
Chapter 3.....	77
1. Introduction .....	80
2. Materials and methods.....	84
2.1 Ethical statements.....	84
2.2 Sample collection, microscopic examination and sample preservation..	84
2.2.1 Isolation of <i>P. fastosum</i> adult fluke from the necropsy of cat carcasses .....	84
2.2.2 Recovery of <i>P. fastosum</i> eggs from cat fecal and bile samples ...	85
2.3 Carmine staining.....	86
2.4 Histological examination of <i>P. fastosum</i> adult worm.....	87
2.5 Scanning electron microscopy (SEM) of <i>P. fastosum</i> adult worms and eggs.....	87
2.5.1 Necropsy-derived <i>P. fastosum</i> adult worms .....	87
2.5.2 Bile-derived <i>P. fastosum</i> eggs.....	88
2.6 Transmission electron microscopy (TEM) of <i>P. fastosum</i> adult worms....	89
3. Results.....	90

3.1	Morphology of <i>P. fastosum</i> adult worm from macroscopic examination	90
3.2	Morphology of <i>P. fastosum</i> adult worm from microscopic examination.	91
3.3	Ultrastructural characteristics of <i>P. fastosum</i> adult examined by scanning electron microscopy (SEM).....	92
3.3.1	Whole ventral body.....	92
3.3.2	Oral sucker and associated papillae .....	94
3.3.3	Ventral sucker and associated papillae.....	97
3.3.4	Cirrus 98	
3.3.5	Anteroventral region of the worm and associated papillae .....	99
3.3.6	Ventral and dorsal tegument of the adult worm .....	102
3.3.7	Dorso-apical and posterior terminal end of the adult worm .....	102
3.4	Morphology of the bile-derived <i>P. fastosum</i> fluke eggs from microscopic examination .....	104
3.5	Morphology of the cat feces-derived <i>P. fastosum</i> fluke eggs from microscopic examination .....	107
3.6	Ultrastructural characteristics of bile-derived <i>P. fastosum</i> eggs using SEM .....	109
3.7	Tegument of <i>P. fastosum</i> adult worm by H&E-stained histological examination .....	111
3.8	Ultrastructural characteristics of <i>P. fastosum</i> adult worm using TEM.....	112
3.8.1	Tegument layers.....	112
3.8.2	Tegumental cells.....	116
3.8.3	Sperms and ova.....	117
4.	Discussion .....	118
5.	Conclusion.....	129

References .....	131
Chapter 4.....	138
1. Introduction .....	141
2. Materials and methods.....	143
2.1 Sample collection and identification .....	143
2.2 Preparation of crude worm antigens.....	144
2.3 Sera sample .....	144
2.4 SDS-PAGE and immunoblotting.....	146
2.5 LC-MS/MS analysis.....	148
2.6 Statistical analyses .....	149
3. Results.....	149
3.1 Immunopattern specific to platynosomiasis in cats .....	149
3.2 Analysis of sensitivity, specificity and predictive values.....	152
3.3 Mass spectrometry analysis.....	153
4 Discussion .....	154
5. Conclusion.....	162
References .....	164
Chapter 5.....	173
General discussion, conclusion and further recommendations.....	173
Appendix.....	176
REFERENCES .....	177
Appendix.....	187
VITA.....	188

## LIST OF TABLES

	<b>Page</b>
Table 1. Demographic data showing signalment, history, coinfections and information on physical examination of 14 naturally <i>P. fastosum</i> -infected cats.....	49
Table 2. Microscopic examination of fecal and bile sample of 14 naturally <i>P. fastosum</i> -infected cats .....	50
Table 3. Differences of fluke egg number from bile and fecal sample of each <i>P. fastosum</i> -infected cat.....	51
Table 4. Clinical parameters of 14 naturally <i>P. fastosum</i> -infected cats.....	52
Table 5. Normal parameters of liver, pancreas and tumor markers .....	54
Table 6. Imaging alterations of hepatobiliary system of 14 naturally <i>P. fastosum</i> -infected cats .....	55
Table 7. Occurrence of microbes from 4 naturally <i>P. fastosum</i> -infected cats .....	57
Table 8. Measurements of <i>P. fastosum</i> eggs with variable sizes (n = 68) in which these eggs were recovered from fecal and bile samples of 14 infected cats.....	106
Table 9. Number of sera sample and diagnosis methods.....	145
Table 10. Reactivities percentage of antigenic components against <i>P. fastosum</i> -infected sera, healthy control sera and other parasites infected sera .....	150
Table 11. Cumulative sensitivity, specificity, positive predictive value and negative predictive value of potential antigenic bands.....	152
Table 12. Identification of candidate proteins from crude worm extracts of <i>P. fastosum</i> using a nano LC-MS/MS.....	153
Table 13. Fecal egg number, bile egg number, blood biochemistry and imaging parameters of <i>P. fastosum</i> -infected cats.....	175

Table 13. Fecal egg number, bile egg number, blood biochemistry and imaging parameters of *P. fastosum*-infected cats..... 186



## LIST OF FIGURES

	<b>Page</b>
Figure 1. Proposed life cycle of <i>Platynosomum fastosum</i> .....	28
Figure 2. Experimental plan .....	38
Figure 3. Abnormal CBC parameters of 14 naturally <i>P. fastosum</i> -infected cats. ....	52
Figure 4. Liver, pancreas and tumor markers biochemical profiles of 14 naturally <i>P. fastosum</i> -infected cats. ....	53
Figure 5. (A-B). Ultrasonography of dilatation and tortuosity of intrahepatic bile duct of <i>P. fastosum</i> -infected cats (C). Computed tomography of gallbladder wall thickening and (D). Common bile duct dilatation of <i>P. fastosum</i> -infected cats. ....	56
Figure 6. <i>Platynosomum fastosum</i> fluke eggs from (A) Fecal sample; (B) Bile sample and (C) Giemsa stained of infected cats .....	57
Figure 7. Kinetic egg shedding measurements of 5 naturally <i>P. fastosum</i> - infected cats within 2 hrs after defecation.....	58
Figure 8. Microscopic examination of 5 naturally <i>P. fastosum</i> - infected cats feces after 24 hrs .....	59
Figure 9. Morphology of <i>P. fastosum</i> freshly isolated from necropsy of a fresh cat carcass.....	89
Figure 10. Adult <i>P. fastosum</i> observed under the stereomicroscope.....	91
Figure 11. SEM micrographs of the whole ventral body of 3 <i>P. fastosum</i> adult flukes collected from 3 different infected cats by necropsy.....	92
Figure 12. SEM micrographs of <i>P. fastosum</i> adult fluke's oral sucker and associated papillae.....	95
Figure 13. SEM micrographs of <i>P. fastosum</i> adult fluke's ventral sucker and associated papillae.....	97

Figure 14. SEM micrographs of <i>P. fastosum</i> adult fluke's cirrus, a male reproductive organ, collected from 2 different cat carcasses.....	98
Figure 15. SEM micrographs of <i>P. fastosum</i> adult fluke's anteroventral region and associated papillae.....	100
Figure 16. SEM micrographs of <i>P. fastosum</i> adult fluke's ventral and dorsal tegument as well as dorso-apical and posterior terminal end.....	102
Figure 17. Morphology of <i>P. fastosum</i> eggs collected from bile samples of infected cats and microscopic examination.....	105
Figure 18. Morphology of <i>P. fastosum</i> eggs isolated from infected cat fecal samples by centrifugal sedimentation and examined under a light microscope. ....	107
Figure 19. SEM micrographs of <i>P. fastosum</i> eggs collected from bile samples of infected cats. This sample was the same sample as shown in Fig 9C for microscopic examination. ....	109
Figure 20. Histological examination of <i>P. fastosum</i> adult worm. ....	111
Figure 21. TEM micrographs of <i>P. fastosum</i> adult fluke's tegument.....	114
Figure 22. TEM micrographs of <i>P. fastosum</i> adult fluke's tegumental cell cross section.....	116
Figure 23. TEM micrographs of <i>P. fastosum</i> adult fluke's oviduct.....	117
Figure 24. SDS-PAGE protein patterns of crude worm antigens of <i>P. fastosum</i> .....	149
Figure 25. Western blot analyses of <i>P. fastosum</i> crude worm antigens using <i>P. fastosum</i> -infected cat sera, healthy control sera and other endoparasites infected sera as probes. ....	150



## Importance and Rationale

Parasitic infections in domestic cats are common worldwide (Lucio-Forster and Bowman, 2011). In Thailand, hookworms, roundworms, coccidia, liver fluke, flea tapeworms and cat tapeworms were reported in cats (Jitsamai et al., 2021). In Bangkok and vicinities, the cat liver fluke, *Platynosomum fastosum*, seemed to require more attention as the ranking of infection has recently been shifted to the third rank among cat endoparasites found during the past 6 years, 8.9% (57/642) in 2020 (manuscript in prep.). Without using proper fecal examination technique and routine monitoring of cats with history of roaming, this infection is most likely to be underdiagnosed and neglected leading to chronic infection and later potentially succumbed to lizard poisoning disease characterized by severe irreversible hepatic diseases and death. In the case of chronic and/or heavy infection, *P. fastosum* can induce cholangiohepatitis, cholecystitis, periductal fibrosis, biliary cirrhosis and obstruction (Taylor and Perri, 1977; Xavier et al., 2007; Basu and Charles, 2014; Ramos et al., 2016). Also, cholangiocarcinoma and pancreatitis in cats were found to be associated with *P. fastosum* infection (Andrade et al., 2012; Koster et al., 2017). Despite available pre-mortem diagnosis and treatable disease, unfortunately, quite a few numbers of *P. fastosum* infected cats eventually died with the final diagnosis at the necropsy tables (Basu and Charles, 2014).

To detect *P. fastosum* infection in cats early, the challenges exist. Firstly, infected cats with subclinical infection rarely show any clinical signs (Foley, 1994; Ramos et al., 2016). For laboratory assessment, liver biochemical profiles can only give some clues for liver related diseases. Previous studies showed that naturally *P. fastosum* infected cats had elevated level of liver enzymes, (alanine transaminase) ALT, ALP (alkaline phosphatase) and GGT (gamma glutamine transference) (Xavier et al., 2007; Headleay et al., 2012; Ramos et al., 2016). For imaging diagnosis, ultrasonographic and computed tomographic studies were conducted in cats naturally infected with *P. fastosum*. They found hepatomegaly with heterogenous and hyperechoic liver parenchyma, gallbladder distention and bile duct dilatation in which these findings seemed to be associated with chronic *P. fastosum* infection (Salamao et al., 2005; Azevedo et al., 2012; Koster et al., 2016). Based on aforementioned physical and blood examination, there is no pathognomonic signs and specific biomarkers for final diagnosis of this liver fluke infection.

Secondly, although the positive results from fecal examination can yield specific and final diagnosis for *P. fastosum*-infected cats, the false negative results can occur from several reasons. Fecal examination using centrifugal sedimentation technique is recommended as conventional microscopic method to detect liver fluke eggs based on its operculum-containing nature (Bowman et al., 2002; Eisenbraun et al., 2020). Unlike detection of cat hookworm and roundworm by simple flotation, liver fluke egg detection requires a centrifuge which is not readily

available in most of the clinics. Despite availability of equipment, some practitioners may consider this technique somewhat tedious to routinely perform. Additionally, the sensitivity of detection by this method is low in case of light infection and of possibly intermittent egg shedding (Shell et al., 2015). We also suspect that *P. fastosum* eggs may present in typical and atypical forms. Experienced microscopic examiner is required to ensure the morphology and to differentiate *P. fastosum* egg from pseudoparasites. So, the false negative results could occur due to these scenarios especially in case of complete biliary obstruction resulting in no egg released in feces. Since *P. fastosum* infect cats via consumption of infected lizards and/or isopods by cats (Pinto et al., 2014), the third challenge is how to collect feces from cats with history of outdoor and hunting that usually defecate outdoor.

Consequently, to overcome all these challenges apart from coprological diagnosis, analysis of imaging profiles, radiology, ultrasonography and computed tomography (CT) from naturally *P. fastosum* infected cats with or without clinical signs combined with the clinical pathologic parameters including complete blood counting, liver, pancreas biochemical profiles and tumor markers will be conducted more completely to reveal that early diagnosis of *P. fastosum* in cats can be made. These parameters can also be established for further monitoring of cat responses to the treatment. To investigate the parasite burden, none of the study has been conducted to compare the difference between the bile-derived liver fluke egg number, obtained by percutaneous ultrasound-guided cholecystocentesis (PUC), and

the fecal egg counting. Although PUC seems to be slightly invasive technique, for non-complicated hepatic and/or systemic cases, it is practical to perform under the sedation and by a keen vet specialist. Since the bile is the first source for initial egg deposition, liver fluke egg recovery from bile could overcome the limitation of detection using fecal sample. Regarding intermittent egg shedding pattern of this liver fluke, no evidence-based report has been published. So, egg shedding kinetics will be performed from feces of naturally *P. fastosum*-infected cats for at least one month. Based on all these parameters, feline practitioners could realize that *P. fastosum* infection is common and should not be neglected by including this infection in their differential diagnostic lists for cats with history of outdoors.

Regarding the treatment, although praziquantel is recommended, the effectiveness and accurate dosage to eliminate the fluke was shown to be ineffective (Shell et al., 2015; Lathroum et al., 2018). To develop the specific treatment and vaccine to control this important infection in cats, the fundamental knowledge about parasite morphology is required to evaluate the effect of dewormer and host immune responses against this worm. So far, the morphology of this liver fluke was reported based on carmine staining of adult fluke and microscopic evaluation of fluke eggs (Basu and Charles, 2014; Nguyen et al., 2017). So, in this study we plan to use a comprehensive approach using scanning electron microscope (SEM), transmission electron microscope (TEM) and histology to investigate the

ultrastructural details of tegument, sensory organ and tissue architecture of *P. fastosum*.

In order to develop an early diagnosis and/or to follow cats up after treatment without fecal collection, investigation of antigenic profiles and the most promising candidate antigen are crucial for development of immunodiagnostic tool (Dar et al., 2019). Up to present, no study has been conducted for *P. fastosum*. Nowadays, mass spectrometry-based proteomics become a powerful tool for not only disease diagnostic biomarker identification but also for following up the progressiveness of disease (Tiberti et al., 2010). So, in the present study we would like to identify and characterize the potential candidate antigen(s) using mass spectrometry technique for further development of serodiagnosis to detect biomarker of *P. fastosum* infection in cats.

## Objectives

### Chapter 1: Clinical diagnosis of naturally *Platynosomum fastosum* infected cats

1. To evaluate clinical signs of naturally *P. fastosum*-infected cats
2. To assess hematological, liver, pancreatic blood biochemistry and tumor markers (carcino embryonic antigen; CEA, alpha-feto protein; AFP) of naturally *P. fastosum*-infected cats
3. To determine clinical imaging profiles of naturally *P. fastosum* infected cats using radiology, ultrasonography and computed-tomography
4. To detect presence of microorganism in the bile sample of naturally *P. fastosum*-infected cats
5. To detect the presence of *P. fastosum* adult or eggs and to determine the parasite burden collected from gallbladder of naturally *P. fastosum*-infected cats pertaining positive egg findings from fecal examination
6. To analyze the difference between bile-derived *P. fastosum* egg number and fecal egg number from naturally *P. fastosum*-infected cats
7. To assess the association between clinical pathology parameters, imaging profiles and parasite burden retrieved from fecal examination and from bile of naturally *P. fastosum*-infected cats
8. To assess the kinetics egg shedding of naturally *P. fastosum*-infected cats

CHULALONGKORN UNIVERSITY

### Chapter 2: Morphology and ultrastructural characteristics of *Platynosomum fastosum* Kossack, 1910 adults and eggs

1. To investigate basic morphology and surface histology of *P. fastosum* adult worm by carmine staining and H&E staining, respectively
2. To investigate morphology and to measure the *P. fastosum* egg size obtained from the bile and feces of infected cats by using a light microscope
3. To examine ultrastructural characteristics of *P. fastosum* adult worm and eggs using scanning electron microscope and transmission electron microscope

**Chapter 3: Antigenic profile and candidate antigen characterization of crude extract of *Platynosomum fastosum* using mass spectrometry**

1. To investigate antigenic profile of CWAs specific to *P. fastosum* infection and determine potential candidate antigen bands
2. To identify the candidate antigen specific to *P. fastosum* infection using mass spectrometry



## Hypotheses

### Chapter 1: Clinical diagnosis of naturally *Platynosomum fastosum* infected cats

1. Cats naturally infected with *P. fastosum* could present subclinical and/or overt clinical signs.
2. Cats naturally infected with *P. fastosum* could show abnormal elevation of liver and pancreatic biochemical parameters and tumor markers.
3. Based on radiologic, ultrasonographic, CT examination, significant hepatobiliary alterations would be detected in naturally *P. fastosum* infected cats.
4. Presence of microbes in bile might have association with inflammation of hepatobiliary system.
5. *P. fastosum* infection in cats can be diagnosed by examining of bile for the presence of fluke or fluke eggs as well as grading for the severity of infection based on the parasite burden.
6. The number *P. fastosum* eggs collected from bile and from feces of naturally *P. fastosum*-infected cats would be statistically different.
7. Abnormal values of each clinical pathology parameters and imaging profiles might be associated with high number of parasite burden retrieved from fecal examination and from bile of naturally *P. fastosum*-infected cats.
8. *P. fastosum* is most likely shed the eggs inconsistently.



## Chapter 2: Morphology and ultrastructural characteristics of *Platynosomum fastosum* Kossack, 1910 adults and eggs

1. Carmine staining could reveal the morphology of *P. fastosum* adult for confirmation of species and surface characteristics of *P. fastosum* may be similar to other dicrocoeliid flukes.
2. Typical and atypical forms and their sizes with detailed morphology of *P. fastosum* eggs can be identified from the bile and feces.
3. *P. fastosum* might have unique ultrastructural characteristics both externally and internally compared to other digenetic trematodes.

## Chapter 3: Antigenic profile and candidate antigen characterization of crude extract of *Platynosomum fastosum* using mass spectrometry

1. Antigen(s) containing in CWAs of *P. fastosum* could be used for differential diagnosis of *P. fastosum* infection.
2. Antigen(s) specific to *P. fastosum* infection could be identified by mass spectrometry.

### Advantages of study

1. Once the sub-clinically and clinically *P. fastosum* infected cats are diagnosed early, they could be treated before the clinical signs become severe and more chronic in which it is more challenging to be managed.
2. If our hypotheses are correct, cats infected by *P. fastosum* would be increasingly more identified and no longer be neglected by using more sensitive methods.
3. The number of cats with hepatic and carcinoma diseases related to *P. fastosum* infection would be much reduced.
4. The basic morphology, morphometry and ultrastructural characteristics of *P. fastosum* adult worm and eggs could be revealed with the evidence.
5. Antigenic profile of crude worm extracts *P. fastosum* would be identified.
6. The potential candidate antigen(s) of *P. fastosum* for serodiagnosis could be determined and characterized for further studies.

## Chapter 1

### 1. Literature reviews

#### 1.1 Epidemiology

*Platynosomum fastosum*, a liver fluke, resides in biliary tract and gall bladder of domestic cats in which it causes a disease called feline platynosomiasis, also known as “lizard poisoning”. The infection is worldwide especially in the areas favor for developmental life cycle of intermediate hosts (Basu and Charles, 2014). The prevalence of *P. fastosum* infection ranged between 15% and 85% and reported worldwide especially in the tropical and subtropical countries, including Brazil, Columbia, USA, Venezuela, Nigeria, Mexico, Malaysia and Thailand (Basu and Charles, 2014). In Thailand, the prevalence of *P. fastosum* was reported between 0.1% and 4.0% between year 2005 and 2015 from different provinces of Khon Kaen, Kanchanaburi, Nakhon Nayok, Pathum Thani and Nakhon Pathom (Jittapalapong et al., 2007; Muksombat K, 2008; Rojekittikhun W et al., 2008; Rojekittikhun W, 2013; Rojekittikhun W et al., 2015). In Bangkok and vicinities between year 2014 and 2015, the prevalence of *P. fastosum* was 3.7% (19/509) considering as the third rank of cat endoparasites (Jitsamai et al., 2021). Between year 2019 and 2020, with the higher sensitivity of detection by increasing sampling numbers, the prevalence of this neglected worm was shifted to 8.9% (57/642) with the same rank of cat endoparasitic infection in Bangkok and vicinities. Also, there was a case report by necropsy of accidental finding of *P. fastosum* co-infection with *Clonorchis sinensis* in a cat

(Nimsuphan et al., 2001). However, no other case report has been published since then.

## 1.2 Life cycle

### 1.2.1 General proposed life cycle

Regarding the nomenclature, *P. fastosum* is synonymous to *P. concinnum* and *P. illiciens* (Braun, 1901) based on morphology and genomic-based evidence (Pinto et al., 2018). The life cycle of *P. fastosum* is not completely documented. Felids are served as definitive host and become infected by eating lizards carrying metacercaria, an infective stage of the fluke. Apart from domestic cats, *P. fastosum* can also be capable of parasitizing avian hosts and also marmosets (Pinto et al., 2014).

The snail *Subulina octona* is considered as the first intermediate host (Maldonado, 1945) and terrestrial isopods (*Oniscidea spp.* and *Nagurus nanus*) are served as the second intermediate host in which it pertains encysted metacercaria in their body cavities capable of transmitting to domestic cats via consumption. Studies showed that terrestrial isopods are a part of diet for domestic cats. Also, excysted metacercaria were found in the biliary ducts of house geckos and lizards (*Hemidactylus mabouia* and *Anolis cristatellus*) in which they could serve as a paratenic host to transmit this infection (Figure. 1) (Pinto et al., 2014).



Figure 1. Proposed life cycle of *Platynosomum fastosum*.

Adapted from (Maldonado, 1945; Pinto et al., 2014)

### 1.2.2 Experimental life cycle

As attempted to pursue morphological and morphometric analysis, the parasite developmental stages, sporocysts and cercariae were obtained from snail *Subulina octona*. Infective stage metacercariae were recovered from body cavities of terrestrial isopods and biliary ducts of naturally infected tropical house geckos (*Hemidactylus mabouia*). Experimental AKR/J strain mice were force-fed with infective stage metacercariae. The mice were euthanized, and adult parasites were recovered after 120-160 days post infection. The morphological analysis was done

using light microscope and alum acetocarmine staining (Pinto et al., 2014; Pinto et al., 2018). The prepatent period from this experiment was about 8 weeks whereas natural infection was 8-12 weeks (Basu and Charles, 2014).

### 1.3 Morphology

#### 1.3.1 General morphology

The adult parasite is about 5 mm long and 2 mm wide. The two suckers are almost the same in size. The oral sucker on subterminal region while ventral sucker was situated one-fourth of the body length. The vitelline glands were seen at the middle of the body and genital pore is presented between the two suckers. The uterus was filled with eggs and occupied almost posterior one-third of the body length (Bowman, 2002).

##### 1.3.1.1 Adult worm

The size of *P. fastosum* fluke varies from 2.9 to 8 mm in length and 0.9 to 2.5 mm in width with prominent oral and ventral sucker. As digenetic trematode, the parasite is hermaphroditic and composed of paired horizontal testes located on either side of ventral sucker and the ovary is elongated and situated behind one of the testes. The large number of golden-brown, oval and thick-shelled eggs were found inside the uterus. The vitelline glands are very prominent and lie mainly on the lateral portions perhaps adult stage (Basu and Charles, 2014; Nguyen et al., 2017).

##### 1.3.1.2 Eggs

*P. fastosum* eggs are golden-brown and embryonated with one-end operculum. The size is 34–50  $\mu\text{m}$  in length  $\times$  23–35  $\mu\text{m}$  in width. Inside the mature

egg, a fully developed miracidium is present, and germ may be discernible under the light microscope. Immature eggs are found to be transparent, elliptical and slightly smaller in size (27–30  $\mu\text{m}$   $\times$  16–20  $\mu\text{m}$ ) (Basu and Charles, 2014; Mati, 2015).

#### 1.3.1.3 Developmental stages

The first intermediate host, a terrestrial snail, *Subulina octona*, releases sporocyst containing cercariae to the environment. The size of sporocyst is about 990  $\mu\text{m}$   $\times$  260  $\mu\text{m}$ , which contains approximately eighteen mature cercariae. In the second intermediate host, the oval or spherical shape of encysted metacercaria is further developed inside the body cavity of isopods. The size of encysted metacercaria is 230  $\mu\text{m}$   $\times$  160  $\mu\text{m}$  in which the active stage of larva may be seen inside. The excysted one, free living metacercaria is found inside the gallbladder and ducts of infected geckos (paratenic hosts) with the measurements of 430  $\mu\text{m}$   $\times$  120  $\mu\text{m}$  (Pinto et al., 2014).

#### 1.3.1.4 Scanning electron microscopy and transmission electron microscopy

To evaluate new drug efficacy by disrupting parasite tegument, fundamental morphological characteristics of parasite is required since the tegument is most important for host-parasite interaction such as nutrient absorption, immune responses, homeostasis and osmoregulation. Previous studies on ultrastructural characteristics of closely related digenetic species were conducted including *Schistosoma mansoni* (Morris and Threadgold, 1967), *Dicrocoelium dendriticum* (Cifrian and Garcia-Corrales, 1988), *Fasciola hepatica* (Bennett, 1975), *Echinostoma*

*reolutum* (Fried and Takahiro, 1984), *Opisthorchis viverrini* (Apinhasmit et al., 1994), *Fasciola hepatica* (Bennett and Threadgold, 1975), *Fasciola gigantica* (Dangprasert et al., 2001), *Faschoederius cobboldi* (Anuracpreeda et al., 2012), *Eurytrema coelomaticum* (Pinheiro et al., 2012), *Orthocoelium parvipapillatum* (Anuracpreeda et al., 2016), *Clonorchis sinensis* (Lee et al., 2012) and also rumen fluke *Paramphistomum cervi* (Panyarachun et al., 2010) and stomach fluke *Carmyerius spatiosus* (Anuracpreeda et al., 2015). However, there was no report for ultrastructural characteristics of *P. fastosum*. In this study, we are going to perform a comprehensive approach to understand surface topography, tissue architectures and tegument of *P. fastosum* using light microscopy, scanning electron microscopy and transmission electron microscopy.

#### 1.4 Diagnosis

Although lizard poisoning is a treatable disease, poor efficacy was demonstrated (Lathroum et al., 2018). So, diagnosis should be made early using fecal examination since positive detection of liver fluke egg is a definitive diagnosis. Since the disease outcome can be changed from asymptomatic and mostly subclinical and severely clinical cases, the combined diagnosis methods are required based on the following parameters.

##### 1.4.1 Clinical signs

In the subclinical *P. fastosum*-infected cats, non-specific clinical signs are clearly present. Clinical recognition can be based on physical examinations through signs of anorexia, dull coat, lethargy, loss of appetite, depression, dehydration, weight



loss, fever, vomiting, diarrhea, emaciation, abdominal tenderness, progressive icterus and occasionally jaundice (Taylor and Perri, 1977; Ramos et al., 2016).

#### 1.4.2 Imaging techniques

Imaging techniques such as X-ray, ultrasonography and computed tomography become important tools for evaluation of liver abnormalities in veterinary practice (Leveille et al., 1996). Comparison of sonographic alteration of *P. fastosum* infected cats were determined between egg eliminated and non-egg eliminated cats (Salamao et al., 2005). Sonographic changes on liver, bile ducts and gallbladder occurred in the presence of the parasite but it was difficult to specifically identify the fluke due to its tiny size.

Since fecal examination procedures are considered as less sensitive in case of biliary obstruction, evaluation of hepatic alteration by computed tomography are frequently used as diagnostic tool in feline medicine (Nakamura M, 2005). With respect to the assessment of hepatobiliary system, hepatomegaly, dilatation of gallbladder and common bile ducts were correlated with the presence of *P. fastosum* infection (Azevedo et al., 2012).

Percutaneous ultrasound-guided cholecystocentesis (PUC) is helpful method to examine gallbladder in cats via transhepatic approach (Savary-Bataille et al. 2003). In case of false negative fecal examination results during biliary obstruction, bile might serve as pure source of parasite origin enabling to detect the presence of parasite with the parasite burden. PUC (percutaneous ultrasound guided

cholecystocentesis) for known platynosomiasis cases becomes a method of choice especially in chronic cholangitis and cholecystitis (Koster et al., 2016).

#### 1.4.3 Blood biochemistry

On the aspects of hematology and liver biochemistry, abnormal white blood cell and hepatic enzymes such as ALT, ALP, AST and GGT are elevated since they are secreted from hepatocytes and biliary epithelium. Evaluation of these parameters are normally used to indicate liver parenchymal cell damage and abnormalities of hepatobiliary system as biliary system was ultimately affected based on histopathological studies of *P. fastosum* infection (Xavier et al., 2007; Ramos et al., 2015). The enzymes ALT, ALP, AST and GGT are mainly secreted from the liver with different half-life. So, the level of these enzymes might be significantly changed in chronic hepatic cell damage associated with *P. fastosum* infection. With the finding of pancreatitis that could be induced by *P. fastosum* infection (Koster et al., 2017), the level of enzyme pancreatic lipase might be helpful as it was the most specific and sensitive enzyme to assess pancreas abnormalities. In chronic cases with prolonged damage to hepatobiliary system, it might have abnormal level of tumor markers in case of developing cholangiocarcinoma induced by *P. fastosum* (Andrade et al., 2012). The tumor markers, CEA (carcinoembryonic antigen) and AFP (alpha-fetoprotein) have been widely used as not only diagnosis biomarkers for liver cancer in veterinary practice (Ano et al., 2011) but also prognosis biomarkers to predict disease progression (Bai et al., 2017).

#### 1.4.4 Gross and histopathology

The common gross lesions of *P. fastosum* infection included hepatomegaly, friable liver, biliary duct distension (both extrahepatic and intrahepatic), gallbladder distension, mesenteric lymphadenopathy and sometimes parasite specimen inside liver section and gallbladder (Ferreira et al., 1999, Headley et al., 2012; Basu and Charles, 2014). On the aspect of microscopic histopathological lesions, biliary hyperplasia, periportal fibrosis, hepatic infiltration of leukocytes and eosinophils, cholangiectasis, cholangiohepatitis and adult parasite inside the bile ducts would occur (Andrade et al., 2012; Basu and Charles, 2014). In chronic cases of *P. fastosum* infection, cholestasis, cholangiohepatitis and cholangiocarcinoma (CCA) was found and 27% of *P. fastosum*-infected cats were succumbed to CCA (Andrade et al., 2012).

#### 1.4.5 Fecal examination

With regards to fecal microscopic examination techniques, direct wet mount, zinc sulphate flotation, sucrose flotation, modified detergent flotation, formalin ether sedimentation and spontaneous sedimentation techniques are conventional and non-invasive techniques appropriate for detection of operculated trematode eggs (Foreyt, 2001; Mati et al., 2015; Eisenbraun et al., 2020). However, quite a few cats were left undiagnosed earlier and unfortunately diagnosed by post-mortem (Basu and Charles, 2014). This may be due to the limitation of getting fecal samples of roaming cats and of performing centrifugal sedimentation required for cat liver fluke egg detection from feces. Also, intermittent egg shedding, low parasite burden (2-10

eggs/g) and obstructive biliary tract in the advanced stage of disease could result in false-negative findings (Willard, 2000). Apart from these reasons, fecal eggs are not detected within prepatent period and centrifugal sedimentation may not be applied in clinics since centrifuge may not be available, hence these facts become challenges and cats may eventually be diagnosed at necropsy table.

### **1.5 Antigen detection for serodiagnosis of parasitic infection**

Though conventional microscopic examination is a basic diagnosis tool to detect parasite eggs in the feces, whereas the sensitivity of detection by this method is low in case of light infection and possibly intermittent egg shedding. These techniques could also favor only in the stage of parasite matured in which release of eggs in the host feces, so false negative result during prepatent period could occur due to these scenarios and in case of complete biliary obstruction. On regards of this, serological tests become the method of choice to detect presence of parasites even in non-productive stage. Although the reliability of these tests could be challenged in case there were common antigens reported from different parasite helminths. To overcome this issue, investigation of immunodominant antigens from parasite secreted products could be beneficial. In the process of representing serodiagnosis, the antigens that secreted from the parasite especially crude worm extracts, excretory secretory extracts and parasite tegument extractions are mentioned as high immunogenic and might be beneficial to develop early serodiagnosis tool (Wongratanacheewin et al., 1988). To identify this fact, specific

novel antigen from this liver fluke play crucial part. Understanding the fundamental antigenic components of parasite itself and investigating the potential candidate antigen, that could involve in host immune response, therefore, of great importance to develop early diagnosis tool and vaccine intervention.

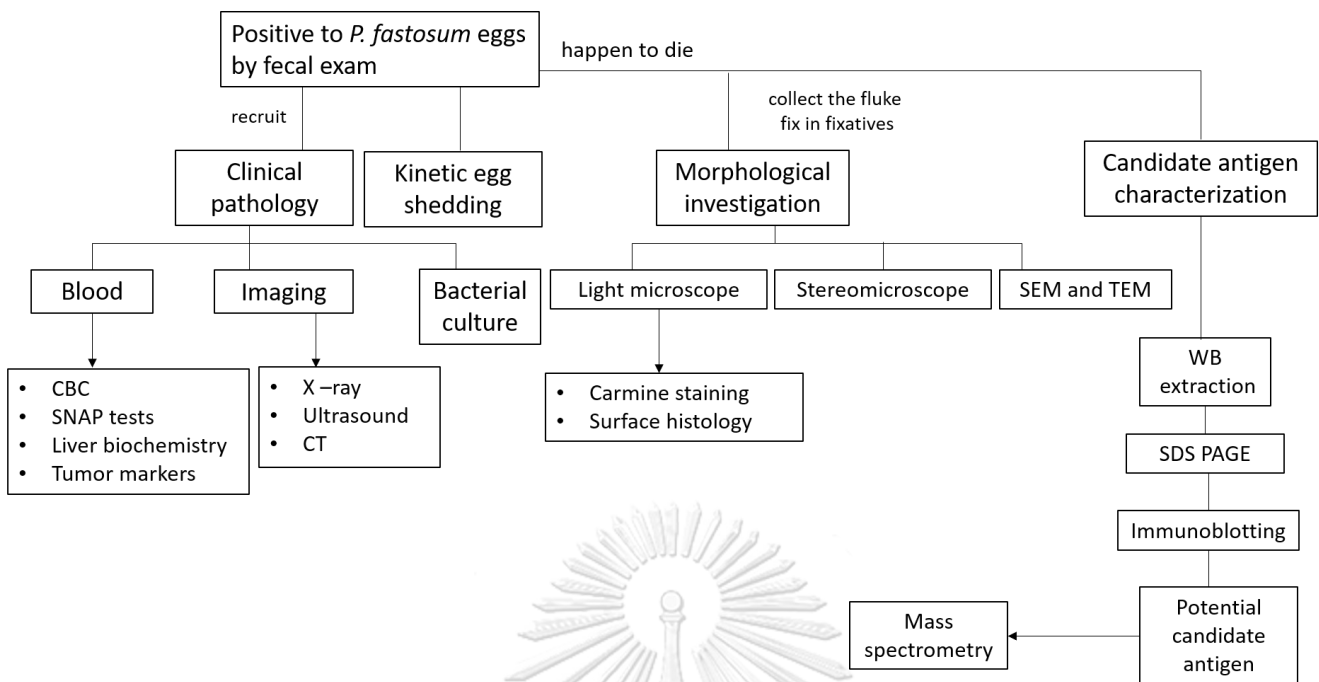
### **1.6 Mass spectrometry- based parasitic proteomics**

On behalf of new technologies, mass spectrometry-based proteomics become the preferable approach to analyze complex protein mixtures, since it can provide massive information with high reproducibility and high resolution. In order to obtain desired data of protein profiling, post translational modification and protein - protein interaction, mass spectrometry- based techniques play pivotal role as it allows to understand the cell at the protein level (Aebersold and Mann, 2003; Reamtong, 2008). Recently, mass spectrometry based parasitic proteomics studies were done to enhance disease diagnosis (Ndao et al., 2010; Khoontawad et al., 2012; Thezenas et al., 2013; Zhang et al., 2019), drug targets and vaccine intervention (Dea- Ayuela et al., 2006; Chemale et al., 2010; Wongkamchai et al., 2011; Boamah et al., 2012; Nuamtanong et al., 2019), it was also used to elucidate the host-parasite interaction (Gonzalez-Miguel et al., 2012) also for ectoparasites (Xavier et al., 2018). Moreover, concern with feline platynosomiasis, there was no previous studies has been conducted for detection of antibodies or circulating antigens in *P. fastosum*-infected cases. Basically, parasitic diseases are diagnosed by conventional microscopic technique in which it relies on the interpretation of skillful microscopic

examiner. Hence, mass spectrometry is suggested as indispensable tool to identify protein of interest, the candidate antigen revealed by immunoblotting technique in this study, will be further pursued for characterization using mass spectrometry.

### 1.7 Treatment

In literatures, praziquantel is recommended as referenced treatment for *Platynosomum fastosum* infection in which single dose of 20mg/kg BW (Evans, 1978), three consecutive doses (10mg/kg BW) and repeated dose 12 weeks apart (Foley, 1994) were used. In a case study of treatment for *P. fastosum* infection revealed that 5.7mg/kg once and booster dose at 3 to 4 weeks apart seemed to be effective (Shell et al., 2015). To determine the effectiveness between high dose and low dose of praziquantel, two group of experimental cats were used and evaluated the results by demonstrating post-mortem fluke counts (Lathroum et al., 2018). They found that only 50% efficacy of praziquantel even in high dose. On regards of this, praziquantel might only kill the adult flukes, then immature flukes remained and may subsequently mature to eliminate the eggs. In addition to this, praziquantel was shown to have limited efficacy depending upon trematode species, the developmental stage of parasite and the host (Mahanty S, 2011). So, further studies are still needed to evaluate effect of praziquantel on *P. fastosum*. Since, adopted cats without hunting behavior found to be infected with *P. fastosum*, it revealed that strayed once in a lifetime could be carrier for infection.



CBC:

CT:

SEM:

TEM:

SDS PAGE:

complete blood count

computed tomography

scanning electron microscope

transmission electron microscope

sodium dodecyl sulfate poly-acrylamide gel electrophoresis

CHULALONGKORN UNIVERSITY

Figure 2. Experimental plan

## Chapter 2

### Clinical diagnosis of naturally *Platynosomum fastosum*-infected cats

Babi Kyi Soe<sup>a</sup>, Nardtiwa Chaivoravitsakul<sup>b</sup>, Kongthit Horoongruang<sup>c</sup>, Rampaipat Penchome<sup>d</sup>, Siwaporn Pengpis<sup>e</sup>, Vachira Hunprasit<sup>f</sup>, Somporn Techangamsuwan<sup>g</sup>, Woraporn Sukhumavasi<sup>a,\*</sup>

<sup>a</sup>Parasitology Unit, International Graduate Program of Veterinary Science and Technology, Faculty of Veterinary Science, Chulalongkorn University, Bangkok 10330, Thailand

<sup>b/c/d</sup>Radiology Unit, Small Animal Teaching Hospital, Faculty of Veterinary Science, Chulalongkorn University, Bangkok 10330, Thailand

<sup>e</sup>Feline Center, Small Animal Teaching Hospital, Faculty of Veterinary Science, Chulalongkorn University, Bangkok 10330, Thailand

<sup>f</sup>Department of Medicine, Faculty of Veterinary Science, Chulalongkorn University, Bangkok 10330, Thailand

<sup>g</sup>Department of Pathology, Faculty of Veterinary Science, Chulalongkorn University, Bangkok 10330, Thailand

<sup>a,\*</sup>Parasitology Unit, Department of Pathology, Faculty of Veterinary Science, Chulalongkorn University, Bangkok 10330, Thailand

\*Corresponding email: [vetkwan@hotmail.com](mailto:vetkwan@hotmail.com)

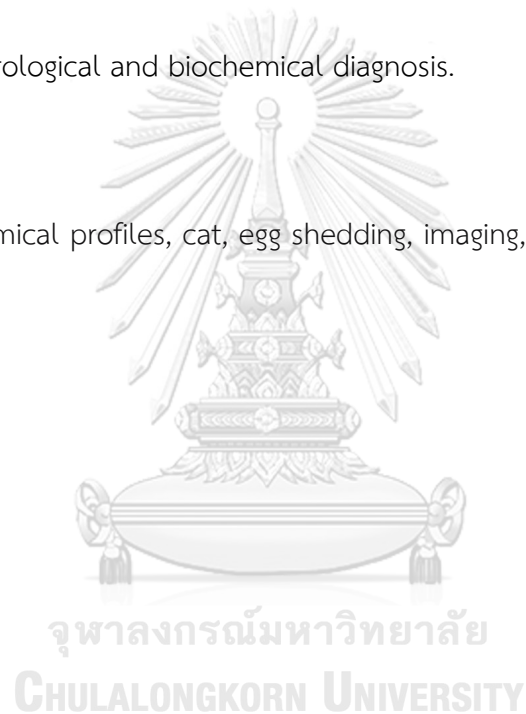


## Abstract

*Platynosomum fastosum* is a causative agent of lizard poisoning in cats in which the range of disease outcome can be from asymptomatic to severe hepatobiliary disease. Since the coprological diagnosis can yield false negative results due to possible inconsistent egg shedding and/or biliary obstruction, combined physical examination and laboratory assessment are required to help in early diagnosis and treatment. To detect the presence and the burden of parasite from bile and to compare this with the fecal-derived *P. fastosum* egg shedding number, percutaneous ultrasound-guided cholecystocentesis (PUC) was used to collect the bile to evaluate the *P. fastosum* eggs from 14 naturally infected cats previously diagnosed by centrifugal sedimentation as well as tracking of fecal egg shedding kinetics of 5 cats for 1 month. Also, to evaluate the abnormality of infected cats, hematology, biochemical profiles of liver, pancreas, tumor markers, retroviral and *Dirofilaria immitis* infection status in conjunction with radiography, ultrasonography, bacterial culture of bile were analyzed. On the physical examination day, 57.0% (8/14) and 78.6% (11/14) of naturally-infected cats were positive to *P. fastosum* by fecal sedimentation and PUC, respectively. The average of the bile egg number was significantly higher than fecal egg number ( $p=0.001$ ) and fecal egg shedding pattern was inconsistent. Out of 14, 2 cats had with eosinophilia. Elevated level of liver enzymes, ALT and GGT, were found in 57.1% (8/14) of *P. fastosum*-infected cats. For tumor biomarkers, 50% (7/14) of infected cats had elevated AFP. Based on

ultrasonogram, bile sediments were present in 85.7% (12/14) of *P. fastosum*-infected cats. There was no correlation between bile egg number and hepatobiliary abnormalities. Consequently, this study revealed that subclinical infection of *P. fastosum* was common with either low number and inconsistent fecal egg shedding or undetectable egg finding. PUC could be encouraged to be implemented in suspected cases due to sensitive detection from the pure source of *P. fastosum* together with coprological and biochemical diagnosis.

Keywords: biochemical profiles, cat, egg shedding, imaging, *Platynosomum fastosum*, tumor markers



## 1. Introduction

Parasite infections are common worldwide and it can cause several complications, especially in young and immunocompromised animals (Epe, 2009). Among companion animals, felids serve as definitive host for many endoparasitic infection (Lucio-Forster and Bowman, 2011). *Platynosomum fastosum*, a hepatic fluke, resides in biliary duct and gallbladder of infected cats. The disease is known as “lizard poisoning” since the cats become infected by ingestion of prey animal, that carried infective stage metacercariae. The disease found to be worldwide distribution, especially tropical and subtropical region (Basu and Charles, 2014). In Thailand, hookworms, roundworms, coccidia, liver fluke, flea tapeworms and cat tapeworms were most common endoparasites in cats (Jitsamai et al., 2021). In Bangkok and vicinities, prevalence of *P. fastosum* became shifted to 8.9% (57/642) with the ranking of third position between year 2019 and 2020 (personal communication).

Without using proper fecal examination technique and routine monitoring, this infection is most likely to be underdiagnosed and neglected leading to chronic infection and later potentially succumbed to severe irreversible hepatic diseases and death (Andrade et al., 2012). In the case of chronic and/or heavy infection, *P. fastosum* can induce cholangiohepatitis, cholecystitis, periductal fibrosis, biliary cirrhosis and biliary obstruction (Taylor and Perri, 1977; Basu and Charles, 2014; Ramos et al., 2016). Also, cholangiocarcinoma and pancreatitis in cats were found to be associated with *P. fastosum* infection (Andrade et al., 2012; Koster et al., 2016).

Despite available pre-mortem diagnosis, quite a few numbers of *P. fastosum* infected cats eventually died with the final diagnosis at the necropsy tables (Basu and Charles, 2014). It has been noted for asymptomatic in case of subclinical infection (Foley, 1994; Ramos et al., 2016). For laboratory assessment, liver biochemical profiles can only give some clues, such as elevated level of liver enzymes, ALT (alkaline transaminase), ALP (alkaline phosphatase) and GGT (gamma glutamine transference) in presence of *P. fastosum* infection (Xavier et al., 2007; Headley et al., 2012; Ramos et al., 2016). Assessment of sonographic alteration have been done to determine the association with *P. fastosum* infection (Salamao et al., 2005; Azevedo et al., 2012; Koster et al., 2017). However, specific pathognomonic signs and biomarkers for final diagnosis of this liver fluke has not been determined yet.

For conventional microscopic techniques, light infection and of possibly intermittent egg shedding could favor false negative results as low sensitivity of detection (Carreira et al., 2008; Shell e al., 2015). In addition, complete biliary obstruction may also result with false negative as the eggs can't pass through in the feces (Pinto et al., 2014). Considering this, experienced microscopic examiner is required to ensure morphology of *P. fastosum* in order to differentiate with pseudoparasites. With regard to these scenarios, combined different techniques such as analyses of imaging profiles from naturally *P. fastosum* infected cats with the pathologic parameters including complete blood counting, liver, pancreas biochemical profiles and tumor markers was conducted in current study. Since the

bile is source of origin to deposit fluke eggs, PUC (percutaneous ultrasound-guided cholecystocentesis) technique could overcome the limitation of detection using fecal sample. As previous mentioned, *P. fastosum* fluke eggs were sporadically found in the feces (Palumbo et al., 1976), no evidence-based report has been published yet for egg shedding pattern. So, egg shedding kinetics of *P. fastosum* has been investigated in this study.

## 2. Materials and methods

### 2.1 Sample size calculation and sample collection procedure

This study was approved by the Animal Care and Use committee, Faculty of Veterinary Science, Chulalongkorn University (Protocol no. 2031011) and by Institutional Biosafety Committee (Protocol no. 2031013). The sample size was calculated using G-Power software 3.1.9.4. From conventional diagnosis of 2 previously approved research project (Protocol no. 1931058, 2031011), a total of 14 naturally *P. fastosum* infected cats were recruited to study with the owner's consent. Interviewing of owner was conducted using questionnaires to record on signalment and history (gender, age, access to outdoors, multi-cat household, hunting behavior and deworming)

### 2.2 Blood sample collection

Blood sample were collected either cephalic or femoral vein using 22 G needle. After that, blood sample were sent to Veterinary Diagnostic Laboratory within 2 hr. Hematology was performed using (BC-5000Vet, Shenzhen, China) and blood chemistry analysis were done using flow cytometer (Calibur™, USA). AST level was

analyzed using (iLab-650, Spain) at Veterinary Diagnostic Unit, Faculty of Veterinary Science, Chulalongkorn University. SNAP Triple test for screening for feline leukemia virus (FeLV), feline immunodeficiency virus (FIV) and heartworm infection, SNAP bile acid test and SNAP fPL tests (IDEXX laboratories, USA) were performed in-house on the same day. The reference interval of blood biochemical parameters were checked with (Cornell University College of Veterinary Medicine, 2020). For cancer biomarker test, CEA (carcinoembryonic antigen) and AFP (alpha-fetoprotein) tests were performed with automated immunoassay analyzer (AIA-360, TOSOH, Japan). The reference interval of these tumor markers in cats were not available, so we checked these parameters compared to reference interval previously mentioned for dogs (Kitao et al., 2006); Camos et al., 2012).

### 2.3 Sedation, general anesthesia, imaging and bile collection using PUC

Total of 14 *P. fastosum*-infected cats were recruited to the study by the consent of owners. Prior to diagnosis, sample cats were not allowed to have meal and water for 12 hours for blood collection and sedation/anesthesia. Then, they were sedated with 15 µg/kg dexmedetomidine via intramuscular route and let them rest for 5-15 minutes. After sedation, cats were gently carried and placed on the right lateral and ventro-dorsal recumbency for taking thoracic and abdominal radiographs (Brivo DR-F, GE Healthcare, USA) followed by induction with 4 mg/kg propofol intravenously. Before intubation, 0.1 ml 2% lidocaine solution was locally dropped at the laryngeal area to prevent the laryngospasm. Endotracheal tubes, size 3.5-4.5mm,

was intubated with lubricant covering the cup of endotracheal tubes. The tubes was related to the ventilator machine and maintained with isoflurane.

During the anesthetic process, the heart rates, respiratory rates, indirect blood pressure and oxygen saturation of patient cats were closely monitored. In CT session, images were obtained using 64-slice CT scanner (Optima 660, GE Healthcare, USA). Pre-contrast abdominal scan was performed and repeatedly scanned after infusion of intravenous contrast medium (iohexol 600 mgI/kg) with rate of 2 ml per second. Abdominal ultrasonography was examined using ultrasonography machine (LOGIQ P6, GE healthcare, USA). Sonographic alterations were checked as previously (Griffin, 2020).

#### 2.4 Bile sample collection

The 22G, 1.5 inch-needles and 5-10 ml syringes was applied for percutaneous ultrasound guided cholecystocentesis (PUC) with standard aseptic technique. Briefly, 3-5 ml of bile was collected with the attempt for emptying the gall bladder to prevent from bile leakage inside the peritoneal cavity. After that, the bile sample was examined for cytology using Giemsa staining, and then check for presence of microbes using collection swab (CITOSWAB, China). Bile microscopic examination was performed to observe fluke eggs and enumerate the fluke eggs. In addition, bile sample was centrifuged at 500 xg at 4°C for 5 min. The bile sediments were stored in sterile eppendorf at -20°C for further scanning electron-microscopic study and PCR confirmation.

## 2.5 Fecal sample collection

Recovery of *P. fastosum* egg from the fecal samples was performed using PBS-ethyl acetate centrifugal sedimentation technique as previously described (Jitsamai et al., 2021). Briefly, fecal samples were collected per rectum and/or colon flushing technique using 10 ml sterile normal saline with feeding tube no. 6-8 during anesthesia. The fecal sample were kept in sterile plastic bag or 15 ml conical tube and cold chain was used prior to fecal examination. After that, fecal samples were microscopically examined using a light microscope (OLYMPUS, Japan).

## 2.6 Kinetic egg shedding

Total of 5 cats from this project were involved to determine kinetic egg shedding of *P. fastosum*. Briefly, fecal samples were collected within 2 hr from litter tray and examined as soon as possible. To investigate the fluke egg shedding nature, routine fecal examination was done at least one month. In addition, the fecal sample were kept inside 4°C refrigerator and examined the next day to determine the differences of egg shedding after 24 hrs. The egg number were also calculated according to the gram of feces used to examine.

## 2.7 Data analysis

For this purpose, the resulted data were analyzed using SPSS program. Differences between egg number retrieved from bile sample and fecal sample was calculated using Mann Whitney 'U' test. Non-parametric Spearman correlation test was used to determine association between bile egg number and damage of hepatobiliary system. Statistical significance was considered when  $P < 0.05$ .



### 3. Results

#### 3.1 History taking

From a total of 14 naturally *P. fastosum*-infected cats, 8 male and 6 female cats were recruited. None of these cats were icteric and all of them were clinically healthy. Based on physical examination including anal temperature measurement, observation of perfusion rate and mucous membrane color, palpation of internal organs including lymph nodes and thyroid glands and auscultation, all of them were normal with bright, alert and responsive status with normal heart and respiratory rates. With regard to their history, all infected cats were currently reared indoor with multi-cat household, and 12 cats were previously strayed and later adopted by the current owner (Table. 1).

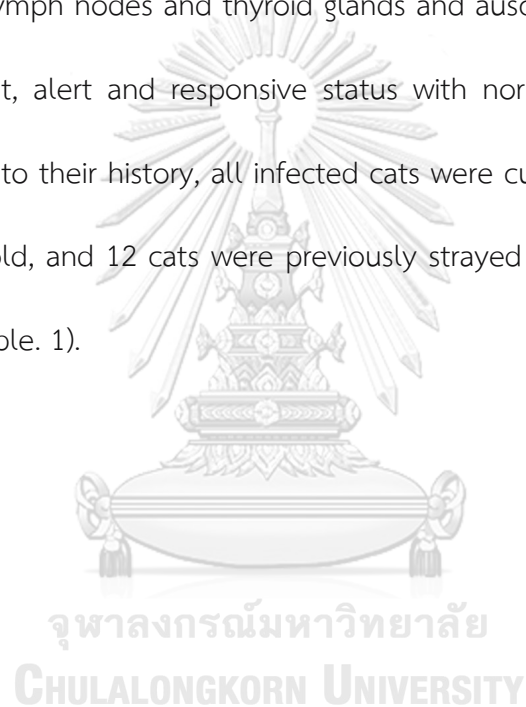


*Table 1.* Demographic data showing signalment, history, coinfections and information on physical examination of 14 naturally *P. fastosum*-infected cats

Demographic data	% (n)
<b>Gender</b>	
Male	57.1 (8)
Female	42.8 (6)
<b>Age</b>	
>6months	21.4 (3)
1-5years	78.6 (11)
Multi-cat household	100 (14)
Strayed history	85.7 (12)
Hunting behavior	57.1 (8)
Outdoor accessed	85.7 (12)
Coinfected with other parasites	57.1 (8)
No regular deworming	85.7 (12)
SNAP triple test (+)	14.2 (2)

### 3.2 Fecal and bile microscopic examination

Both fecal and bile sample were examined on the day of clinical diagnosis. For conventional examination technique, at least two times sampling was done to get high sensitivity. As result, 57.1% (8/14) of infected cats showed positive of fluke eggs in fecal sample with range of 14 – 201 eggs/g. However, 78.57% (11/14) cats were observed for presence of fluke eggs in bile sample with high parasite load (55 – 7800 eggs/ml). Both qualitative and quantitative measurements of fluke eggs were shown in (Table. 2). According to analysis, there was highly significant difference between bile and fecal egg number, ( $P= 0.001$ ). The differences of fluke egg

numbers retrieved from the bile and fecal sample of each *P. fastosum*-infected cat was shown in (Table. 3). As results, only 0-14.5 % of bile eggs were most likely passed through feces.

*Table 2.* Microscopic examination of fecal and bile sample of 14 naturally *P. fastosum*-infected cats

Cat no.	Prior to physical exam day	Examination results on physical examination date				Total vol: of bile (ml)
		Fecal examination	Fecal examination		Bile examination	
		Qualitative no. of eggs/40ul	Quantitative (eggs/g)	Qualitative no. of eggs/40ul	Quantitative (eggs/ml)	
1.	+	NF	NF	NF	NF	3
2.	+	2	40	1	55	5
3.	+	NF	NF	100	2750	4
4.	+	1.8	33	NA	350	2
5.	+	4	40	8	178	1.6
6.	+	8	40	6	150	3
7.	+	4	40	133	3300	2
8.	+	NF	NF	NF	NF	2.2
9.	+	2	14	41	1025	0.6
10.	+	NF	NF	25	625	2.3
11.	+	NF	NF	NF	NF	1
12.	+	35	201	184	7800	5
13.	+	NF	NF	112	280	3.5
14.	+	5	137	42	1050	2
<b>Positive cats %</b>	<b>100% (14/14)</b>	<b>57.1% (8/14)</b>		<b>78.57% (11/14)</b>		

NF: nothing found; NA: not available

Table 3. Differences of fluke egg number from bile and fecal sample of each *P. fastosum*-infected cat

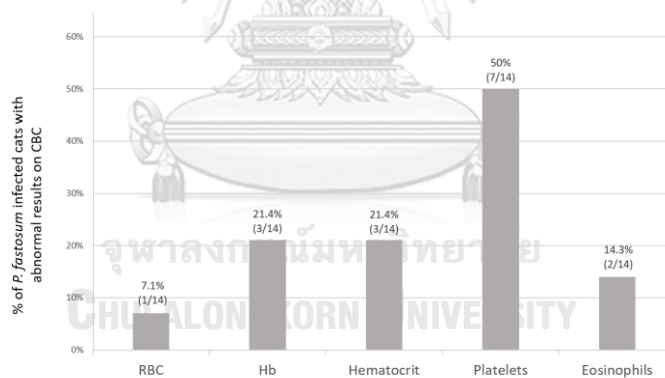
Cat No.	Fecal egg number (eggs/g)	Bile egg number (eggs/ml)	Total vol: of bile (ml)	Total no. of bile eggs (Tot. vol. of bile x bile egg number)	% Difference
1.	NF	NF	3	NF	NF
2.	40	55	5	275	14.5 %
3.	NF	2750	4	11,000	0 %
4.	33	350	2	700	4.7 %
5.	40	178	1.6	284.8	14 %
6.	40	150	3	450	8.9 %
7.	40	3300	2	6,600	0.6 %
8.	NF	NF	2.2	NF	NF
9.	14	1025	0.6	1,640	0.9 %
10.	NF	625	2.3	1437.5	0 %
11.	NF	NF	1	NF	NF
12.	201	7800	5	39,000	0.5 %
13.	NF	280	3.5	980	0 %
14.	137	1050	2	2,100	6.5 %

### 3.3 Hematology

Hematology was done with quantitative investigation in which packed cell volume (PCV), total red blood cell count (RBC), hemoglobin (Hb) concentration, total white blood cell count (WBC), differential WBC count and platelet count were determined. Abnormal clinical parameters of *P. fastosum*-infected cats were shown in (Table. 4). As a result, 50% (7/14) of infected cats showed thrombocytopenia and 28.6% (3/14) with abnormal level of hemoglobin and hematocrit. Moreover, two out of fourteen cats (14.3%) were found to have blood eosinophilia (Figure. 3).

Table 4. Clinical parameters of 14 naturally *P. fastosum*-infected cats

No.	Parameters	<i>P. fastosum</i> -infected cats			Reference values
		Diagnosed values	Elevated/decreased	% (number of infected cats with abnormal parameters/total number of infected cats)	
1.	RBC ( $\times 10^6$ )	3.9-9.87 per $\mu\text{l}$	Decreased	7.1% (1/14)	4.95-10.53 per $\mu\text{l}$
2.	Hemoglobin	6.1-15.9 g/dl	Elevated Decreased	14.3% (2/14) 7.1% (1/14)	8.5-14.4 g/dl
3.	Hematocrit	18.4-44.2 %	Elevated	21.4% (3/14)	25.8-41.8 %
4.	WBC	3,800-19,000 per $\mu\text{l}$	-	-	3,800-19,000 per $\mu\text{l}$
5.	Platelets ( $\times 10^3$ )	42-371 per $\mu\text{l}$	Decreased	50% (7/14)	160-660 per $\mu\text{l}$
6.	Neutrophils	2,500-12,500 per $\mu\text{l}$	-	-	2,500-12,500 per $\mu\text{l}$
7.	Eosinophils	260-2,230 per $\mu\text{l}$	Elevated	14.3% (2/14)	0-1,500 per $\mu\text{l}$
8.	Basophils	0-1 %	-	-	0-1 %
9.	Lymphocytes	1,500-7,000 per $\mu\text{l}$	-	-	1,500-7,000 per $\mu\text{l}$
10.	Monocytes	0-850 per $\mu\text{l}$	-	-	0-850 per $\mu\text{l}$

Figure 3. Abnormal CBC parameters of 14 naturally *P. fastosum*-infected cats.

### 3.4 Liver, pancreas biochemical profile and tumor markers

For blood chemistry, remarkably elevated liver enzymes, ALT 57.1% (8/14) and GGT 57.1% (8/14) were observed, followed by elevated level of blood urea nitrogen (BUN), alkaline phosphatase (ALP) and total protein in 35.7% (5/14), 21.4%

(3/14), 14.3% (2/14) of infected cats, respectively. According to SNAP test results, 14.3% (2/14) cats were positive to FIV antibody. The normal parameters of liver, pancreas and tumor markers were shown in (Table. 5). None of them showed abnormal level of serum bile acid and feline pancreatic lipase. With regards to tumor markers, 50% (7/14) of *P. fastosum* infected cats with elevated AFP (alpha-fetoprotein) whereas CEA within the normal limit for all infected cats (Figure 4).

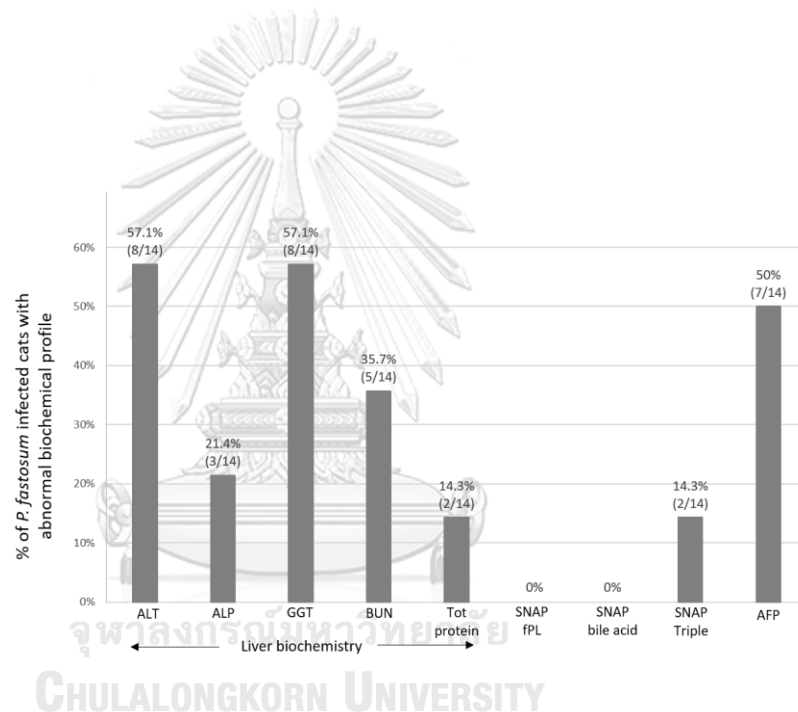


Figure 4. Liver, pancreas and tumor markers biochemical profiles of 14 naturally *P. fastosum*-infected cats.

Table 5. Normal parameters of liver, pancreas and tumor markers

No.	Parameters	<i>P. fastosum</i> -infected cats		Reference values
		Elevated/decreased	% (number of infected cats with abnormal parameters/total number of infected cats)	
1.	Alanine aminotransferase (ALT)	Elevated	57.1% (8/14)	13-75 units
2.	Alkaline phosphatase (ALP)	Elevated	21.4% (3/14)	3-61 units
3.	Gamma-glutamyl transferase (GGT)	Elevated	57.1% (8/14)	<2 units
4.	Blood urea nitrogen (BUN)	Elevated	35.7% (5/14)	10-30 mg%
5.	Tot protein	Elevated	14.3% (2/14)	6.1-8.8 g%
6.	Feline pancreatic lipase (fPL)	Normal	-	<3.6 ug/l
7.	Bile acid	Normal	-	<5 umol/L
8.	Alpha fetoprotein (AFP)	Elevated	50% (7/14)	<8.5 µg/dL
9.	Bilirubin	Normal	-	0-600 mg%

### 3.5 Alteration by imaging

For imaging alteration, 50% (7/14) of infected cats had hepatomegaly based on radiographic finding with round margin of the liver on ultrasound. Heterogenous liver parenchyma was observed in two cats. Interestingly, 85.7% (12/14) of infected cats had bile sediments in which these cats had liver fluke eggs in their bile samples. In addition, thickening of gallbladder wall was found in 42.9% (6/14) of sample cats. Most of cats, the biliary duct appear normal on ultrasonographic and computed tomographic examination. Dilatation of cystic duct and common bile duct in 35.7% (5/14) of infected cats, followed by extrahepatic and intrahepatic bile duct dilatation in 28.6% (4/14) of infected cats. Bile ducts tortuosity was occurred in 14.3% (2/14) of naturally *P. fastosum*-infected cats. The occurrence of imaging alterations in each organ was shown in (Table 6). The abnormalities images of hepatobiliary system was

shown in (Figure. 5 A-D). After analysis, there was no correlation between bile egg number and pathological grades of hepatobiliary system ( $p>0.05$ ).

*Table 6.* Imaging alterations of hepatobiliary system of 14 naturally *P. fastosum*-infected cats

No.	Structure	Parameters	References	<i>P. fastosum</i> -infected cats		
				% (number of infected cats with abnormal parameters/total number of infected cats)	Findings	Interpretation
1.	Liver	Size	Not extend beyond costal arch and right ventral kidney	50% (7/14)	Enlargement	Hepatomegaly
		Margin	Sharp	50% (7/14)	Round	
		Parenchymal homogeneity	Homogenous parenchyma	14.3% (2/14)	Heterogenous	Cholangitis/ cholangiohepatitis
2.	Gallbladder	Echogenicity of the contents	Normal	85.7% (12/14)	Intra-luminal contents	Bile sediment
		Wall thickness	Not visible	42.9% (6/14)	Wall thickness >1mm	Cholecystitis
		Wall distension	Not visible	42.9% (6/14)	Distended	Biliary stasis
3.	Biliary tracts	Hepatic duct	Not visible	28.6% (4/14)	> 0.1cm	Dilatation
		Cystic duct	Not visible	35.7% (5/14)	>0.3cm	Dilatation
		Common bile duct	<0.4cm	35.7% (5/14)	>0.4cm	Dilatation
		CBD wall	Normal	21.4% (3/14)	Thicken	Thickening
		Shape	Normal	14.3% (2/14)	Tortuosity	Tortuous bile duct

CBD; common bile duct



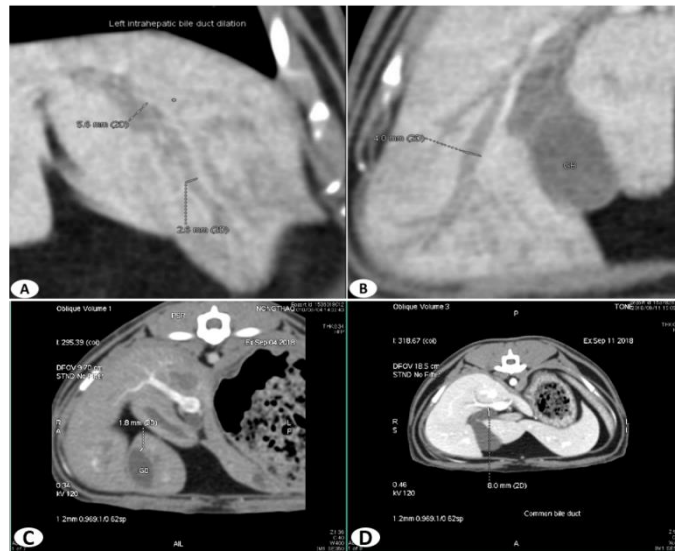


Figure 5. (A-B). Ultrasonography of dilatation and tortuosity of intrahepatic bile duct of *P. fastosum*-infected cats (C). Computed tomography of gallbladder wall thickening and (D). Common bile duct dilatation of *P. fastosum*-infected cats.

### 3.6 Giemsa staining and bacterial culture

By Giemsa staining, *P. fastosum* fluke eggs of deep blue color with thick egg shell were observed. The fluke eggs from fecal sample, bile sample and Giemsa stain were shown in (Figure. 6 A-C). According to bacterial culture results, the bile sample from 28.6% (4/14) of *P. fastosum*-infected cats were cultured for *Staphylococcus coagulase*, *Pseudomonas* spp. and *Bacillus* spp.. In further detail, these four cats had bile sediments inside gallbladder and three out of four observed hepatomegaly by imaging. Occurrence of microbes from four infected cats and their bile egg number were shown in (Table. 7).

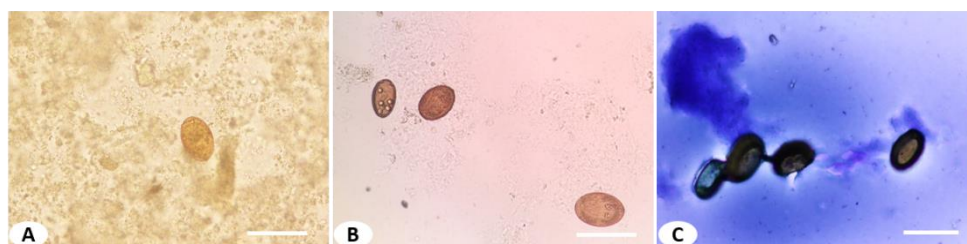


Figure 6. *Platynosomum fastosum* fluke eggs from (A) Fecal sample; (B) Bile sample and (C) Giemsa stained of infected cats

Scale bar; 50  $\mu$ m

Table 7. Occurrence of microbes from 4 naturally *P. fastosum*-infected cats

Cat no.	Culture results	Imaging findings	Bile egg number (eggs/ml)
9	<i>Staphylococcus coagulase</i> (-)	Bile sediment and biliary dilatation	1025
10	<i>Pseudomonas</i> spp.	Hepatomegaly, bile sediment, gallbladder distension and tortuous bile duct	625
11	<i>Bacillus</i> spp.	Hepatomegaly, bile sediment and tortuous bile duct	NF
12	<i>Staphylococcus coagulase</i> (-)	Hepatomegaly, bile sediment, tortuous bile duct and biliary dilatation	7800

NF: nothing found

### 3.7 Egg shedding pattern

For this aspect, five *P. fastosum* infected cats have been investigated for regular fecal examination at least one month. According to results shown in (Figure. 7A-F), *P. fastosum* shed the fluke eggs inconsistently with different egg shedding rates. The infected cats appeared to shed fecal eggs 2-6 days interval. After first day examination, the remaining fecal sample was kept in 4°C however, the eggs were mostly no longer detected in the feces (Figure. 8A-F). In case, fecal eggs were found after 24 hrs, fecal egg per gram was totally different with the result which was examined within 2 hrs after defecation.

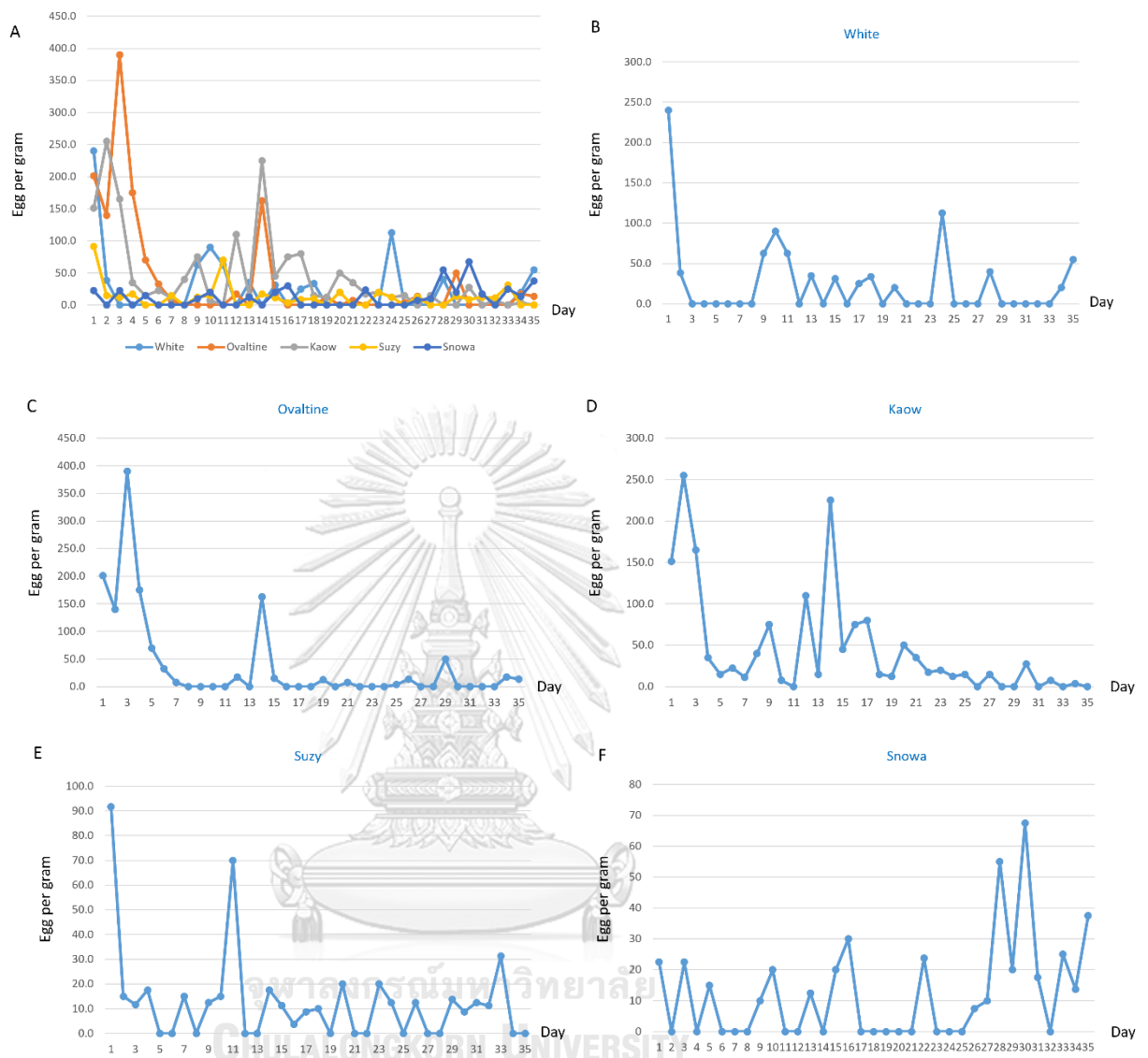


Figure 7. Kinetic egg shedding measurements of 5 naturally *P. fastosum*-infected cats within 2 hrs after defecation.

(A), The graph showed the egg shedding pattern of total 5 cats; (B-F), The graphs showed egg shedding pattern of each cat



Figure 8. Microscopic examination of 5 naturally *P. fastosum*-infected cats feces after 24 hrs .

(A), The graph showed the findings of fecal eggs from total 5 cats; (B-F), The graphs showed findings of fecal eggs from each cat

#### 4. Discussion

*Platynosomum fastosum* infection is widely distributed in both tropical and subtropical region (Basu and Charles, 2014). In Thailand, the prevalence rate reached to 8.9% within year 2019-2020, become the third rank of feline endoparasitic infection in Bangkok and vicinities (Manuscript in prep.). To diagnose this infection, centrifugal sedimentation method was used as it shown high sensitivity to detect presence operculated fluke eggs (Garcia et al., 2018). Nowadays, limited number of studies have been done for clinical diagnosis of feline platynosomiasis. In addition to this, the specific clinical parameters related to *P. fastosum* infection have not been identified yet. Therefore, we have investigated possible clinical parameters that might be useful to diagnose the infection.

The sample cats in current study did not show noticeable clinical symptoms and thus they are subclinically infected. Therefore, *P. fastosum* infection is most likely asymptomatic and might not be able to show the symptoms as previously described (Taylor and Perri, 1977). According to our results, strayed for once could be able to carry infection for their lifetime. Therefore, routine fecal examination should be performed for the cats with outdoor accessed.

In current study, 3 out of 11 cats were not detected from both fecal and bile sample. Sample cats from this study was recruited from previous project that aimed to determine prevalence of *P. fastosum* infection. So, it might be wrong interpretation of false positive results by examiners.

For complete blood count, 50% of infected cats showed low level of platelets as compared with normal reference range. Platelets are produced from bone marrow stem cells, and they are mainly responsible for hemostasis function. Platelets were found to be involved in innate immune system (Ali et al., 2015). Considering, low level of platelets is commonly occurred in *P. falciparum* infection with poor prognosis (Kho et al., 2018). However, involvement of platelets in helminth infection is still overlooked. Herein, flowcytometry technique was used to determine complete blood count (CBC). So, it is possible that the cytometer might be missed to count some platelets then resulted in thrombocytopenia. Manual counting of platelets would reveal different results compared to automatic analyzers (O'Brien et al., 1998).

Blood eosinophilia was occurred in two out of fourteen cats (14.3%). As previously mentioned, helminth infections were considered as one of the potential causes of eosinophilia (Mehta and Furuta, 2015), in which these two cats were also infected with *Ancylostoma* spp. and *Toxocara* spp.. However, these two cats showed 1,025 eggs/ml and 3,300 eggs/ml of bile egg number. So, it still need to discuss blood eosinophilia was related with either *P. fastosum* infection or not. Out of fourteen, three cats showed abnormal level of hemoglobin and hematocrit. Since these levels were associated with gastrointestinal hemorrhage (Walker et al., 1990), two out of three cats were infected with *Ancylostoma* spp.. Moreover, the sample

cats were deprived of food and water prior to anesthesia, thus dehydration and stress factors would favor to increase red blood cells (Winter, 1991).

As results, ALT, GGT and ALP level were elevated in 57.1%, 57.1% and 21.4% of *P. fastosum*-infected cats similar to previous studies (Taylor and Perri, 1977; Xavier et al., 2007; Headley et al., 2011; Ramos et al., 2016). It has been noted that, increased in both ALT and ALP are signal for hepatocellular injury (Iluz-Freundlich et al., 2020), whereas 21.4% (3/14) cats with elevated liver enzymes, ALT and ALP. Addition to this, GGT is an enzyme released from the biliary epithelium and used to indicate hepatobiliary diseases with high diagnostic efficacy, specificity of 87% (Center et al., 1986). Elevated GGT level has been reported together with bile duct hypertrophy and cholestasis in post mortem findings of *P. fastosum*-infected cats (Headley et al., 2011). So, it was interesting to see this parameter increased in 57.1% (8/14) cats correlating where adult parasites live. In addition, elevation of both ALP and GGT suggests for cholestasis (Vroon and Israili, 2011), in which one cat with increased ALP and GGT. In current study, total protein, albumin and globulin were within normal ranges as previously described (Taylor and Perri, 1977), indicating that biliary epithelial cell damage caused by *P. fastosum* seemed to be insufficient to observe these abnormalities. Since only 21.42% (3/14) cats showed elevated ALP level, non-remarkable changes might be found due to short half-life (6hr in cat). Since biliary epithelium was shown to be habitat site of *P. fastosum*, ALP level could be normal in low parasite burden case, as it is produced mainly from hepatocytes

cytoplasm. Although BUN was elevated in 5 cats (35.71%), three out of five cats were not detected for fluke eggs in bile sample. Considering that, BUN was remarkable biomarker for kidney function in companion animal (English, 1974). As above mentioned facts, abnormal liver enzyme parameters, especially ALT and GGT might be elevated in *P. fastosum* infected cases. However, the association between actual parasite burden and specific pathognomonic changes still need to be discussed.

In current study, 7 out of 14 cats were tested for AST and showed in normal ranges. AST level was appeared to be elevated in case of hepatocellular degeneration during migrating of juvenile flukes in *Fasciola* spp. infection (Hodzic et al., 2013). Therefore, we suggested that this enzyme could probably back to normal range when the fluke settled inside biliary duct or gallbladder. Probably, short half-life (1.5hr in cat) of this enzyme made unremarkable changes in *P. fastosum* infection (Ramery et al., 2010).

According to SNAP triple test, only two cats showed positive to FIV antibody. Therefore, immunosuppressive diseases did not seem to be associated with *P. fastosum* infection. However, limited sample would not favor to determine this immunosuppressive disease as risk factor for *P. fastosum* infection (Jitsamai et al., 2021). All sample cats showed in normal ranges for serum bile acid level. Considering, bile acid were profoundly elevated in liver dysfunction and cholestasis cases in cats. However, the normal bile acid level with high level of certain liver



enzymes in current study indicated functional hepatobiliary system is less likely (Schlesinger and Rubin, 1993).

*Platynosomum* spp. found to be collected from pancreatic ducts in cats (Purvis, 1931). To determine feline pancreatitis, assessment of fPL concentration is method of choice in which high sensitivity and specificity value, 67% and 91% have been reported previously (Forman et al., 2004). In current study, none of the sample cats showed abnormal fPL concentration as feline platynosomiasis rarely induced pancreatitis (Koster et al., 2017).

Attempt to diagnose cancer in companion animals, the diagnostic value of tumor markers remain controversial. For better understanding of neoplastic cells in cancer, quite a few studies have been reported potential biomarkers in both human and veterinary practice. Among them, AFP is the most widely used serum biomarker to establish diagnosis while upregulated AFP level was associated with pathological grades, disease progression and survival time of patient (Bai et al., 2017). Due to its oncogenic effect, AFP can promote tumor cell proliferation (Zhu et al., 2016). Interestingly, a half of *P. fastosum* infected cats showed elevated AFP level. In hepatocellular carcinoma, high diagnostic efficacy of AFP was documented specificity, 88%, although sensitivity was only 56%, (Hu et al., 2018). Thus, AFP might be possible biomarker hence 27% of *P. fastosum* infected cats has been proposed carcinogenesis (Andrade et al., 2012). With regards to CEA, normal range was shown in all sample cats. CEA is the serum biomarker, that produced from neoplasm of

epithelial origin. Elevation of this protein was mostly related to malignant histiocytosis, fibrosarcoma, colorectal and gastric cancer in both human and veterinary medicine (Hanglund et al., 1991; Teixeira et al., 2014). In addition, low diagnostic value of CEA, 52% sensitivity and 55% specificity has been reported in cholangiocarcinoma (Lumachi et al., 2014). Considering this, CEA might not be specific biomarker for cholangiocarcinoma and/or this tumor marker has not been detected due to its low diagnostic efficacy.

Feline biliary infection are still overlooked due to absence of specific clinical symptoms. Histopathological examination and bile fluid for microbiology and cytology could be helpful diagnosis with high sensitivity (Otte et al., 2017). On the aspect of bacterial culture, we found the bacterial growth in four out of fourteen cats, in which these cats showed high number of fluke eggs (625-7800 eggs/ml) in bile. Biliary pathologies were found to be associated with secondary bacterial colonization (Begley, 2005). Bile sediment could lead to cholestasis and cholecystitis that favor bacterial growth by increasing biliary pressure (Koster et al., 2016). Considering as contaminants, *Bacillus* spp. was identified from one cat with no bile eggs. So, proper specimen handling in step-by-step procedures is highly recommended. However, sample size was too small to evaluate bacterial growth as a factor for predictive significance. The association between positive culture results and *P. fastosum* infection should be further pursued.

Nowadays, imaging techniques were used to identify abnormalities of biliary ducts in veterinary practice (Azevedo et al., 2012). As results in current study, cystic duct and common bile duct were dilated in 35.71% (5/14) of infected cats. Liver fluke infection was considered as one of the most common cause of biliary duct dilatation (Spain et al., 2017). Thus, *P. fastosum* might induce hepatobiliary abnormalities. Interestingly, hepatomegaly was revealed in 50% (7/14) of *P. fastosum*-infected cats. Enlargement of liver with biliary dilatation have been reported previously (Salamao et al., 2005; Azevedo et al., 2012). In contrary, hepatic ducts have been found as mostly affected in *P. fastosum* infection (Salamao et al., 2005). However, normal ranges of biliary parameters cannot rule out biliary obstruction as previously described (Griffin, 2019). Apart from that, *Eurytrema procyonis*, a pancreatic fluke have been reported in consistent with enlargement of pancreas, pancreatic duct distension whereas mild hepatomegaly and reduced in portal veins diameter compared to hepatic veins in ultrasound findings in which this fluke is the same family of *P. fastosum* (Vyhnal et al., 2008). Conceivably, bile sediment might be possible for concurrent cholangitis, cholecystitis and cholangiohepatitis. Despite of histopathological findings have performed in current study, the severity of lesions that could lead to sonographic changes is still unsolved.

Bile sediment was detected in 85.7% (12/14) of infected cats. However, it was difficult to specifically identify presence of fluke inside gallbladder due to its tiny size. Cholestasis could occur in case bile sediments could obstruct biliary flow as

described previously (Salamao et al., 2005; Azevedo et al., 2012; Braga et al., 2016; Koster et al., 2016).

Since bile egg number was significantly different from fecal egg number ( $p=0.001$ ), then PUC technique revealed high sensitivity beyond fecal examination. Nonetheless it was slightly invasive technique, PUC could be established as final diagnosis for false negative cases.

Bile eggs 0-14.5% was shown to be eliminated through feces, thus false negative would come out in low parasite burden case. We have investigated that *P. fastosum* shed the eggs inconsistently by subsequent findings of fluke eggs in the fecal sample. Freshness of fecal sample is very important as *P. fastosum* eggs were no longer detected after 24 hrs even these fecal sample were kept in . Therefore, fecal microscopic examination should be performed quickly. As mentioned, inconsistent egg shedding might be due to intermittent shedding nature of fluke (Palumbo et al., 1976). Therefore, routine fecal examination should be performed in outdoor accessed cats. Although we have performed multiple diagnostic approaches to determine *P. fastosum* infection, it still insufficient to interpret accurately. In case of suspicious cats with undetectable fluke eggs in feces but elevated clinical parameters and hepatobiliary abnormalities, positive result of liver fluke egg from bile examination via PUC can be final diagnosis. Our results might be helpful to interpret reasonably of feline platynosomiasis.

## 5. Conclusion

In conclusion, we have investigated potential clinical parameters associated with liver fluke *P. fastosum* infection. However, most of liver and pancreatic biochemical parameters were in normal range, then regular examination of parasite eggs in fecal sample is strongly recommended. Despite of PUC is slightly invasive, the most appropriate parasite egg number can determine, and imaging techniques would favor to evaluate sonographic alterations. Since *P. fastosum* infection become one of most neglected endoparasites with third rank in Bangkok and vicinities, feline practitioners can realize that this infection could be listed as one of the etiological agents of feline liver abnormalities. According to *P. fastosum* egg shedding nature, conventional fecal examination technique should be routinely practice. The owners should aware since the cats with outdoor access still favor to get infection. Since different combined diagnosis would favor reliable results, fine needle aspiration should be done in cats with abnormal clinical and imaging parameters with positive fluke egg results. Further studies with large sample size are still needed to determine associate risk factors to make appropriate preventive measures and treatment regime.

## Acknowledgements

This research was financially supported to WS by the grant of Faculty of Veterinary Science, Feline Health and Infectious Disease Research Unit, Animal Vector-Borne Disease Research Unit, Chulalongkorn University. In addition, this research was

financially supported to Babi Kyi Soe by the 90<sup>th</sup> Anniversary of Chulalongkorn University Scholarships (Rachadaphiseksomphot Endowment Fund), Grant of Faculty of Veterinary Science, Chulalongkorn University. The authors would like to thank IDEXX for partial support of SNAP test kits, staff from Feline clinic, Veterinary Diagnostic Laboratory, Imaging Unit of Veterinary Teaching Hospital and Parasitology Unit, Department of Pathology, Faculty of Veterinary Science, Chulalongkorn University for their kind support to use laboratory supplies. Authors would like to gratefully thank Prof. Dr. Chollada Buranakarl and the Department of Livestock Development for the opportunity to join the public veterinary services. Moreover, authors would like to thank undergraduate student volunteers and graduate students in parasitology unit, Faculty of Veterinary Science, Chulalongkorn University for cooperating in sample collection and processing. Moreover, the authors would like to thank Mr. Shane Thiha Soe and Ms. Shin Moe Aoke for kind participating during clinical assessment and kinetic egg shedding study.

## REFERENCES

- Ali, R.A., Wuescher, L.M. and Worth, R.G. 2015. Platelets: essential components of the immune system. *Curr. Trends. Immunol.*, 16, 65.
- Andrade, R.L., Dantas, A.F., Pimentel, L.A., Galiza, G.J., Carvalho, F.K., Costa, V.M. and Riet-Correa, F. 2012. *Platynosomum fastosum*-induced cholangiocarcinomas in cats. *Vet. Parasitol.*, 190(1-2), 277-280. doi:10.1016/j.vetpar.2012.04.015
- Azevedo, F.D., da Veiga, C.C.P., Scott, F.B., Azevedo, T.R.C., de Souza, B.G. and Vulcano, L.C. 2012. Computer Tomography Evaluation of The Liver and Gallbladder in Domestic Cats (*Felis catus domesticus*) Parasitized by *Platynosomum illiciens* (BRAUN 1901) Kossack 1910. *Revista Brasileira de Medicina Veterinária.*, 34(4), 275-278.
- Bai, D.S., Zhang, C., Chen, P., Jin, S.-J. and Jiang, G.Q. 2017. The prognostic correlation of AFP level at diagnosis with pathological grade, progression, and survival of patients with hepatocellular carcinoma. *Sci. Rep.*, 7(1), 1-9.
- Basu, A.K. and Charles, R.A. 2014. A review of the cat liver fluke *Platynosomum fastosum* Kossack, 1910 (Trematoda: Dicrocoeliidae). *Vet. Parasitol.*, 200(1-2), 1-7. doi:10.1016/j.vetpar.2013.12.016
- Begley, M. 2005. Gahan CG, Hill C. The interaction between bacteria and bile. *FEMS Microbiol. Rev.*, 29, 625-651.
- Bowman, D.D., Hendrix, C.M., Lindsay, D.S. and Barr, S.C. 2002. *Feline Clin. Parasitol.* (Vol. 206): Wiley Online Library.
- Carreira, V.S., Vieira, R.F., Machado, G.F. and Luvizotto, M.C. 2008. Feline cholangitis/cholangiohepatitis complex secondary to *Platynosomum fastosum* infection in a cat. *Revista Brasileira de Parasitologia Veterinária.*, 17(1), 184-187.
- Center, S., Baldwin, B., Dillingham, S., Erb, H. and Tennant, B. 1986. Diagnostic value of serum gamma-glutamyl transferase and alkaline phosphatase activities in hepatobiliary disease in the cat. *J. Am. Vet. Med. Assoc.*, 188(5), 507-510.
- English, P. 1974. Acute renal failure in the dog and cat. *Aust. Vet., J.*, 50(9), 384-392.
- Epe, C. 2009. Intestinal nematodes: biology and control. *Veterinary Clinics: Small Anim. Pract.*, 39(6), 1091-1107.

- Foley, R.H. 1994. *Platynosomum concinnum* infection in cats. The Compendium on continuing education for the practicing veterinarian (USA).
- Forman M., Marks S.L., De Cock H., Hergesell E., Wisner E.R., Baker T., Kass P.H., Steiner J. and Williams D. 2004. Evaluation of serum feline pancreatic lipase immunoreactivity and helical computed tomography versus conventional testing for the diagnosis of feline pancreatitis. *J. Vet. Intern. Med.*, 18(6): 807-815.
- Garcia, L.S., Arrowood, M., Kokoskin, E., Paltridge, G.P., Pillai, D.R., Procop, G.W. and Visvesvara, G. 2018. Practical guidance for clinical microbiology laboratories: laboratory diagnosis of parasites from the gastrointestinal tract. *Clin. Micro. Rev.*, 31(1).
- Griffin, S. 2019. Feline abdominal ultrasonography: what's normal? what's abnormal? The biliary tree. *J. Feline Med. Surg.*, 21(5), 429-441.
- Haglund, C., Kuusela, P., Roberts, P. and Jalanko, H. 1991. Tumour marker CA 125 in patients with digestive tract malignancies. *Scandinavian J. Clin. Lab.*, 51(3), 265-270.
- Headley, S., Gillen, M., Sanches, A. and Satti, M. 2012. *Platynosomum fastosum*-induced chronic intrahepatic cholangitis and *Spirometra* spp. infections in feral cats from Grand Cayman. *J. Helminthol.*, 86(2), 209.
- Headley, S.A., Ferioli, R.B., Reis, A.C. and Bracarense, A. 2011. *Platynosomum fastosum*-induced infections in domestic shorthair cats: a retrospective study of seven cases. *Braz. J. Vet. Pathol.*, 4(3), 227-234.
- Hodžić, A., Zuko, A., Avdić, R., Alić, A., Omeragić, J. and Jažić, A. 2013. Influence of *Fasciola hepatica* on serum biochemical parameters and vascular and biliary system of sheep liver. *Iranian J. Parasitol.*, 8(1), 92.
- Hu, J., Wang, N., Yang, Y., Ma, L., Han, R., Zhang, W. and Wang, X. 2018. Diagnostic value of alpha-fetoprotein combined with neutrophil-to-lymphocyte ratio for hepatocellular carcinoma. *BMC Gastroenterol.*, 18(1), 1-7.
- Iluz-Freundlich, D., Zhang, M., Uhanova, J. and Minuk, G.Y. 2020. The relative expression of hepatocellular and cholestatic liver enzymes in adult patients with liver disease. *Annals Hepatol.*, 19(2), 204-208.



- Jitsamai, W., Khrutkham, N., Hunprasit, V., Chandrashekar, R., Bowman, D. and Sukhumavasi, W. 2021. Prevalence of endoparasitic and viral infections in client-owned cats in metropolitan Bangkok, Thailand, and the risk factors associated with feline hookworm infections. *Vet. Parasitol., Regional Studies and Reports*, 100584.
- Jittapalapong, S., Inparnkaew, T., Pinyopanuwat, N., Kengradomkij, C., Sangvaranond, A. and Wongnakphet, S. 2007. Gastrointestinal parasites of stray cats in Bangkok metropolitan areas, Thailand. *J. Agric. Nat. Res.*, 41(5), 69-73.
- Kho, S., Barber, B.E., Johar, E., Andries, B., Poespoprodjo, J.R., Kenangalem, E. and William, T. 2018. Platelets kill circulating parasites of all major *Plasmodium* species in human malaria. *Blood*, 132(12), 1332-1344.
- Kitao S., Yamada T., Ishikawa T., Madarame H., Furuichi M., Neo S., Tsuchiya R. and Kobayashi K. 2006. Alpha-fetoprotein in serum and tumor tissues in dogs with hepatocellular carcinoma. *J. Vet. Dia. Invest.*, 18(3): 291-295.
- Köster, L., Shell, L., Illanes, O., Lathroum, C., Neuville, K. and Ketzis, J. 2016. Percutaneous ultrasound-guided cholecystocentesis and bile analysis for the detection of *Platynosomum* spp.-induced cholangitis in cats. *J. Vet. Intern. Med.*, 30(3), 787-793.
- Köster, L.S., Shell, L., Ketzis, J., Rajeev, S. and Illanes, O. 2017. Diagnosis of pancreatic disease in feline platynosomosis. *J. Feline Med. Surg.*, 19(12), 1192-1198.
- Lucio-Forster, A. and Bowman, D.D. 2011. Prevalence of fecal-borne parasites detected by centrifugal flotation in feline samples from two shelters in upstate New York. *J. Feline Med. Surg.*, 13(4): 300-303.
- Lumachi, F., Re, G.L., Tozzoli, R., D'aurizie, F., Facomer, F., Chiara, G.B. and Basso, S.M. 2014. Measurement of serum carcinoembryonic antigen, carbohydrate antigen 19-9, cytokeratin-19 fragment and matrix metalloproteinase-7 for detecting cholangiocarcinoma: a preliminary case-control study. *Anticancer Res.*, 34(11), 6663-6667.
- Maldonado, J.F. 1945. The life-history and biology of *Platynosomum fastosum* Kossak, 1910 (Trematoda : Dicrocoeliidae). *Puerto Rico J. Publ. Heal. Trop.*

- Med., 21(1), 17-39. Retrieved from <https://www.cabdirect.org/cabdirect/abstract/19450801019>
- Mehta, P. and Furuta, G.T. 2015. Eosinophils in gastrointestinal disorders: eosinophilic gastrointestinal diseases, celiac disease, inflammatory bowel diseases, and parasitic infections. *Immunol. Allergy Clin.*, 35(3), 413-437.
- Nguyen, H.M., Van Hoang, H. and Ho, L.T. 2017. *Platynosomum fastosum* (Trematoda: Dicrocoeliidae) from cats in Vietnam: morphological redescription and molecular phylogenetics. *The Korean J. Parasitol.*, 55(1), 39.
- Nimsuphan, B., Prihirunkij, K., Pinyopanuwat, N. and Chimnoi, W. 2001. Case report: mixed infection of *Platynosomum fastosum* and *Clonorchis sinensis* in cat. *Warasan Sattawaphaet*.
- O'Brien, M., Murphy, M.G. and Lowe, J.A. 1998. Hematology and clinical chemistry parameters in the cat (*Felis domesticus*). *J. Nutri.*, 128(12), 2678S-2679S.
- Otte, C.M., Penning, L.C. and Rothuizen, J. 2017. Feline biliary tree and gallbladder disease: aetiology, diagnosis and treatment. *J. Feline Med. Surg.*, 19(5), 514-528.
- Palumbo, N., Taylor, D. and Perri, S. 1976. Evaluation of fecal technics for the diagnosis of cat liver fluke infection. *Lab. Anim. Sci.*, 26(3), 490-493.
- Pinto, H.A., Mati, V.L. and de Melo, A.L. 2014. New insights into the life cycle of *Platynosomum* (Trematoda: Dicrocoeliidae). *Parasitol Res.*, 113(7), 2701-2707. doi:10.1007/s00436-014-3926-5
- Pinto, H.A., Pulido-Murillo, E.A., Braga, R.R., Mati, V.L., Melo, A.L. and Tkach, V.V. 2018. DNA sequences confirm low specificity to definitive host and wide distribution of the cat pathogen *Platynosomum illiciens* (= *P. fastosum*) (Trematoda: Dicrocoeliidae). *Parasitol. Res.*, 117(6), 1975-1978.
- Purvis, G. 1931. The species of *Platynosomum* in felines. *Vet. Rec.*, 1931; 11: 228-229.
- Ramery, E., Papakonstantinou, S. and O'Brien, P.J. 2010. Clinical pathology tests for assessment of liver disease in dogs & cats. *North. Ireland Vet., Today*.
- Ramos, R.A., Lima, V.F., Monteiro, M.F., Santana Mde, A., Lepold, R., Faustino, M.A. and Alves, L.C. 2016. New insights into diagnosis of *Platynosomum fastosum*

- (Trematoda: Dicrocoeliidae) in cats. *Parasitol Res.*, 115(2), 479-482.  
doi:10.1007/s00436-015-4763-x
- Rojekittikhun W.M.A., Prummongkol, S., Puangsa-art, S., Chaisiri, K. and Kusolsuk, T. 2013. Prevalence of Gastrointestinal Parasitic Infections in Refuge Dogs and Cats and Evaluation of Two Conventional Examination Techniques. *J. Trop. Med. Parasitol.*, 36, 58-67.
- Salomão, M., Souza-Dantas, L.M., Mendes-de-Almeida, F., Branco, A.S., Bastos, O.P., Sterman, F. and Labarthe, N. 2005. Ultrasonography in hepatobiliary evaluation of domestic cats (*Felis catus*, L., 1758) infected by *Platynosomum* Looss, 1907. *Intern. J. Appl. Res. Vet. Med.*, 3(3), 271-279.
- Schlesinger, D.P. and Rubin, S.I. 1993. Serum bile acids and the assessment of hepatic function in dogs and cats. *The Canadian Vet. J.*, 34(4), 215.
- Shell, L., Ketzis, J., Hall, R., Rawlins, G. and du Plessis, W. 2015. Praziquantel treatment for *Platynosomum* species infection of a domestic cat on St Kitts, West Indies. *J. Feline Med. Surg.*, 1(1), 2055116915589834.
- Spain, H.N., Penninck, D.G., Webster, C.R., Daure, E. and Jennings, S.H. 2017. Ultrasonographic and clinicopathologic features of segmental dilatations of the common bile duct in four cats. *J. Feline Med. Surg.*, 3(1), 2055116917716881.
- Taylor, D. and Perri, S. 1977. Experimental infection of cats with the liver fluke *Platynosomum concinnum*. *Am. J. Vet. Res.*, 38(1), 51-54.
- Teixeira, L., Guerra, T., Conrado, F.D.O., Terra, S.R., Gerardi, D.G. and González, F. 2014. Evaluation of tumor markers carcinoembryonic antigen, cytokeratin 19 fragment and cancer-associated antigen 72-4 in neoplastic and non-neoplastic canine effusions differentiation. *Arquivo Brasileiro de Medicina Veterinária e Zootecnia*, 66(5), 1311-1316.
- Vroon, D.H. and Israili, Z. (2011). Alkaline phosphatase and gamma glutamyltransferase.
- Walker, H.K., Hall, W.D. and Hurst, J.W. 1990. *Clinical methods: the history, physical, and laboratory examinations*: Butterworth-heinemann.

- Winter, M. 1991. Cornell University College of Veterinary Medicine Annual Report., 1990-91.
- Xavier, F.G., Morato, G.S., Righi, D.A., Maiorka, P.C., and Spinosa, H.S. 2007. Cystic liver disease related to high *Platynosomum fastosum* infection in a domestic cat. J. Feline Med. Surg., 9(1), 51-55.
- Zhu, M., Lu, Y., Li, W., Guo, J., Dong, X., Lin, B. and Li, M. 2016. Hepatitis B virus X protein driven alpha fetoprotein expression to promote malignant behaviors of normal liver cells and hepatoma cells. J. Cancer, 7(8), 935.



### Chapter 3

#### Morphology and ultrastructural characteristics of *Platynosomum fastosum*

##### Kossack, 1910 adults and eggs

Babi Kyi Soe<sup>a</sup>, Arin Ngamniyom<sup>b</sup>, Poom Adisakwattana<sup>c</sup>, Somporn Techangamsuwan<sup>d</sup>,  
Panat Anuracpreeda<sup>e</sup>, Dwight Bowman<sup>f</sup>, Woraporn Sukhumavasi<sup>a,\*</sup>

<sup>a</sup>Parasitology Unit, The International Graduate Program of Veterinary Science and  
Technology, Faculty of Veterinary Science, Chulalongkorn University, Bangkok 10330,  
Thailand

<sup>b</sup>Major Environment, Faculty of Environmental Culture and ECO tourist,  
Srinakharinwirot University, Bangkok 10100, Thailand

<sup>c</sup>Department of Helminthology, Faculty of Tropical Medicine, Mahidol University,  
Bangkok 10400, Thailand

<sup>d</sup>Department of Pathology, Faculty of Veterinary Science, Chulalongkorn University,  
Bangkok 10330, Thailand

<sup>e</sup>Institute of Molecular Biosciences, Mahidol University, Bangkok 73170, Thailand

<sup>f</sup>Department of Microbiology and Immunology, College of Veterinary Medicine,  
Cornell University, Ithaca, NY, USA

<sup>a,\*</sup>Parasitology Unit, Department of Pathology, Faculty of Veterinary Science,  
Chulalongkorn University, Bangkok 10330, Thailand

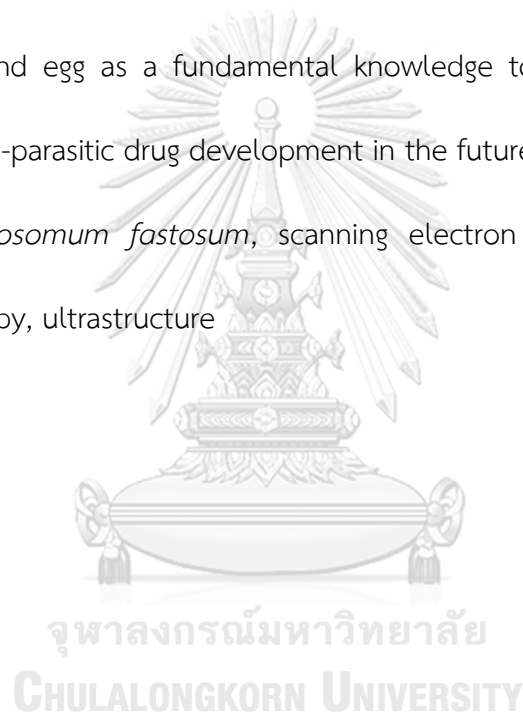
\*Corresponding author: [vetkwan@hotmail.com](mailto:vetkwan@hotmail.com)

## Abstract

Cats harbor a wide variety of parasites including *Platynosomum fastosum*, a liver fluke of domestic cats. This liver fluke residing in biliary tract can induce cholangitis, cholangiohepatitis and biliary obstruction especially in chronic and/or high parasite burden. Although praziquantel is recommended, the efficacy of this drug was ineffective. To evaluate any new rational drugs, fundamental knowledges of parasite morphology and ultrastructural characteristics are crucial but has not yet been investigated. To study macroscopic, microscopic and ultrastructural morphology, *P. fastosum* adult worms and eggs were evaluated using a light microscope, a stereomicroscope, a scanning electron microscopy (SEM) and a transmission electron microscopy (TEM). Under a stereomicroscope, the fluke was reddish brown and dorsoventrally flattened with leaf-like body shape. The body measurement was about 4.5 mm in length and 1.5 mm in width. Under SEM, the tegument surface of *P. fastosum* was spineless and covered with slender villous-like projections. The oral sucker was located on the anterior subterminal region and ventral sucker was located one fourth of the body. Four types of papillae were found and all were non-ciliated. *P. fastosum* fluke egg was dark brown in color with operculum and had thick and smooth egg shell surface with inconspicuous posterior abopercular knob. From both fecal and bile samples, at least 3 types of eggs were present. The average size of typical *P. fastosum* egg was 44.2 in length and 31.8 in width ( $1.7 \times 2.2 \pm \text{SD}$ ). Under TEM, tegument syncytium was analyzed into three layers. The first layer was

outermost trilaminate membrane covered by glycocalyx. The second layer was tegument cytoplasm composed of 2 types of tegumental granules (TG<sub>1</sub> and TG<sub>2</sub>) with electron lucent and electron dense matrix, lysosomes, mitochondria and microtubules. The third layer lied on basal lamina and contained basal membrane infoldings. Both TG<sub>1</sub> and TG<sub>2</sub> granules were produced by only one type of tegumental cell. This study revealed the first ultrastructural characteristics of *P. fastosum* adult and egg as a fundamental knowledge to use as basic criteria for assessment of anti-parasitic drug development in the future.

Keywords: *Platynosomum fastosum*, scanning electron microscopy, transmission electron microscopy, ultrastructure



## 1. Introduction

*Platynosomum fastosum*, a liver fluke belonging to the family Dicrocoeliidae, is a causal agent of feline platynosomiasis or lizard poisoning which is a neglected hepatobiliary disease in cats. Since this cat liver fluke becomes mature and stay in biliary tracts and gallbladder, it can induce the inflammatory processes depending upon the parasite burden and chronicity. Hence, the infection outcome can be ranged from asymptomatic to severe and lethal infection. In case of chronic and/or heavy infection, *P. fastosum* can induce cholangiohepatitis, cholecystitis, periductal fibrosis, biliary cirrhosis, and biliary obstruction (Basu and Charles, 2014; Ramos et al., 2015; Ramos et al., 2015; Ramos et al., 2016). Besides, *P. fastosum* infection was found to be associated with cholangiocarcinoma (Andrade et al., 2012).

Prevalence of *P. fastosum* infection was reported worldwide with ranges between 15% and 85% in both tropical and subtropical regions (Basu and Charles, 2014). In Thailand, between year 2017 and 2020, this parasite seemed to be more recognized and detected than did previous local reports. In year 2020, the prevalence was reached to (8.9%) in Bangkok and vicinities presumably due to increased sampling numbers to yield higher sensitivity of fecal egg detection (manuscript in prep.).

Cats can be infected by consuming *P. fastosum* metacercaria-containing preys that serve as either the second intermediate or paratenic hosts. The terrestrial lizards



have been suspected to play a role in *P. fastosum* life cycle as a paratenic host in which they consume metacercaria-infected terrestrial isopods. The terrestrial isopods receive the sporocyst by ingestion from the land snails that previously consumed the environmentally contaminated *P. fastosum* eggs. So far, *Subulina octona* was reported as one of the first intermediate host whereas species of terrestrial lizard (*Anolis cristatellus*) was reported as paratenic (Pinto et al., 2014). Although praziquantel is recommended as a specific treatment for *P. fastosum* infection in cats, the efficacy of this drug is ineffective, only 50% efficacy, even at high dose, 20 mg/kg, as the adult worms were still present in the cat livers without egg shedding (Lathroum et al., 2018). Whenever the new generation of anti-trematode is available and dosage titration study are required for drug efficacy evaluation, the fundamental knowledge of *P. fastosum* tegument structure is critical to use for mode of action and drug efficacy analyses.

Parasite tegument is an interface layer that plays vital role to maintain the homeostasis of the parasite, for example, nutrient absorption, waste product exchange, osmoregulation, self-protection from host digestive enzymes and immune responses. Therefore, parasite has to protect their functionate tegument from any disruption by perception of sensory stimuli (Sobhon et al., 2000). Since tegument releases infinite antigens which can stimulate host immune system, thus tegument is considered as primary target for any rational drugs and vaccines (Loukas et al., 2007).

Electron microscopic techniques have been used to elucidate the effect of dewormers on across tegument (JC, 1999). These techniques can be used to determine the surface topography of parasite and to investigate the common and unique characteristics among the family (Sobhon et al., 2000). Previous studies on ultrastructural characteristics of tegument were conducted with the following trematodes: *Schistosoma mansoni* (Morris and Threadgold, 1967), *Dicrocoelium dendriticum* (Cifrian and Garcia-Corrales, 1988), *Fasciola hepatica* (Bennett and Threadgold, 1975), *Ehinostoma revolutum* (Fried and Takahiro, 1984), *Opisthorchis viverrini* (Apinhasmit et al., 1994), *Fasciola gigantica* (Dangprasert et al., 2001), *Paramphistomum cervi* (Panyarachun et al., 2010), *Eurytrema coelomaticum* (Pinheiro et al., 2012), *Orthocoelium parvipapillatum* (Anuracpreeda et al., 2016), *Carmyerius spatiosus* (Anuracpreeda et al., 2015) and *Clonorchis sinensis* (Yun-Liang Shi, 2018). However, to the authors' knowledge, none of the study has been conducted with both adult worm and egg of *P. fastosum*.

The pre-mortem diagnosis of feline platynosomiasis is mainly relied on conventional coprological and microscopic techniques to demonstrate the *P. fastosum* egg from cat fecal samples. Centrifugal sedimentation technique is the method of choice to detect operculated fluke eggs (Willard, 2000). However, conventional microscopic examination yielded low sensitivity of detection in case of light infection and due to the nature of *P. fastosum* intermittent egg shedding (Willard, 2000; Shell et al., 2015). According to previous reports, the size of *P.*

*fastosum* egg was 34-50  $\mu\text{m}$  in length and 23-35  $\mu\text{m}$  in width. The egg was operculated, brown, oval in shape and fully developed miracidium is present (Basu and Charles, 2015). To avoid diagnosing the false positive result, the experienced microscopic examiner is required to differentiate this egg from other helminth eggs and pseudoparasites. Also, if variable size and shape differences of *P. fastosum* eggs would exist depending upon their maturation and fertilization phases as well as inconsistent egg shedding pattern, the knowledge on these variations should be established in order to achieve the accurate final diagnosis of *P. fastosum* infection.

Consequently, the purposes of this study were to perform a comprehensive approach using a stereomicroscope, a light microscope, a scanning electron microscope (SEM) and a transmission electron microscope (TEM) to reveal the macroscopic morphology, microscopic morphology with or without carmine staining, histological features by hematoxylin and eosin staining and ultrastructural morphology of *P. fastosum* adult worm as well as structural organization of *P. fastosum* tegument, respectively. Also, the morphology and size of *P. fastosum* eggs could be assessed using microscopic examination together with topographic ultrastructural assessment for the first time. This valuable information could provide fundamental knowledge as a basis for anthelmintic drug and vaccine efficacy evaluation that may affect tegument structures and functions of *P. fastosum* in the future.

## 2. Materials and methods

### 2.1 Ethical statements

The protocol of this study was approved from the Faculty of Veterinary Science, Animal Care and Use Protocol (VET-ACUP) and Institutional Biosafety Committee (CU-VET-IBC), Chulalongkorn University (IACUC No. 2031011 and IBC No. 2031054). All the cats that were recruited to this study had their owners' consent.

### 2.2 Sample collection, microscopic examination and sample preservation

#### 2.2.1 Isolation of *P. fastosum* adult fluke from the necropsy of cat carcasses

*Platynosomum fastosum* adult flukes were dissected from the liver and gallbladder of naturally infected cats by necropsy at Pathology Unit, Faculty of Veterinary Science, Chulalongkorn University. Three *P. fastosum*-infected carcasses were recruited in this study to compare the differences of adult fluke morphology by SEM in which the flukes were collected from partially autolyzed and fresh carcasses. The first and the second *P. fastosum*-infected carcasses were stored in 4°C for 2 days and 3 days, respectively, before the necropsy day whereas the third carcass was freshly obtained soon after death. Since the last cat yielded the fresh and alive *P. fastosum* adult flukes, its adult worms were selected for detailed tegumental surface study using SEM. During necropsy of all these 3 carcasses, the sterile normal saline was used to thoroughly flush biliary tracts and gallbladder. The collected adult fluke samples were rinsed for at least 3 times with 50 ml sterile normal saline followed by quickly rinsed through distilled water to remove the salt. For unstained adult samples, a randomly selected intact fluke was immediately brought for size

measurement using a ruler and for morphology record using a stereomicroscope (OLYMPUS, Japan). To preserve adult fluke samples for carmine staining, the parasite specimens were fixed in 10% formalin for 4 days. For sample preparation for scanning and transmission electron microscopy, adult worms were fixed in 2.5% glutaraldehyde in 0.1 M, phosphate buffer, pH 7.2 at 4°C for 2 days and 8 days, respectively.

#### 2.2.2 Recovery of *P. fastosum* eggs from cat fecal and bile samples

*Platynosomum fastosum*-infected cats were previously diagnosed by the coprological diagnosis from other study. For recovery of *P. fastosum* egg from the fecal samples, as previously described (Jitsamai et al., 2021), briefly, fecal samples were collected per rectum and/or colon flushing technique using sterile normal saline followed by PBS-ethyl acetate centrifugal sedimentation technique and microscopic examination using a light microscope (OLYMPUS, Japan). All images of *P. fastosum* eggs were recorded for further morphological analysis.

Five of these fecal egg-positive cats were recruited to pursue bile sample collection for other clinical study and for ultrastructural morphology analysis of *P. fastosum* egg. They were not allowed to feed and drink for 12 hours before blood collection for blood chemistry and hematology assessment to ensure their safety during sedation and anesthetization. Then, they were sedated with 15 µg/kg dexmedetomidine via intramuscular route and were allowed to rest for 5-10 minutes. After sedation, cats were induced with 4 mg/kg propofol intravenously. Before

intubation, 0.1 ml 2% lidocaine solution was locally dropped at the laryngeal area to prevent the laryngospasm. An endotracheal tube, size 3.5-4.5 mm, was intubated with lubricant covering the cup of endotracheal tube. The tube was related to the ventilator machine and maintained with isoflurane.

During the anesthetic process, the heart rates, respiratory rates, indirect blood pressure and oxygen saturation of patient cats were closely monitored. Using ultrasound-guided percutaneous cholecystocentesis (PUC) method performed under the recovery of anesthesia, 3-5 ml of bile sample was totally drawn from a gallbladder of each cat using 22G, 1.5 inch-needle. Wet bile mount was performed on a glass slide followed by microscopic examination of the eggs with morphological assessment. For the *P. fastosum* egg-containing bile sample preparation for SEM, a collected bile sample was centrifuged at 500xg for 5 min at 4°C and the supernatant was discarded to obtain *P. fastosum*-containing bile sediment. To rinse the bile sediment, the sample was then resuspended with phosphate buffer saline and centrifuged for 10 min with repeated steps followed by washing with distilled water. Thereafter, the fluke egg-containing sediment was fixed in 2.5% glutaraldehyde in 0.1 M phosphate buffer, pH 7.2 at 4°C for 6 days before SEM processing.

### 2.3 Carmine staining

Carmine staining was performed according to the method previously described by (Marhaba and Haniloo, 2018). Briefly, after the fixation of the *P. fastosum* adult parasites in 10% formalin for at least 24 hours, they were stained

with Semichon's acetic carmine overnight and then destained with 1% HCl for 5 min and 70% ethanol for 5 min. In addition, dehydration step was done using graded series of ethanol (30%, 50%, 70%, 95%, 100% for 10 min each and 100% twice), followed by clearing in xylene for 5 min and mounting the specimen with permanent medium (Permount, Sigma-Aldrich Co).

#### 2.4 Histological examination of *P. fastosum* adult worm

The formalin-fixed paraffin-embedded (FFPE) adult parasite specimens were prepared as previously described with slight modification (Anuracpreeda et al., 2016). Briefly, the adult worms were fixed in 10% formalin for 24 hr, then rinsed with tap water followed by putting in 70% ethanol for 24 hr at room temperature. After that, dehydration with graded series of ethanol (30%, 50%, 70%, 95%, 100% for 10 min each) and cleaning steps were performed using automatic tissue processor (SAKURA ATP140, Japan). Subsequently, the specimens were embedded in paraffin and sliced to a 5- $\mu$ m-thick section using a microtome (HESTION ERM3000, Australia), followed by staining with hematoxylin and eosin (H&E) using automatic tissue staining machine (MYREVA SS-30, Spain) and mounting with a permanent medium (Neo-Mount, Germany) before microscopic examination.

#### 2.5 Scanning electron microscopy (SEM) of *P. fastosum* adult worms and eggs

##### 2.5.1 Necropsy-derived *P. fastosum* adult worms

The 2.5% glutaraldehyde-fixed adult parasite specimens were prepared according to the method previously described (Anuracpreeda et al., 2015). Briefly,

the specimens were rinsed twice with phosphate buffer saline and washed once with distilled water for 10 min each. After washing, the specimen was dehydrated with graded series of ethanol (30%, 50%, 70%, 95%, 100% for 10 min each and 3 rounds for 100%), followed by drying in critical point dryer (Leica model EM CPD300, Austria). The specimens were later mounted on aluminium stubs and coated with gold using sputter coater apparatus (Blazers model SCD 040, Germany), at 15 mA for 3 min. Finally, the specimens were examined under a scanning electron microscope (JEOL JSM-IT300LV, Japan).

#### 2.5.2 Bile-derived *P. fastosum* eggs

A 2.5% glutaraldehyde-fixed fluke egg sediment retrieved from a cat bile sample was further processed for SEM according to previously published protocol (Shin et al., 2009). Cover slip was prepared by cutting into small pieces (size less than 1cm<sup>2</sup>). The specimen was coated with poly-L-lysine one drop and then waited for 10 min. After that, poly-L-lysine coated sample one drop was applied on cover slip and waited for 15 min. Subsequently, the cover slip was rinsed two times with phosphate buffer and once washed with distilled water (3-5 min in each step). After washing, the specimen was dehydrated with graded series of ethanol (concentration of 30%, 50%, 70%, 95%, 100% for 10 min in each step and 3 rounds for 100%). The specimen was then dried in critical point dryer (Leica model EM CPD300, Austria). After drying, the sample eggs were stuck on aluminium stubs using double sided carbon adhesive tape and coated with gold using sputter coater apparatus (Blazers model SCD 040,



Germany) at 25 mA for 2 min. Then, the sample was examined under SEM (JEOL JSM-IT300LV, Japan).

## 2.6 Transmission electron microscopy (TEM) of *P. fastosum* adult worms

The 2.5% glutaraldehyde-preserved *P. fastosum* adult samples were prepared according to the protocol described (Anuracpreeda et al., 2016) with slight modification on filtration step. For washing step, phosphate buffer saline was used to wash 3 times and post-fixed in 1% osmium tetroxide in 0.1 M sodium cacodylate buffer, pH 7.2 at 4°C for 1 hr. Thereafter, the specimen was washed in distilled water and subsequently incubated in 0.5% aqueous solution of uranyl acetate, pH 5.0, containing 45 mg/ml sucrose, at 4°C for 20 min. Then, the specimen was washed 3 times in distilled water, followed by dehydration in graded series of ethanol 30%, 50%, 70%, 95% and 100%, 10 min for each step. Subsequently, the tissue blocks were infiltrated using 1:1 ratio of propylene oxide and resin mixture containing (Araldite-502+DDSA+DMP-30) at room temperature overnight. Then, the specimens were transferred to pure Araldite-502 for at least 12 hr at room temperature and incubated at 60°C for 48 hr. Thin sections were cut and collected on formvar-coated 300-mesh copper grids. Then, ultrathin sections were stained with uranyl acetate and lead citrate for 30 min each. Finally, ultrastructural characteristics of *P. fastosum* was checked using TEM (JEOL JEM, 2100, Japan), operating at 80 kV.

### 3. Results

#### 3.1 Morphology of *P. fastosum* adult worm from macroscopic examination

By necropsy, several adults *P. fastosum* worms were dissected from the biliary tracts and a gallbladder of a naturally infected cat carcass and placed inside a sterile normal saline-containing 60 mm-Petri Dish. The natural color of this worm was reddish brown and the size is very small (Fig. 9A). Based on a ruler placed underneath the Petri Dish, the size of this selected worm was 4.5 mm in length and 1.5 mm in width. The uterus filled with eggs were remarkably present in dark brown color from around the beginning of the two third of the worm's body extending downwards to the terminal end (Fig. 9B).

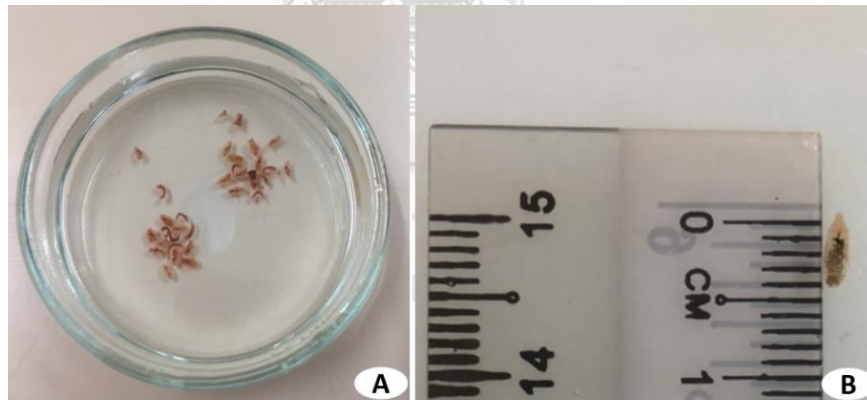


*Figure 9.* Morphology of *P. fastosum* freshly isolated from necropsy of a fresh cat carcass.

(A) *P. fastosum* adult flukes dissected from a cat's liver and placed inside a sterile normal saline-containing 60 mm Petri Dish. (B) The size measurement of *P. fastosum* showed the estimated size of this fluke about 4 mm in length and its color was reddish-brown.

### 3.2 Morphology of *P. fastosum* adult worm from microscopic examination

With the higher magnification of *P. fastosum* adult observed under the stereomicroscope, the shape of this fluke was lanceolate (Fig. 10). All the worm's internal organs were clearly visible regardless of making the worm more flatten for the carmine staining process (Fig. 10A). Unstained *P. fastosum* was translucent whereas better contrast of certain organs, testes, ovary and vitelline glands of this worm were clearly demonstrated by carmine staining (Fig. 10B). The bilateral intestinal caeca extending to the terminal end and vitelline ducts were present in unstained worm whereas they were not present in this carmine-stained worm. These two selected worms had the size of 4.4 mm in length and 1.2 mm in width. The whole body was flat, spineless, and elongated with two prominent suckers, oral and ventral. The anterior end was slightly rounded with the part of oral sucker and tapered posterior end. Both oral and ventral suckers were circular in shape. The beginning of cirrus sac occurred nearby bifurcation of intestinal caeca. Similar sizes of two lobular testes were arranged in tandem position and located in the anterior half of the worm. Below the testes, an oval-shaped ovary was located just to the right of the median vertical axis of the worm. The dark coiled uterus filled with several hundred dark brown eggs appeared to start from the cirrus sac area and pass through the same alignment of the middle of ventral sucker then occupied from two third of the body toward the terminal end. Additionally, numerous vitelline follicles are formed into glands on both sides at the middle region of the body (Fig. 10).

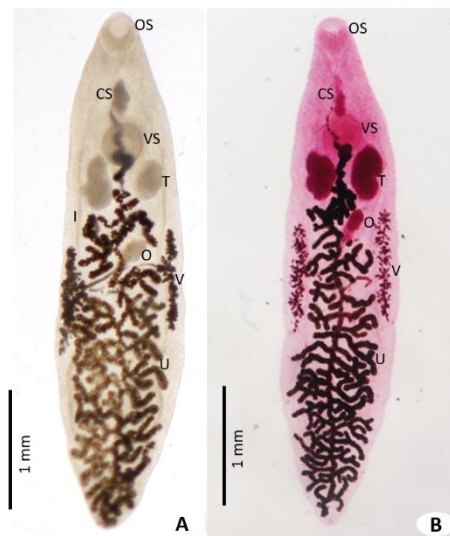


Figure 10. Adult *P. fastosum* observed under the stereomicroscope.

(A) Fresh and unstained *P. fastosum* adult fluke had a translucent leaf-like shape. (B) Carmine staining of adult fluke revealed a different contrast and clear visibility of certain organs. Note: oral sucker (OS), cirrus sac (CS), ventral sucker (VS), two testes in tandem (T), intestinal caeca (I), ovary (O), vitelline gland (V) and uterus filled with eggs (U).

### 3.3 Ultrastructural characteristics of *P. fastosum* adult examined by scanning electron microscopy (SEM)

#### 3.3.1 Whole ventral body

To compare the morphology of *P. fastosum* whole ventral body collected from the different stages of carcasses, 3 *P. fastosum* adult flukes were collected from 3 different naturally infected cats by necropsy. The worm in Fig. 3A and 3B were not freshly collected from cat carcasses as the carcasses were kept at 4°C for 2 days and 3 days, respectively, prior to the necropsy days and followed by worm fixation. From the scanning electron micrograph, the body of both worms was relaxed with protruded cirrus from the midway between oral sucker and ventral sucker (Fig. 11A and 11B). In contrast, the worm isolated from a recently dead cat and immediately fixed with 2.5% glutaraldehyde seemed to be slightly contracted without protruded

cirrus (Fig. 11C). The general morphology of all these 3 flukes was symmetrical leaf like and dorsoventrally flattened. The mean body size of these 3 worms (mean  $\pm$  SD) was  $4.1 \pm 0.21$  mm in length and  $1.2 \pm 0.14$  mm in width. The oral sucker was located subterminal position and the ventral sucker was located about one fourth of the body length from the anterior end. The size of oral sucker is smaller compared to that of ventral sucker. Opening of oral sucker faced anteroventrally whereas that of ventral sucker faced ventrally. For this freshly preserved fluke (Fig. 11C), the common genital pore without protruded cirrus was located at the middle region between oral and ventral suckers. When the body length of this worm was arbitrarily divided into three regions, anterior, middle, and posterior, the widest part of the body was located around the end of the two thirds of the body. Next to the widest part, the body was slightly tapering down to posterior end (Fig. 11C).

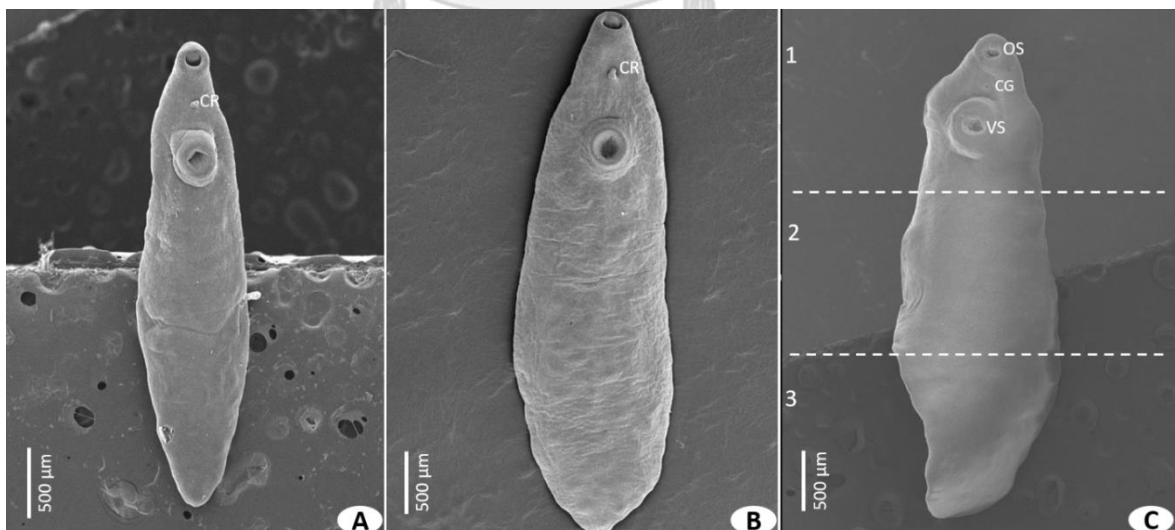


*Figure 11.* SEM micrographs of the whole ventral body of 3 *P. fastosum* adult flukes collected from 3 different infected cats by necropsy.

(A and B) Before fixation, both adult worms were not freshly collected from cat carcasses as the carcasses were kept at 4°C for 2 days and 3 days, respectively, before the necropsy days. The cirrus (CR) of both worms were protruded from the midway between oral sucker (OS) and ventral sucker (VS). (C) The worm was isolated from a recently dead cat and immediately fixed with 2.5% glutaraldehyde at 4°C. The common genital pore (CG) was seen without protruded cirrus. When the body length of this worm was arbitrarily divided into 3 regions: anterior, 1; middle, 2, and posterior, 3, the widest part of the body was located around two thirds of the body. Note for the image magnification: A, 35x; B and C, 30x.

### 3.3.2 Oral sucker and associated papillae

From the worm in Fig. 11C, detailed structures were further demonstrated with higher magnification (Fig. 12). The oral sucker of this *P. fastosum* adult fluke was slightly ellipsoidal in shape. The dimension of oral sucker opening was 125 µm in horizontal diameter and 75 µm in vertical diameter (Figure. 12A). When the apical area of the oral sucker was further enhanced, a number of papillae and pores of gland cells were presented. The tegument at the apical region of oral sucker shows wrinkle surface. The papillae were scattered on apical region and perimeter of oral sucker's aperture. In some area between each papilla, pores of gland cells are clustered (Fig. 12B). For the perimeter of the oral sucker's aperture, concentric arrangement of papillae with 8 papillae on each side was somewhat symmetrically demonstrated. From the lining of these papillae, the corrugated folds and grooves were radially arranged towards the center of the oral sucker opening. These corrugations structurally made the oral sucker discrete from the body tegument. Inside the concave side of oral sucker, a pair of papillae was located on the roof of both sides (Figure. 12C). On the oral sucker, at least 3 types of papillae were

demonstrated composed of a plate papilla, a button papilla and a dome papilla. The plate papilla was flat and associated with cross-linking folds. The size of a plate papilla was  $>5\ \mu\text{m}$  in diameter (Fig. 12D). The button papilla was constructed from extensive binding of tegument folds and immersed their lining inside the tegument depression. The diameter of a button papilla was  $>5\ \mu\text{m}$  (Fig. 12E). The domed papilla protruded from the surface and surrounded by tegumental folds with a diameter of  $<10\ \mu\text{m}$  (Fig. 12F).



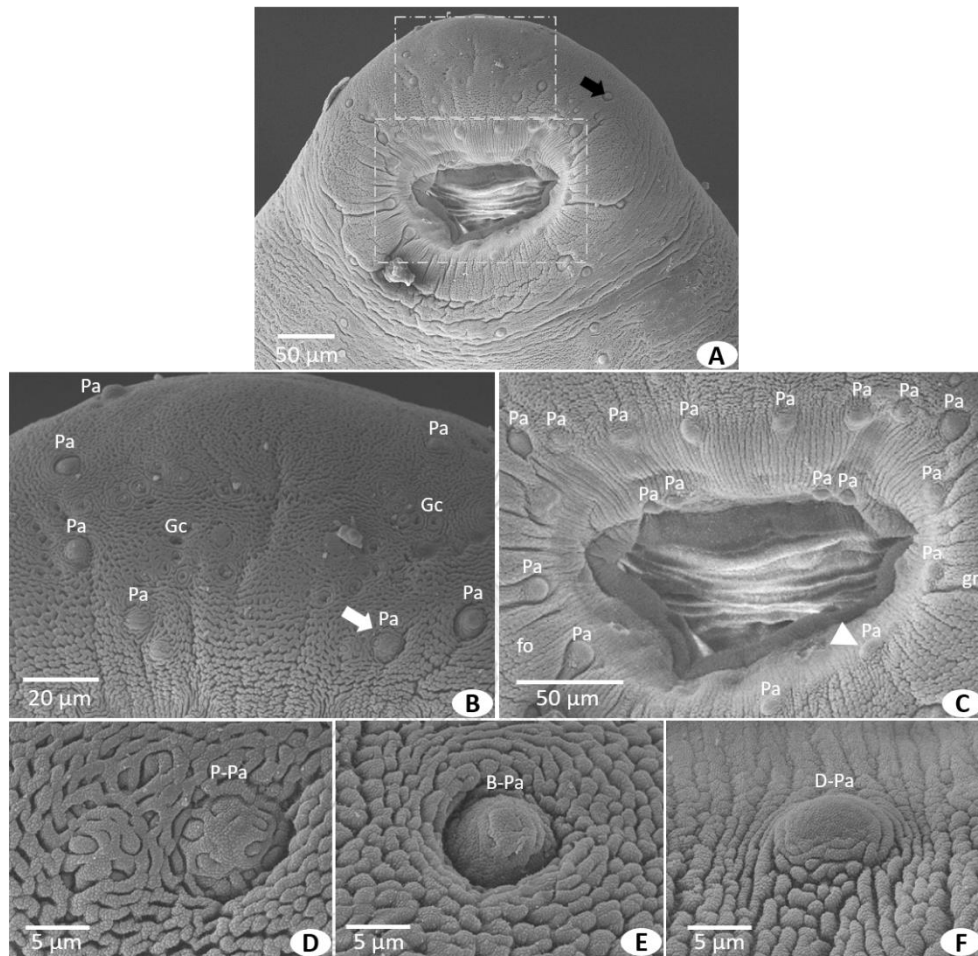


Figure 12. SEM micrographs of *P. fastosum* adult fluke's oral sucker and associated papillae.

(A) The apical and central areas of the oral sucker were shown and further enhanced in (B) and (C), respectively. (B) On the apical surface of the oral sucker, a number of papillae (Pa) and pores of gland cells (Gc) were presented. (C) A number of papillae (Pa) and an example of fold (fo) and groove (gr) were presented in radial arrangement on the perimeter of the oral sucker's aperture. (D-F) At least 3 types of papilla were demonstrated composed of a plate papilla (P-Pa), a button papilla (B-Pa) and a dome papilla (D-Pa) in which the papillae indicated with a white arrow, a black arrow, and a white arrowhead in Fig. 4B, Fig. 4A, and Fig. 4C were respectively enhanced. Note for the image magnification: A, 300x; B, 800x; C, 566x (digital zoom); D-F, 5,000x.



### 3.3.3 Ventral sucker and associated papillae

The surrounding tegument surface of ventral sucker seemed to be protruded with large corrugating structures. A number of papillae were systematically dispersed on both outer and inner rims of the ventral sucker. On the outer rim, 6 papillae were arranged in hexagonal shape as shown by a connecting imaginary broken line with radially arranged folds and grooves. The aperture of this ventral sucker was about 175  $\mu\text{m}$  in horizontal diameter and about 100  $\mu\text{m}$  in vertical diameter (Fig. 13A). Interestingly, another worm collected from the same cat carcass, happened to have a naturally everted ventral sucker making the original internal hollow structure of the concavity become exposed as a smooth dome shape decorated with papillae at its base and its surface. The similar hexagonal arrangement of papillae located on the outer rim of the ventral sucker were also found (Fig. 13B). At the 430x magnification to enhance the square inset in Fig. 13A, circular arrangement of 10 papillae on the inner rim of the ventral sucker was shown (Fig. 13C). At 5,000x magnification to enhance the papillae on outer and inner rim of ventral sucker indicated in Fig. 13A with a white arrow and a black arrow, respectively, the domed papillae on the outer rim seemed to have a couple of crossing folds on the surface with incomplete tegument depression at their base of papilla (Fig. 13D), whereas a dome-shaped papilla on the inner rim had a smooth surface (Fig. 13E). The size of these papillae were similar about 10  $\mu\text{m}$  in diameter.

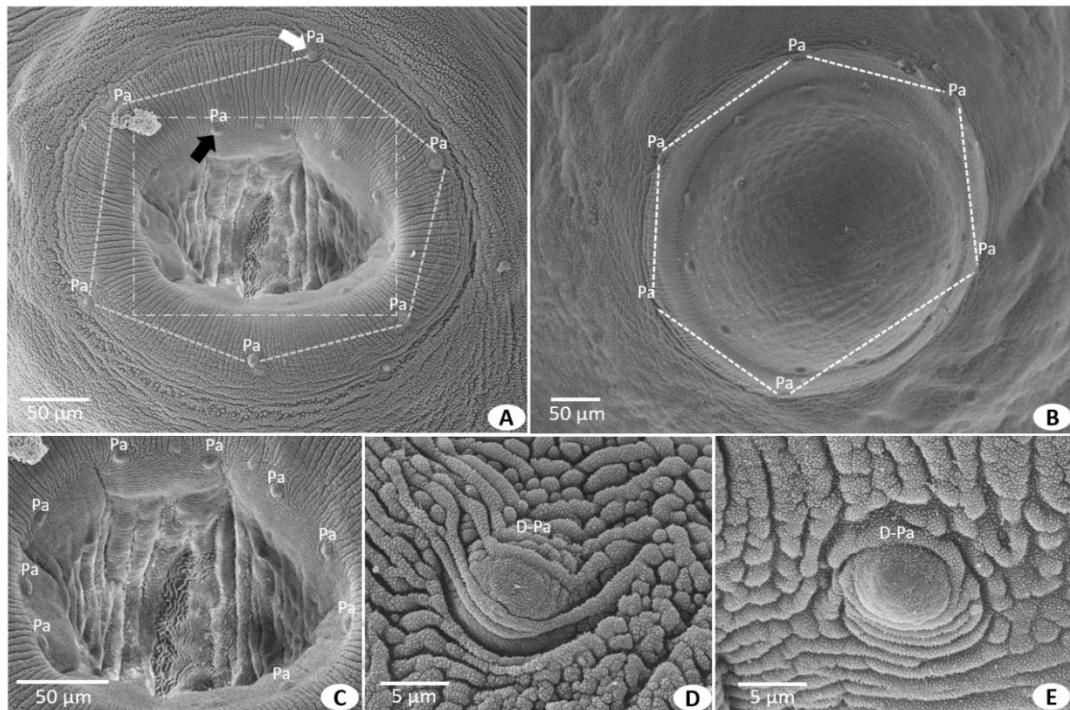


*Figure 13.* SEM micrographs of *P. fastosum* adult fluke's ventral sucker and associated papillae. (A) On the outer rim of the ventral sucker, 6 papillae (Pa) were arranged in hexagonal shape as shown by a connecting broken line. (B) The ventral sucker of another worm, collected from the same cat carcass, happened to be naturally everted making the original internal hollow structure of the concavity become exposed as a smooth dome shape decorated with papillae at its base and its surface. The similar hexagonal arrangement of papillae (Pa) located on the outer rim of the ventral sucker were also shown through a connecting broken line. (C) As the square inset in Fig. 5A was enhanced, circular arrangement of papillae on the inner rim of the ventral sucker was shown. (D and E) From a white arrow and a black arrow indicated in Fig. 5A, dome-shaped papillae (D-Pa) were shown. Note for the image magnification: A, 300x; B, 250x; C, 430x (digital zoom); D and E, 5,000x.

### 3.3.4 Cirrus

Enhanced the mid area between the oral and ventral suckers, cirrus collected from 2 different cat carcasses were demonstrated. From the same worm presented in Fig. 11A, retrieved from a partially autolyzed carcass kept at 4°C for 2 days before necropsy followed by fixation of the worm, the surface of this protruded

cirrus revealed an annularly folded structure (Fig. 14A) whereas the cirrus of the worm isolated from a recently dead cat carcass followed by immediate preservation had a reverse funnel shape with a wrinkle surface (Fig. 14B).

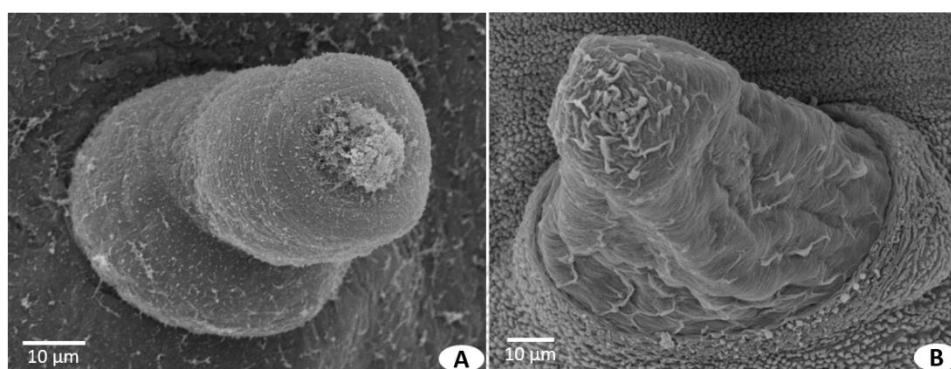


*Figure 14.* SEM micrographs of *P. fastosum* adult fluke's cirrus, a male reproductive organ, collected from 2 different cat carcasses.

(A) From the same worm presented in Fig. 3A, retrieved from a partially autolyzed carcass kept at 4°C for 2 days before necropsy followed by fixation of the worm, the surface of this protruded cirrus revealed an annularly folded structure. (B) From the worm isolated from a recently dead cat carcass followed by immediate preservation, a reverse funnel shape with a wrinkle surface of this cirrus was shown. Note for the image magnification: A, 1,600x and B, 1,200x.

### 3.3.5 Anteroventral region of the worm and associated papillae

To demonstrate the tegument and associated papillae in the areas below the oral and ventral suckers, 2 square inset images were further enhanced (Fig. 15A). Below the oral sucker towards the upper area of the ventral sucker, papillae were bilaterally lined up in a vertical row (Fig. 15B). The tegumental surface below a ventral sucker was decorated with the same type of papillae sparsely scattered (Fig. 15C). The papillae found in both regions seem to be similar in shape. From the 2 representative papillae below the ventral sucker area indicated with white arrows in

Fig. 15C, these papillae were embedded among tightly dense columnar tegumental projection (Fig. 15D). From the square inset image in Fig. 15D, a rosette papilla was classified based on cauliflower-like with a series of tightly packed tegumental projections and outgrowth of the surface. The size of this rosette papilla was  $<5\mu\text{m}$  in diameter (Fig. 15E).



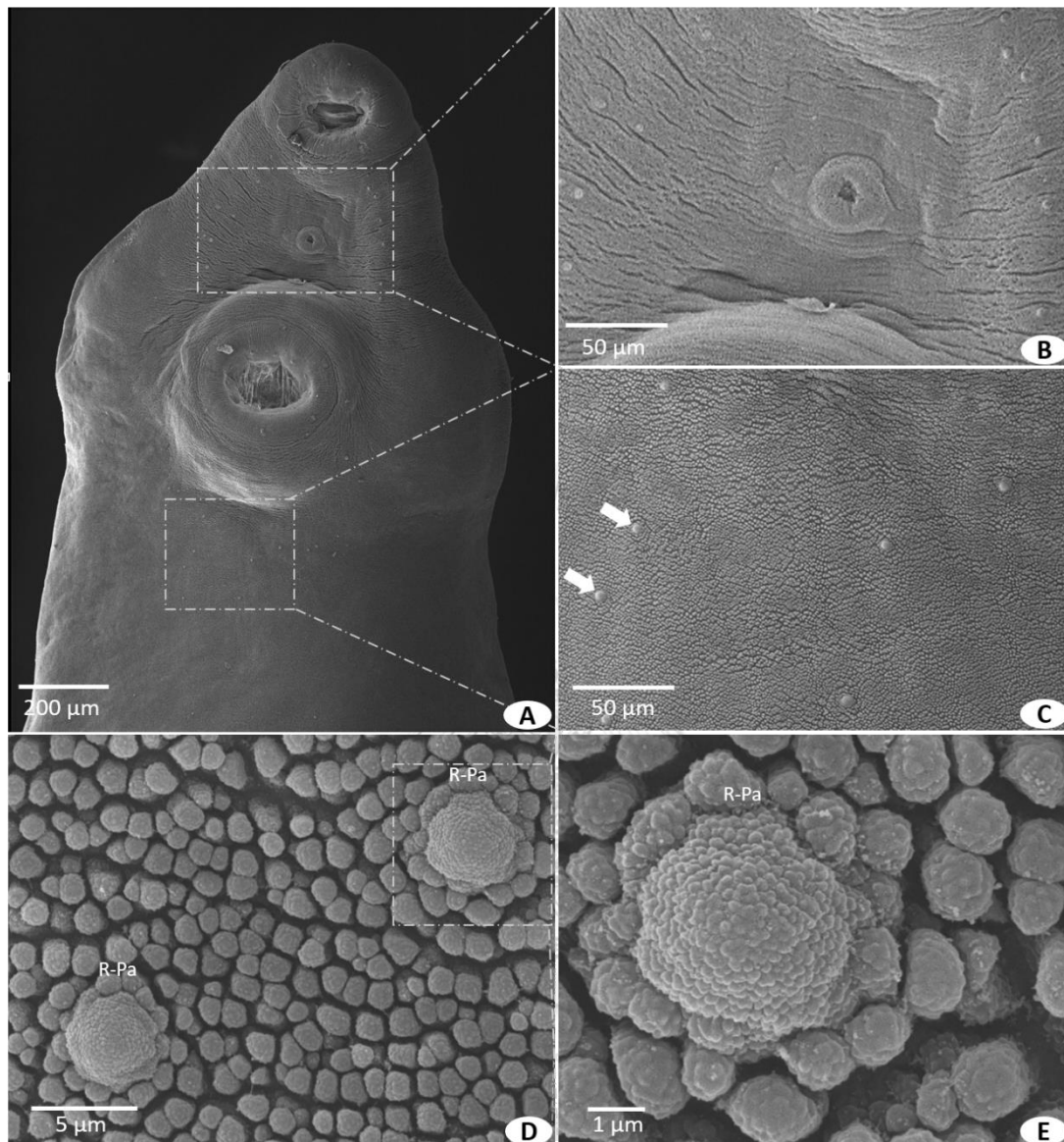


*Figure 15.* SEM micrographs of *P. fastosum* adult fluke's anteroventral region and associated papillae.

(A) Two square inset images of the tegument area between the oral and ventral suckers and the area below ventral sucker were further enhanced in (B) and (C), respectively. (B) Below the oral sucker towards the upper area of the ventral sucker, a row of papillae was arranged in a linear pattern on both sides. (C) The tegumental surface below a ventral sucker was decorated with the same type of papillae sparsely scattered. (D) Two representative papillae indicated with white arrows in (C) were further enhanced. These papillae were embedded among tightly dense columnar tegumental projection. (E) From the square inset image in (D), a rosette papilla (R-Pa)

was classified based on cauliflower-like and outgrowth of the surface. Note for the magnification: A, 80x; B, 376x (digital zoom); C, 500x; D, 5,000x; E, 10,000x.

### 3.3.6 Ventral and dorsal tegument of the adult worm

Based on 3 randomly selected ventral tegument as shown in inset images (Fig. 16A), the topographical arrangement of anteroventral region was covered with the different height of slender villous-like projections that were densely packed (Fig. 16B). For the middle part of the ventral body, a lattice of irregular size of knob-like projection surrounded by shallow furrows made the tegumental surface look knobby (Fig. 16C). For the posteroventral part, the short finger-like projections were consistent in size and were densely packed thus the bottom of the furrow was not able to be seen (Fig. 16D). For the tegument of the dorsal side, 3 inset images were randomly selected for examination of the anterior, middle, and posterior regions (Fig. 16E). For the anterodorsal region, villous-like projections of tegument were formed as transverse bundle or fold alternating with horizontal groove (Fig. 16F). At the middle part of the dorsal tegument, a lattice of irregular size of lumps incorporated with shallow furrows made the surface look lumpy (Fig. 16G). For the posterodorsal part, the short finger-like projections were consistent in size and were densely packed thus the bottom of the furrow was not able to be seen (Fig. 16H).

### 3.3.7 Dorso-apical and posterior terminal end of the adult worm

Dorso-apical region showed a few numbers of papillae scattered as a single or in group (Fig. 16I). For this single papilla (arrowhead indicated in I), dome-shaped papilla was presented (Fig. 16J). Indentation at the posterior terminal end was shown

(Fig. 16K). Enhanced of this area, excretory pore (Ep) exhibiting a hole-like structure was clearly present (Fig. 16L).

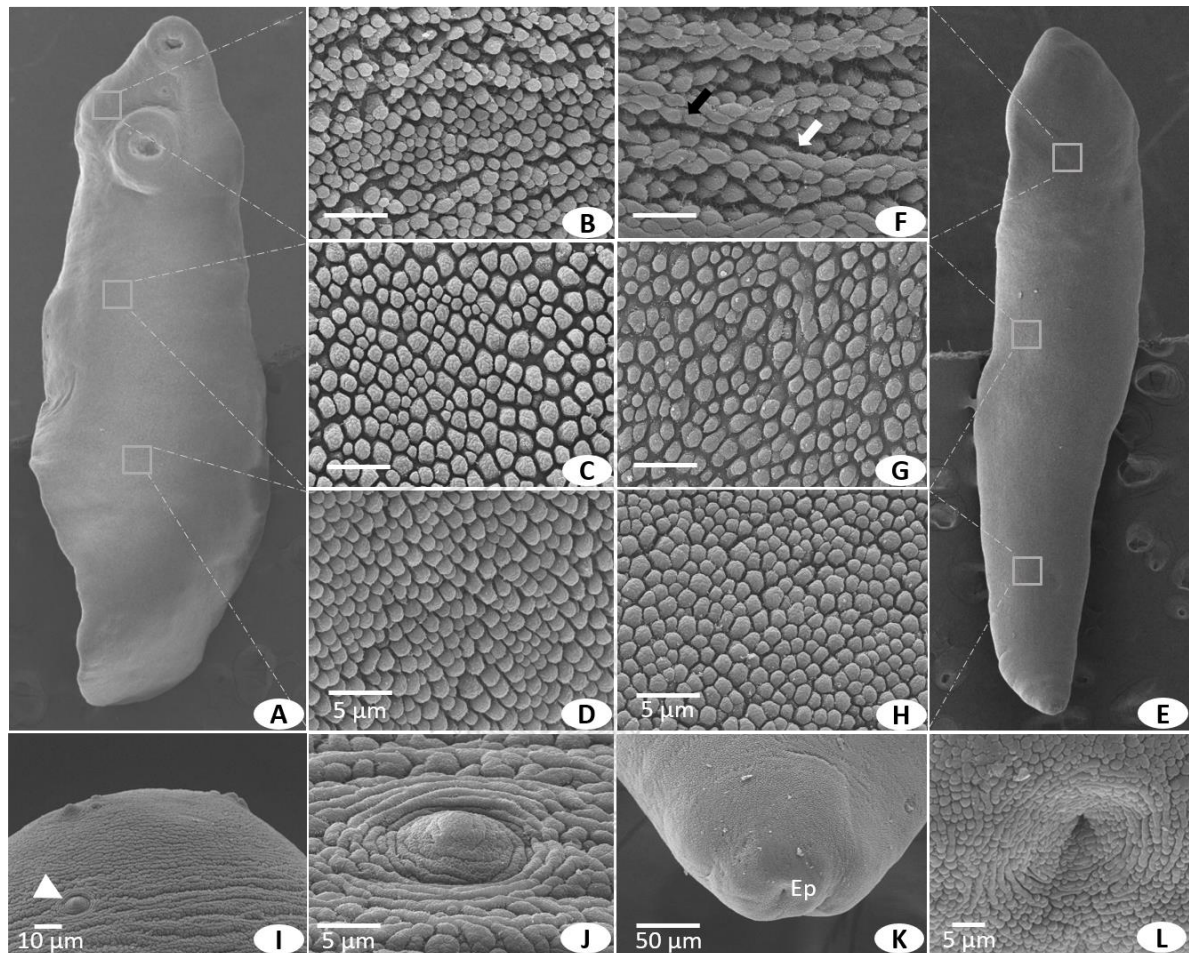


Figure 16. SEM micrographs of *P. fastosum* adult fluke's ventral and dorsal tegument as well as dorso-apical and posterior terminal end.

(A) For the ventral side, the tegument of the anterior, middle, and posterior regions was randomly selected to be enhanced as indicated inset images. (B) For the tegument of anteroventral region, the different height of slender villous-like projection was found densely packed. (C) A lattice of irregular size of knobs surrounded by shallow furrows made the tegumental surface of the middle part of the ventral body knobby. (D) For the posteroventral part, the short finger-like projections with consistent villous size were densely packed without discernible bottom of furrow. (E) For the dorsal side, the anterior, middle, and posterior regions of the tegument were randomly selected as indicated inset images. (F) For the anterodorsal region, villous-like projections of tegument were formed as transverse bundles or folds (black arrow) alternating with horizontal grooves (white arrow). (G) At the middle part of the dorsal tegument, a



lattice of irregular size of lumps incorporated with shallow furrows made the surface lumpy. (H) For the posterodorsal part, the short finger-like projections with consistent villous size were densely packed without discernible bottom of furrow. (I) Dorso-apical region showed a few numbers of papillae scattered as a single or in group. (J) For this single papilla (arrowhead indicated in I), dome-shaped papilla was presented. (K) Indentation at the posterior terminal end was shown. (L) Enhanced of (K), excretory pore (Ep) exhibiting a hole-like structure was clearly present. Note for the magnification: A and E, 30x; B-D, F-G, 5000x; I, 1000x; J, 5000x; K, 500x and L, 3000x.

#### 3.4 Morphology of the bile-derived *P. fastosum* fluke eggs from microscopic examination

To observe the morphology of *P. fastosum* eggs from the original source where the worms shed and deposit the eggs into a gall bladder, PUC was performed to collect the bile from *P. fastosum*-infected cats followed by wet bile mount. Under a light microscope at 40x magnification, the natural dark brown color of *P. fastosum* eggs was clearly discernible without staining (Fig. 17A). At 100x magnification, a varied size of *P. fastosum* eggs was presented (Fig. 17B). Before submission of bile-derived *P. fastosum* egg for scanning electron microscopy (shown in Fig. 19), sampling of eggs post sample preparation by washing and fixing in 2% glutaraldehyde revealed different sizes and color shades of eggs trapped with bile debris in the background (Fig. 17C). Typical and atypical morphology of *P. fastosum* eggs were found. Observed at 400x magnification, this *P. fastosum* egg was operculated, brown, and elliptical in shape containing well-developed ciliated miracidium in which 2 clusters of germ balls were located on its posterior. Its size was 44  $\mu\text{m}$  in length and 32  $\mu\text{m}$  in width. An abopercular knob was present on the thick shell opposite to the



operculum (Fig. 17D). Apart from the typical form in which most of the structures were clearly visible, *P. fastosum* egg morphology with a long elliptical shape containing undefined miracidium and possibly germ balls inside was demonstrated (Fig. 17E). In Fig. 17F, the typical form of *P. fastosum* eggs happened to be next to another form for morphological comparison. The egg in the lower left corner was found to be smaller and lighter in color than did the typical egg. With a distinct operculum and thicker egg shell, this egg had large and scattered germ balls inside the undefined content. In addition to 3 different types of *P. fastosum* egg morphology commonly seen in bile from our study, atypical morphology of *P. fastosum* eggs derived from one cat were also found as smaller in size but with consistent brown color (Fig. 17G-I). Three eggs were subspherical embryonated with one egg having an extended large lobe (Fig. 17G). For the egg in the lower part of this figure compared to the upper one consistent to the morphology found in Fig. 17F, this egg was asymmetrically oval, small with inconsistent thickness of shell and without discernible content (Fig. 17H). Interestingly, there was an embryonated egg with morphology similar to conjoined twins with the atypical germ ball inside (Fig. 17I). Variable size differences of *P. fastosum* eggs selected for analysis were shown (Table. 8). As a result, the bile eggs can be classified into three groups: mature, immature and unfertilized eggs (Figure. 17D-17F).

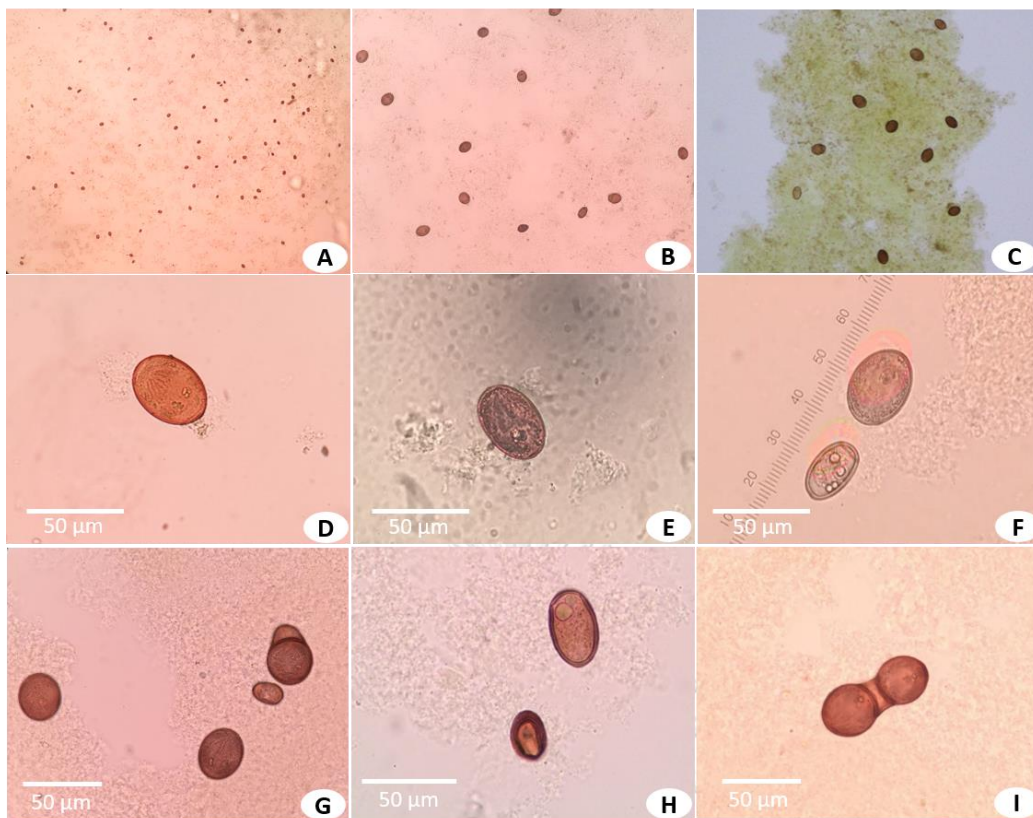


Figure 17. Morphology of *P. fastosum* eggs collected from bile samples of infected cats and microscopic examination.

(A) The natural dark brown color of *P. fastosum* eggs was discernible at low magnification, 40x. (B) At 100x magnification, a varied size of *P. fastosum* eggs was presented. (C) Before submission of bile-derived *P. fastosum* egg for scanning electron microscopy (shown in Fig. 11), sampling of eggs post sample preparation revealed different sizes and color of eggs trapped with bile debris in the background. (D) A mature *P. fastosum* egg was operculated, brown, and elliptical in shape containing well-developed miracidium in which 2 clusters of germ balls were located on its posterior. An abopercular knob was present on the thick shell opposite to the operculum. (E) A *P. fastosum* egg exhibited a long elliptical shape containing undefined miracidium and possibly germ balls inside. (F) A comparison of 2 *P. fastosum* eggs presenting the difference in size and shape. To compare with the mature egg on the top, another type of *P. fastosum* egg was found to be smaller and lighter in color than the mature egg. With a distinct operculum and thicker egg shell, this egg had large and scattered germ balls inside the undefined content. (G-I) Apart from *P. fastosum* egg morphology commonly seen in bile from our study, atypical morphology of *P. fastosum* eggs derived from one cat were also found as smaller in size but with consistent brown color. (G) Three of the eggs were subspherical embryonated with one egg having an extended large lobe. (H) For the lower egg compared to the upper one relevant to the morphology found

in (F), this egg was asymmetrically small oval with inconsistent thickness of shell but without discernible content. (I) Morphology similar to conjoined twins of embryonated eggs were found with the atypical germ ball inside. Note for the image magnification: A, 40x; B and C, 100x.

*Table 8.* Measurements of *P. fastosum* eggs with variable sizes (n = 68) in which these eggs were recovered from fecal and bile samples of 14 infected cats

	Mean ± SD (LxW) (µm)
<b>Typical mature (n = 24)</b> Dark brown and thick egg shell in elliptical shape, inconspicuous operculum at the anterior end, small knob in the posterior end, fully developed miracidium, bilateral 2 clusters of germ balls	44.2 ± 1.7 × 31.8 ± 2.2
<b>Atypical/immature (n = 21)</b> Dark brown and thick shell in long elliptical shape, unremarkable miracidium and germ balls	43.5 ± 2.0 × 27.1 ± 2.0
<b>Atypical/unfertilized eggs (n = 23)</b> lack of embryo and bubbles inside	35.3 ± 2.8 × 23.1 ± 2.4

### 3.5 Morphology of the cat feces-derived *P. fastosum* fluke eggs from microscopic examination

To observe the morphology of *P. fastosum* eggs isolated from infected cat fecal samples and to compare with the egg morphology found in bile, centrifugal sedimentation was performed followed by microscopic examination under a light microscope. At least 3 forms of *P. fastosum* egg were found. Similar to the *P. fastosum* eggs collected from bile sample, the first form was typical as embryonated with a well-developed miracidium, operculated, brown, and elliptical in shape. Two clusters of germ balls were located on its posterior. An abopercular knob was not evidently present and located opposite to the operculum (Fig. 18A). For the 2<sup>nd</sup> form, operculated and long elliptical in shape containing undefined and granular embryo and possibly germ balls inside egg was observed (Fig. 18B). For the 3<sup>rd</sup> form of *P.*

*fastosum* egg, they were smaller and lighter brown with a distinct operculum and thicker egg shell compared to the typical one. This type of egg had large and scattered germ balls inside the undefined internal content (Fig. 18C).

To show the comparative morphology of *P. fastosum* egg with other parasitic stages commonly found in cat feces, we demonstrated some selected fecal samples that happened to have other eggs beside the *P. fastosum* eggs. Partially sporulated *Cystoisospora felis* oocyst and *Ancylostoma* spp. egg were located next to the *P. fastosum* eggs (Fig. 18D and Fig. 18E, respectively). Importantly, we would like to point out the finding of *Trichuris* spp. egg that was also brown in color and similar in size with *P. fastosum*. However, its barrel shape and bipolar plugs were important characteristics to differentiate *Trichuris* spp. from *P. fastosum* (Fig. 18F).

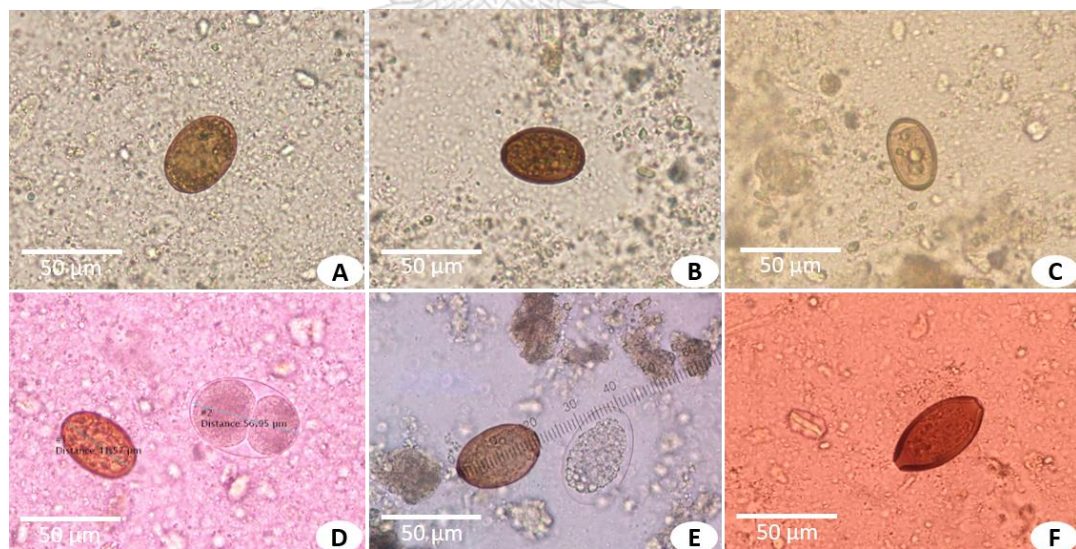


*Figure 18.* Morphology of *P. fastosum* eggs isolated from infected cat fecal samples by centrifugal sedimentation and examined under a light microscope.

(A) A mature *P. fastosum* egg was embryonated, operculated, brown, and elliptical in shape. Two clusters of germ balls were located on its posterior. An abopercular knob was slightly present opposite to the operculum. (B) A *P. fastosum* egg was operculated and long elliptical in shape

containing undefined and granular embryo and possibly germ balls inside. (C) For another form of *P. fastosum* egg, smaller and lighter brown color were found with a distinct operculum and thicker egg shell. This egg had large and scattered germ balls inside the undefined internal content. (D) A *P. fastosum* egg was shown beside partially sporulated *Cystoisospora felis* oocyst. (E) A *P. fastosum* fluke egg was shown next to *Ancylostoma* spp. egg. (F) *Trichuris* spp. egg was also brown in color and similar in size with *P. fastosum* but its barrel shape and bipolar plugs were important characteristics to differentiate *Trichuris* spp. from *P. fastosum*.

### 3.6 Ultrastructural characteristics of bile-derived *P. fastosum* eggs using SEM

To observe the ultrastructural features *P. fastosum* egg's surface, a bile sample of an infected cat, the same sample as shown by microscopic examination in Fig 17C, was directly taken from a gall bladder by PUC. Based on selected SEM micrographs of *P. fastosum* eggs retrieved from bile, the sizes of *P. fastosum* fluke eggs were slightly variable. In Fig. 19A, this egg had an oval shape with the size 37.5  $\mu\text{m}$  in length and 26.2  $\mu\text{m}$  in width. The egg shell surface was smooth with inconspicuous operculum at the anterior end. At 6,000x magnification of the same egg, smooth surfaces of the operculum and egg shell were clearly demonstrated but the shoulder rim was not prominent (Fig. 19B). To demonstrate the posterior end of *P. fastosum* egg, an accidentally shell-broken egg was selected to reveal the operculum, shoulder rim and irregular surface of abopercular knob at the terminal end (Fig. 19C). After image enhancing, the surface of the egg shell in the terminal region was confirmed to be smooth and the knob was still not very distinct (Fig. 19D). For this smaller size of *P. fastosum* egg, 35  $\mu\text{m}$  in length and 25  $\mu\text{m}$  in width,

unremarkable operculum, shoulder rim, and abopercular knob was present (Fig. 19E). An enhanced image of an abopercular knob revealed an irregular and slightly pointy surface at the posterior end (Fig. 19F). From the top view of another *P. fastosum* egg, the shape of the operculum was elliptical in shape (Fig. 19G). In Fig. 19H, the lateral view of this *P. fastosum* egg showed an elongated shape similar to a capsule with an inconspicuous shoulder rim located very close to the apical end. On the surface of this egg, a grape-like cluster of cocci bacteria was found relevant to cholangitis status of this cat based on a culture result.

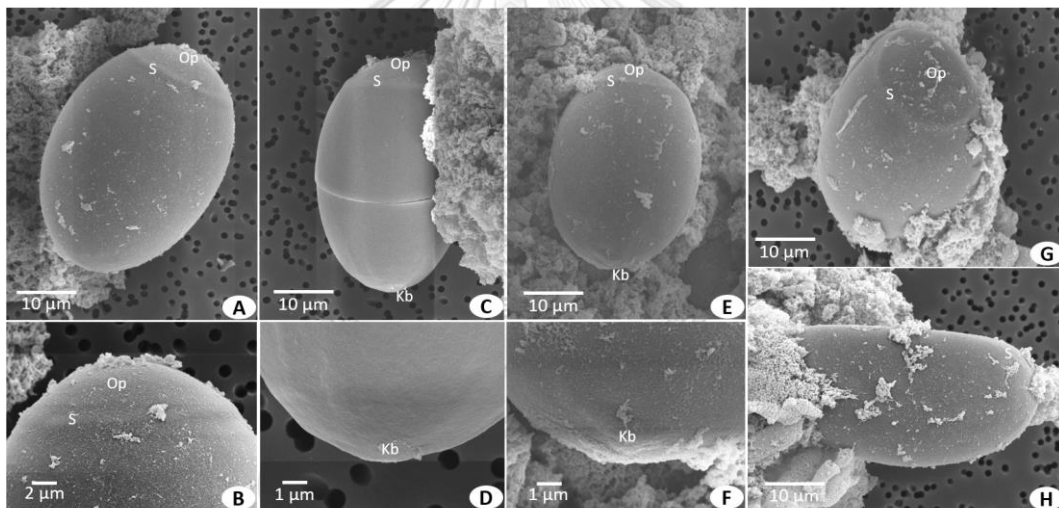


*Figure 19.* SEM micrographs of *P. fastosum* eggs collected from bile samples of infected cats.

This sample was the same sample as shown in Fig 9C for microscopic examination.

(A) Operculum (Op) at the anterior end with lining of shoulder rim (S) were shown from this tilted orientation of *P. fastosum* egg. (B) Smooth surfaces of the operculum (Op) and egg shell were clearly demonstrated but the shoulder rim (S) was not prominent. (C) With an accidentally broken shell, this *P. fastosum* egg revealed operculum (Op), shoulder rim (S) and the irregular surface of abopercular knob (Kb) at the terminal end. (D) The surface of the egg shell in the terminal region was smooth and the knob (Kb) was not very distinct. (E) Another *P. fastosum* egg with visible operculum (Op), shoulder rim (S), and abopercular knob (Kb). (F) An enhanced image of an abopercular knob revealed an irregular and slightly pointy surface of the posterior end. (G)

From the top view of the *P. fastosum* egg, the shape of the shoulder rim (S) bordering operculum (Op) was elliptical. (H) The lateral view of this *P. fastosum* egg showed a capsule shape with shoulder rim (S) located very close to the apical end. On the surface of this egg, a grape-like cluster of cocci bacteria was found due to cholangitis. Note for the image magnification: Top row (A, C, E, G) and H, 2,500x; Bottom row (B, 6,000x; D and F, 10,000x).

### 3.7 Tegument of *P. fastosum* adult worm by H&E-stained histological examination

To reveal the tegument surface and partial internal structures *P. fastosum* adult worms, the formalin-fixed paraffin-embedded adult parasites were prepared and the cross sections were stained with H&E (Fig. 20A). After observing the tissue at the apical part at 1,000x magnification, a thin layer of tegument syncytium without spine was revealed. Tegumental cell are situated deep inside parenchyma area which was not clearly seen. Underneath the reticular lamina layer, parenchyma cells were found in the internal region of the fluke which were connected by loose connective tissues (Fig. 20B). At 1,000x magnification, vitelline glands (V) were composed of lobulated vitelline cells (Fig. 20C). (D) The egg shell of *P. fastosum* was thick, brown and operculated. Inside the egg, a miracidium was visible with 2 clusters of germ balls located in the posterior end (Fig. 20D). A cross section of the worm uterus showed a number of fluke eggs inside (Fig. 20E). With enhancement of this image inset, amorphous shape of fluke eggs was present with thick and brown eggshell. Based on our finding, thick brown eggshell nature of *P. fastosum* has been investigated similar morphology from bile and fecal microscopic examination as above mentioned (Figure. 20E and 20F).



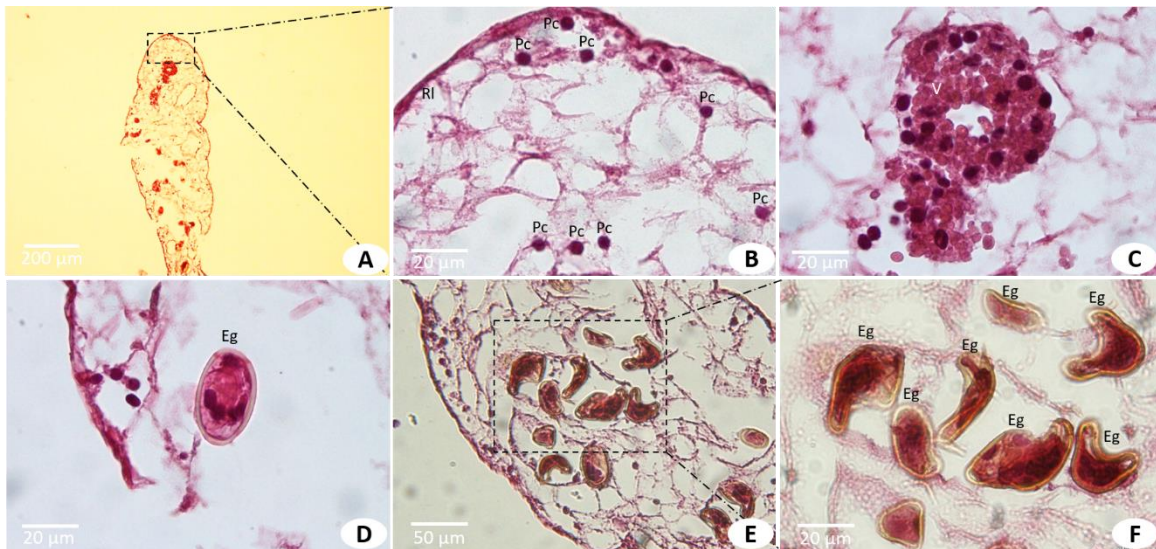


Figure 20. Histological examination of *P. fastosum* adult worm.

(A) Cross section of *P. fastosum* adult was further enhanced in Fig. B, C and D. (B) At 1,000x magnification of the top of the piece in A, a thin layer of tegument syncytium was revealed. Underneath the reticular lamina layer (RI), parenchyma cells (PC) were found in the interior region of the fluke which were connected by loose connective tissues. (C) At 1,000x magnification, vitelline glands (V) were composed of lobulated vitelline cells. (D) For this *P. fastosum* egg (Eg) in upside down orientation, the operculated shell is brown and thick containing miracidium with dark stained 2 clusters of germ balls. (E) Cross section of uterus showed a number of fluke eggs, which were enhanced in (Fig. 20F) revealed similar morphology of fluke eggs (Eg) from microscopic examination with thick brown eggshell. Note: H&E staining.

### 3.8 Ultrastructural characteristics of *P. fastosum* adult worm using TEM

#### 3.8.1 Tegument layers

To observe the ultrastructural characteristics of *P. fastosum* adult worm's tegument, samples were fixed, sectioned and processed for TEM. Based on TEM micrographs across the tegument depth, we divided the tegument of *P. fastosum* into 3 regions composed of tegument syncytium, basal lamina and muscle layer (Fig. 21A). For the tegument syncytium, we further sub-divided it into 3 layers according to components and density of each organelle including apical outermost layer,



tegument cytoplasm and above basal lamina. For the apical outermost layer, it contained villous-like tegumental projections in which their various lengths were alternately separated by tegument indentation. The exterior tegument surface was covered by outer membrane with glycocalyx and devoid of spines (Fig. 21B). Next to the apical outermost layer, the tegument cytoplasm contained tegumental granules, mitochondria, and frequently distributed lysosomes as well as microtrabeculae connecting with the surface syncytium. For tegumental granules, there were 2 types, TG<sub>1</sub> and TG<sub>2</sub>. TG<sub>1</sub> was spherical tegumental granules pertaining electron lucent matrix whereas TG<sub>2</sub> was rod-shape tegumental granules having with electron dense matrix. Tegumental granules are densely packed nearby apical outermost membrane. The tegument cytoplasm appears to be widest area. Due to presence of microtrabeculae, it supports to connect internally to the tegumental cells (Figure 21C).

The third layer lies on basal and reticular laminae. Underneath the tegument syncytium, the areas of basal lamina, reticular laminae, muscle layer and subtegumental layer within tegument cytoplasmic process were enhanced (Fig. 21D). This layer was composed of fibers and slightly stained particles and connected to the tegument syncytium by means of basal membrane infoldings. The basal lamina appeared to have a trilaminar membrane. Tightly packed filamentous structures were seen in this layer that were intertwined with whitish gel like substances. This whitish gel-like process connected to basal plasma membrane appears to fill continuously all the space between basal membrane infoldings. Underneath the

basal lamina, the reticular lamina was composed of fibers that make joining process between the tegument and underlying muscle layers. The lining of basal and reticular laminae was clear and exhibited a fine granular electron lucent matrix (Fig. 21D).

The basal and reticular laminae proceed with a narrow channel that run towards both outer and inner tegument. Under reticular laminae, there are two muscle layers of circular and longitudinal, that ran parallel with reticular laminae crossing tegument cell process.

The subtegumental layer comprised interstitial fibrous connective tissues. This layer contained limited number of secretory granules and trabeculae like structures. The secretory granules and trabeculae are passing across in the granular cytoplasm. Within subtegumental layer, outer circular and inner longitudinal muscle fibers are pass through within tegument cytoplasmic process (Fig. 21D).

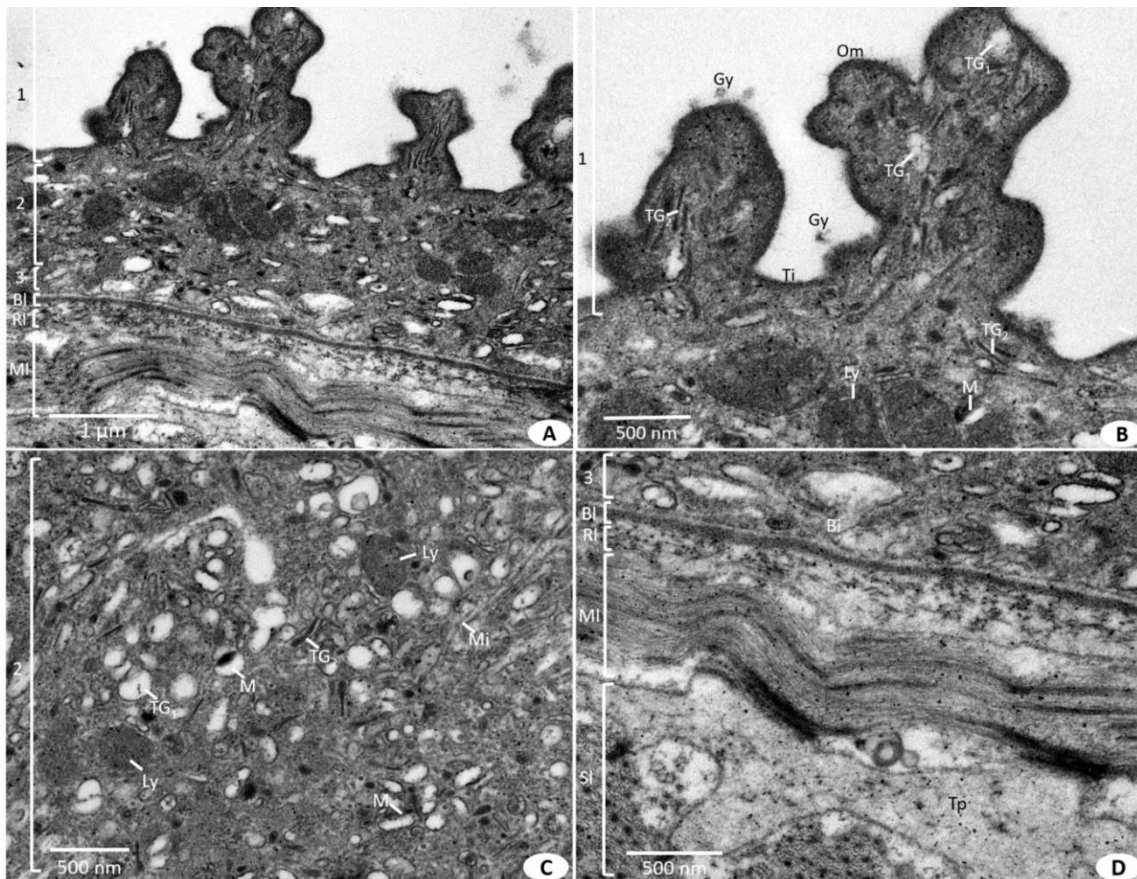


Figure 21. TEM micrographs of *P. fastosum* adult fluke's tegument.

(A) Tegument of *P. fastosum* can be divided into 3 regions across tegument depth; 1, apical outermost layer; 2, tegument cytoplasm; 3, the third layer with basal membrane infoldings. After the third layer, basal lamina layer (BL) is found followed by reticular laminae (RL). Underneath the reticular laminae is muscle layer (ML), followed by subtegumental layer. (B) Apical outermost layer is covered by outer membrane (Om) with cross section of glycocalyx (Gy). Tegument projections are separated by tegument indentation (Ti) were observed in this outermost layer. (C) The second layer is tegument cytoplasm which contained tegumental granules in which spherical tegumental granule with electron lucent matrix (TG<sub>1</sub>) and rod-shape tegumental granule with electron dense matrix (TG<sub>2</sub>), mitochondria (M), lysosomes (Ly) and microtrabeculae (Mi) to connect surface syncytium, whereas number of tegumental granules seem to be reduced in this layer. (D) The third layer lied on the basal lamina with numerous basal membrane infoldings (Bi) followed by reticular laminae (RL). Underneath the reticular laminae, the muscle layer (ML) is followed by subtegumental layer (SL) within tegument cytoplasmic process (Tp). Note for the magnification of each image: A, 25,000x; B, 51,600x; C, 33,536x and D, 41,735x.

### 3.8.2 Tegumental cells

From the TEM micrographs showing below the muscle layer of *P. fastosum*'s tegument, tegumental cell was present with basic cell structures including distinct nucleolus, nuclear envelope and cytoplasmic process (Fig. 22A). From the inset image, it was enhanced to show the components within the cytoplasm of tegumental cell. Both types of tegumental granules (TG<sub>1</sub> and TG<sub>2</sub>), secretory granules and Golgi bodies were demonstrated next to the nuclear envelope. Ribosomes, mitochondria and rough endoplasmic reticulum were also seen. Inside the nucleus, patches of heterochromatin and euchromatin were present (Fig. 22B). In addition, the tegumental cell processes seem to be packed up with microtubules, that are connected with tegument syncytium by passing through the basal lamina. Moreover, the tegumental cell membrane are connected to nearby parenchymal cells, nonetheless their junctions are not clearly observed (Figure 22A and 22B).

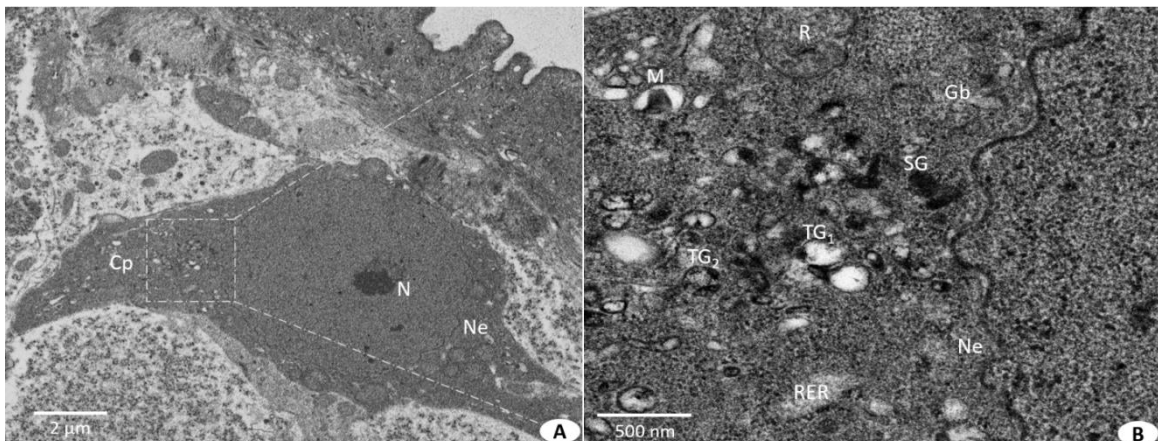


Figure 22. TEM micrographs of *P. fastosum* adult fluke's tegumental cell cross section.

(A) Under the muscle layer, tegumental cell showed distinct nucleolus (N), nuclear envelope (Ne) and cytoplasmic process (Cp). (B) From the inset image in (A) to enhance the cytoplasm of tegumental cell, both tegumental granules (TG<sub>1</sub> and TG<sub>2</sub>), secretory granules (SG) and Golgi bodies (Gb) were demonstrated next to the nuclear envelope (Ne). Ribosome (R), mitochondria (M) and rough endoplasmic reticulum (RER) were also present inside the cytoplasm of the tegumental cell. Note for the image magnification: A, 10,600x and B, 50,000x.

### 3.8.3 Sperms and ova

To observe the reproductive-related organelles and gametes, TEM micrographs of *Platynosomum fastosum* adult fluke's oviduct were analyzed. At the edges of Fig. 23A, 2 oocytes were located among several spermatozoa. A number of mitochondria were observed in this area of the oviduct. With the higher magnification, cross sections and possibly sagittal sections of the congregation of several spermatozoa (Sp) showed distinctive sperm heads and sperm tails associated with microtubules. Tail of each spermatozoon showed the presence of microtubules however the pattern of microtubules could not clearly identify. After syngamy, the section of microtubules can be seen at the peripheral area of fertilized ovum. (Fig. 23B).

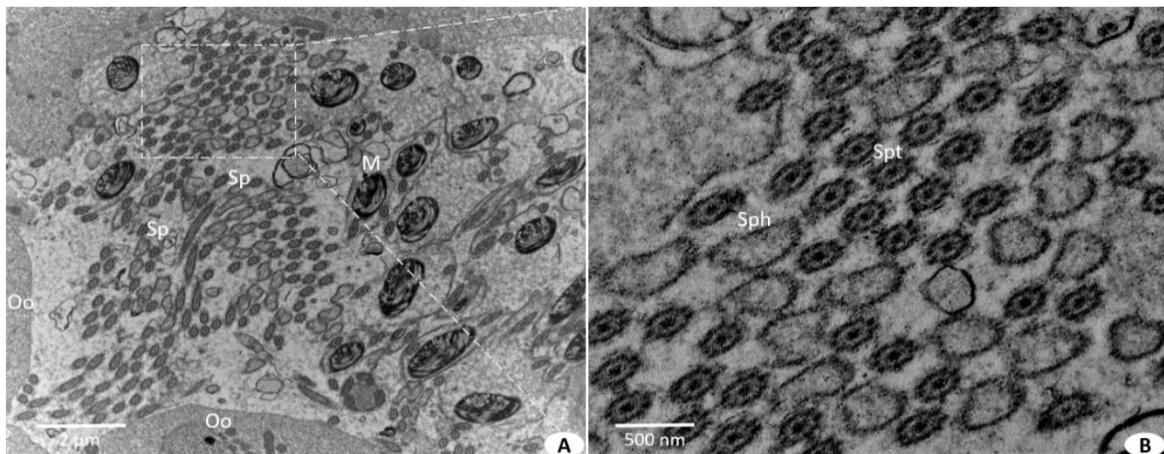


Figure 23. TEM micrographs of *P. fastosum* adult fluke's oviduct.

(A) Two oocytes (Oo) were surrounded by spermatozoa (Sp). A number of mitochondria (M) were observed inside the oviduct. (B) With the higher magnification, a cross section of the congregation of several spermatozoa (Sp) showed distinct sperm heads (Sph) and sperm tails (Spt) associated with microtubules. Note for the magnification of each image: A, 10,000x; B, 35,000x.

#### 4. Discussion

In this study, we have investigated morphology of *P. fastosum* adult fluke and eggs by gross examination and using different combined microscopic techniques. By naked eyes, the size of this parasite was small and its color was very similar to liver tissues (Fig. 9). To avoid overlooking this tiny worm, the eagle eyes with experience and attempt to look for it are needed to diagnose this infection by necropsy especially when associated pathology or overt clinical signs was not present. To make the detection of adult *P. fastosum* more vivid and perhaps easy to spot during necropsy, we would like to compare the size of *P. fastosum* with a tamarind leaf in which most of veterinarians in tropical countries would be more familiar with.

When examined by using a stereomicroscope (Fig. 10), the morphology of unstained and stained adult flukes that we investigated were similar to previous reports on morphological description of *P. fastosum* and *P. concinnum*. Based on the description, paired anterior testes and vitellaria around lateral margin are in line with previously described (Bowman et al., 2002; Basu and Charles, 2014). However, paired anterior testes was presented in tandem positioned of *D. dendriticum* (Otranto et al., 2007), whereas two globular posterolateral testes were presented in *E. coelomaticum* (Leite et al., 2020). In Thailand, additional 2 genera of liver flukes reported in cats (Nimsuphan et al., 2001; Aunpromma et al., 2016) apart from *P. fastosum* were *Opisthorchis viverrini* and *Clonorchis* spp. belonging to a different family, Opisthorchiidae. Although the size of these 2 trematodes is also small, the testes of all Opisthorchids are located in the posterior part of the body (Enes et al., 2010). Therefore, based on adult worm morphology, we confirmed that the trematode used in this study was identified as *P. fastosum*.

Since retrieval of *P. fastosum*-infected cat carcass was challenging at the beginning of our study, we initially obtained 2 partially autolyzed cat carcasses. With the preliminary microscopic examination of the worm morphology, their teguments and internal organs seemed to be intact so they were subjected to sample preparation for SEM and visualization. At low magnification of SEM, the adult worms looked relaxed with protruded cirrus (Fig. 11A-11B) in which it may be its actual shape (Fig. 11A). However, with higher magnification, the tegument and suckers were

all degenerated (data not shown). Later, we obtain another carcass in fresh condition, isolated adult parasites were then subjected to SEM processing. Fresh worm presented complete condition of tegument surface, suckers and papillae, although the body seemed to be slightly contracted and a cirrus of one worm was not protruded (Fig. 11C) or protruded with contracted action (Fig. 11B). To study the ultrastructural features of trematode, we found that the freshness of sample is very critical and cannot be prolonged in the refrigerator longer than one day. Also, to allow the adult worm to be more relaxed, the fixation process should be performed with warm fixative (Gonzalez et al., 2012).

Based on the previous reports, the location of *P. concinnum* genital pore was at or rather anterior to the branching point of the intestinal ceca (Bowman et al., 2002). This was in line with our results (Fig. 10). Also, to observe the location of genital pores with or without cirrus protrusion by the SEM, their locations of all 3 *P. fastosum* worms were in the midpoint between the oral and the ventral suckers (Fig. 11).

On the apical surface of the oral sucker, papillae and pores of gland cells were distributed. Similar to *O. viverrini*, numerous gland cells were found around the oral sucker (Apinhasmit et al., 1993). At least 3 types of papillae composed of plate-, button- and dome-shaped papillae were seen surrounding the oral sucker. The plate and button papillae seemed to be present on the apical region whereas dome papillae were present on the perimeter of oral sucker's aperture (Fig. 12). To



compare with the worm in the same family, plate papillae of *P. fastosum* were resemble to *Dicrocoelium dendriticum* plate papillae which described as knob like structure with hollow pit, surrounded by fine meshwork of tegument ridges (Cifrian and Garcia-Corrales, 1988). For the button papillae found on the oral sucker's apical surface of *P. fastosum*, other trematode species also had similar type, for example, type C papillae of *Clonorchis sinensis* (Fujino et al., 1979), type B papillae of *Gorgoderina attenuate* (Nadakavukaren and Nollen, 1975), and button papillae of *Dicrocoelium dendriticum* (Cifrian and Garcia-Corrales, 1988).

For the presence of *P. fastosum*'s dome papillae on the oral sucker aperture, outer and inner muscular rim of ventral sucker (Fig.11, 12 and 15), they were highly resembled to those described by *Fasciola hepatica* (Bennett and Threadgold, 1975), *Gorgoderina vitelliloba* (Hoole and Mitchell, 1981), *Paramphistomes* spp. (Eduardo, 1982) and *Dicrocoelium dendriticum* (Cifrian and Garcia-Corrales, 1988). However, ciliated papilla was not found in *P. fastosum* whereas a number of them has been reported around oral and ventral sucker of other trematodes, such as *Carmyerius spatiosus* (Anuracpreeda et al., 2015), *Orthcoelium parvipapillatum* (Anuracpreeda et al., 2016), *Fischoederius cobboldi* (Anuracpreeda et al., 2012) and *O. viverrini* (Apinhasmit et al., 1993).

Papillae performed various functions depending upon their locations (Hoole and Mitchell, 1981). As previously described, plate papilla was shown to be responsible for chemoreceptive function since this papilla was located around the

oral sucker (Otubanjo, 1985). Chemoreceptor plays essential role for locating host since it can perceive chemical compound in their surrounding and responsible for sending this signal as intracellular message. Apart from chemoreceptor, button papillae might be involved with contact and mechanoreceptors since this papilla was found at the oral apical portion (Fujino et al., 1979; Hoole and Mitchell, 1981). Dome papillae in the current study with *P. fastosum* was resemble to conical shape domed papilla of *Gorgoderina vitelliloba* and it could be tangoreceptors to respond to touch and pressure. Since domed papillae were situated on outer and inner rim of both muscular suckers, this papilla might also serve as stretch receptors. Stretch receptors plays critical role for parasite movement, feeding and attachment as well (Hoole and Mitchell, 1981). In the presence of different types of papillae and pores of gland cells on the apical region of ventral surface, we suggested that oral apical might play critical for nutrient absorption and firmly attachment to the host tissue (Apinhasmit et al., 1993).

Due to presence of strong muscular suckers, the worm could be able to firmly attach biliary epithelial wall with well-decorated suckers. Suckers have been considered as potential targets for anthelmintics drugs (Krupenko, 2019), then ventral and oral sucker suckers of *P. fastosum* could be potential drug target.

Cirrus, male reproductive organ was everted through the cirrus sac and penetrated to Laurel' canal of other fluke as *P. fastosum* is hermaphroditic . The cirrus was annularly folded and lack of papillae on the surface. So, this feature is

similar to other trematodes of same family such as *D. dendriticum* and *E. coelomaticum*, in which prominent extroverted and smooth surface cirrus has been reported (Cifrian and Garcia-Corrales, 1988; Leite et al., 2020). In contrary, *F. gigantea* showed spinous cirrus dorsally (Dangprasert et al., 2001) and large number of papillae were occurred around the genital pouch of *Paramphistomum* spp. (Eduardo, 1982). As far as we know, there has been very limited reports for surface description of cirrus in other trematodes. Thus, surrounding surface pattern of genital pore and cirrus might be different between species.

Rosette papillae were observed below oral and ventral sucker. These rosette papillae were resembled as described in *Dicrocoelium dendriticum* and *Gorgoderina attenuate* (Cifrian and Garcia-Corrales, 1988; Mata-Lopez and Leon-Regagnon, 2006). Considering their location around ventral midbody, rosette papillae might serve as tangoreceptors (Apinhasmit et al., 1993).

Herein, the tegument of *P. fastosum* shows corrugating surface with slender villous-like projections structures as in *O. viverrini*, in which these projections were mentioned as furrowed tegument (Scholz et al., 1992). Tegument surface with corrugated transverse folds were observed in *Fischoederius cobboldi* and *Fasciola gigantea* (Dangprasert et al., 2001; Anuracpreeda et al., 2012) and oriented ridges network with tegumental vesicles were shown in *Dicrocoelium dendriticum* (Cifrian and Garcia-Corrales, 1988). Considering that, villous-like projections of *P. fastosum* could be beneficial to enhance ionic exchange and osmolarity. As previously

described, the arrangement of folds might be depend upon degree of muscular contraction (Fujino et al., 1979), thus dorsal anterior region with transverse bundles of corrugated folds alternating with horizontal grooves appear to be highly motile area to follow parasite movement.

In current study, we have investigated variable size differences of *P. fastosum* eggs from both bile and fecal sample. We suggest that the egg with distinct operculum, thick egg shell, large and scattered germ balls inside the undefined content could be unfertilized one. Similar to our study, different morphological features and variable size differences of *S. mansoni* eggs has been proposed by (Cancado et al., 1965), in which unfertilized or dead ova was recognized by hemitransparent and granules inside. In addition, atypical helminths eggs deviating from identical morphology have been reported previously (Sapp et al., 2018). However, only two types of *P. fastosum* eggs, mature and immature have been reported previously (Palumbo et al., 1976). As we hypothesized, atypical form of *P. fastosum* eggs were seen in the original bile sample. Thus, microscopic examiner should aware possible finding of typical and atypical *P. fastosum* eggs from fecal sample too, otherwise false negative results would come out.

As observed under SEM, *P. fastosum* eggs are highly resembled to *E. coelomaticum* egg (Pinheiro et al., 2015) by means of shape, size and shell surface smoothness, however abopercular knob was not seen. As compared to ultrastructure of minute intestinal fluke eggs whereas thread-like ridges on egg shell surface of *P.*

*summa*, multiple minute ridges on *Metagonimus yokogawai* egg shell, rough egg shell surface of *Himasthla continua*, and muskmelon-like structure of *Clonorchis sinensis* (Lee et al., 2012) have been reported previously. In contrary with *Opisthorchis viverrini* eggs which showed the distinct melon patterns (Apinhasmit et al., 1994) since this melon pattern played vital role in attachment of aquatic plants to reach their first intermediate host. However, the first intermediate host of *P. fastosum* was land snail, and then smooth eggshell could be helpful to ingest easily.

For H&E staining, the tegument showed thin and homogenous layer with tegument indentations. The parenchyma might provide for firmly attachment, nutrient storage, motility and exchanging materials as described by (Conn et al., 1993). In contrast with other digenetic trematodes, such as *O. parvipapillatum* and *P. gracile* in which their tegument exhibited surface folds and grooves (Panyarachun et al., 2013; Anuracpreeda et al., 2016). Apart from that, cross section of uterus showed fluke eggs morphology with thick brown egg shell, which is similar to microscopic examination. However, we did not see *P. fastosum* tegument in layer by layer. This might be due to fixative time before doing histological staining process. Although we collected the fluke from recently dead cat, there was more than 48 hr in 10% formalin. Therefore, fixatives might have detrimental effect if we could not process specimen immediately. Moreover, some special fixatives for histological observation are recommended to enhance the visualization of this small fluke.

Under TEM, tegument syncytium of *P. fastosum* can be divided into three layers depend on the components and the depth of tegument. Tegument indentations were occurred within various sizes of tegumental projections, and surface membrane is discontinuously covered with glycocalyx. Glycocalyx were said to be typical feature of trematodes, such as *F. hepatica* (Hanna and Trudgett, 1983), *F. gigantica* (Sobhon et al., 2000), *O. viverrini* (Apinhasmit et al., 1993), *C. spatiosus* (Anuracpreeda et al., 2015) and *O. parvipapillatum* (Anuracpreeda et al., 2016). As previously described by (Threadgold, 1976), these glycocalyx elicited negative charge to protect host immune response by repelling hosts' immune cells attachment since these immune cell surfaces are high electronegative charged. Due to presence of these negative-charged molecules, it might be possible to gather small molecules, ion particles and amino acids as their nutrient. Herein, glycocalyx might be produced more abundantly by TG<sub>2</sub> granules, since TG<sub>2</sub> granules are consistently dispersed to the outermost membrane and more likely to be secreted their matrix to tegument surface continuously.

The tegument cytoplasm contained numbers of TG<sub>1</sub> and TG<sub>2</sub> granules, lysosomes, mitochondria and microtubules. Both tegumental granules (TG<sub>1</sub> and TG<sub>2</sub>) occurred in *P. fastosum* are similar to other trematode species. In detail, spherical or ovoid (T<sub>0</sub>) granules of *F. hepatica* (Hanna, 1980), that are critical in juvenile stage to enrich glycocalyx during parasite migration inside host tissues. When parasite reached to habitat site, these T<sub>0</sub> granules are totally replaced by similar T<sub>1</sub> granules. However,

the number of  $T_1$  granules in adult *F. hepatica* become lesser whereas biconcave or rod shape  $TG_2$  granules were replaced. Likewise, cytoplasm of *F. gigantica* tegument contained ovoid granules  $G_1$  and discoid granules  $G_2$ . But,  $G_1$  granules were distributed to surface membrane to secrete their contents to contribute glycoalyx formation (Sobhon et al., 2000). Similar in stomach fluke *C. spatiosus*, two types of granules  $TG_1$  and  $TG_2$  were occurred. However,  $TG_1$  granules shown to be highly dispersed underneath tegument ridges whereas  $TG_2$  granules are diffused within cytoplasm (Anuracpreeda et al., 2015). Considering this,  $TG_1$  granules of *P. fastosum* might be similar to  $T_1$  granules of *F. hepatica*,  $G_1$  granules of *F. gigantica* and  $TG_1$  granules of *C. spatiosus*, whereas  $TG_2$  granules could probably *F. hepatica*  $T_2$  granules, *F. gigantica*  $G_2$  type and *C. spatiosus*  $TG_2$  granule. In contrary, rod shape  $TG_2$  granules of *P. fastosum* are abundantly dispersed near to outermost layer to contribute glycoalyx. The secreted tegumental granules seem to involve in exchanging materials and replacement of damaged membrane. As immediate recovery process, tegument outer membrane was become coated by glycoalyx. Thus, parasite surface membrane coated with glycoalyx are more likely to involve in parasite defense mechanism. Lysosomes have been proposed in endocytosis (Anuracpreeda et al., 2016). So, immune complexes molecules may probably break down by fusion with lysosomes. Numerous mitochondria are distributed throughout cytoplasm together with secretory granules. Due to presence of mitochondria, tegument cytoplasm might involve in energy supplementation to other layers of

tegument by means of microtubules. So, this layer could probably serve as storehouse for granules to create new membrane (Sobhon et al., 2000). It has been noted that, basal membrane infolding structures could be beneficial for enhancement of osmotic and ionic equilibrium (Threadgold, 1976). In addition, tegument sub-syncytial layer of *P. fastosum* exhibited muscle fibers. This characteristics is similar to other related trematodes such as *C. spatiosus* (Anuracpreeda et al., 2015), *F. gigantica* (Sobhon et al., 2000) and *P. gracile* (Panyarachun et al., 2010). These muscle fibers have been considered as main supporter for parasite movement with strong retraction (Sobhon and Upatham, 1990).

According to our findings, only one type of tegumental cell was found in *P. fastosum*. Likewise, one type of tegumental cell was occurred and it can synthesize all types of granules in other digenean species, such as *F. gigantica* (Sobhon et al., 2000), *B. anguillae* (Filippi et al., 2010), *L. musculus* (Filippi et al., 2012), *D. inflata* (Filippi et al., 2013), *O. parvipapillatum* (Anuracpreeda et al., 2016) and *C. spatiosus* (Anuracpreeda et al., 2015). Conversely, *F. hepatica* showed at least 3 types of tegumental cells (Burden et al., 1983). We have investigated that both types of tegumental granules (TG<sub>1</sub> and TG<sub>2</sub>) can be produced by only one type of tegument cell. Due to presence of microtubules within cytoplasmic process, the granules might be easily transported to the surface tegument (Sobhon and Upatham, 1990).



With regard to TEM of reproductive organs, limited studies has been done for trematode fertilization process and intrauterine eggs. Herein, we have investigated the route of *P. fastosum* oviduct, together with cross section of sperm head, sperm tail (microtubules), and oocyte as well. These microtubules are responsible for cytoskeletal function and also being associated with sperm undulatory movement as previously described (Culioli et al., 2006). In addition, microtubules play critical role in fusion process of sperm and oocyte (Swiderski et al., 2004). Despite detail fertilization process of *P. fastosum* was identified in current study, the pattern of microtubules and ultrastructural characteristics of intrauterine eggs still remain to discuss.

## 5. Conclusion

Our study is the first attempt to demonstrate surface topography and ultrastructural characteristics of *P. fastosum* using combined microscopic techniques. Understanding basic surface features of both adult worm and eggs could be useful to differentiate between species and might be able to evaluate efficacy of any rational drug. In current study, the probability of strong muscular sucker that could become potential target for any rational drug has been investigated. Since variable size differences of *P. fastosum* eggs can be occurred, the examiner should be aware to make decision of false negative. However, detail morphological studies on parasite developmental stages should be further pursued. The tegument cell play pivotal role for replacement of damage tegument with massive secretion of granules.

## Acknowledgements

This research was supported to WS by the grant of Faculty of Veterinary Science, Feline Health and Infectious Disease Research Unit, Animal Vector-Borne Disease Research Unit, Chulalongkorn University. Moreover, this research was financially supported to Babi Kyi Soe by the 90<sup>th</sup> Anniversary of Chulalongkorn University Scholarships (Rachadaphiseksomphot Endowment Fund), Grant of Faculty of Veterinary Science, Chulalongkorn University. The authors would like to gratitude to the staff from STREC lab and Department of Pathology, Faculty of Veterinary Science, Chulalongkorn University for their guidance. In addition to this, the staff from Department of Helminthology, Faculty of Tropical Medicine, Mahidol University for their kind support. Moreover, the authors would like to gratitude to Dr. Nardtiwa Chaivoravitsakul, Dr. Kongthit Horoongruang, Dr. Rampapat Penchome and Dr. Siwaporn Pengpis from Feline Center and Radiology Unit, Small Animal Teaching Hospital, Department of Pathology, Faculty of Veterinary Science, Chulalongkorn University for their kind support.

## References

- Andrade, R.L., Dantas, A.F., Pimentel, L.A., Galiza, G.J., Carvalho, F.K., Costa, V.M. and Riet-Correa, F. 2012. *Platynosomum fastosum*-induced cholangiocarcinomas in cats. *Vet. Parasitol.*, 190(1-2), 277-280. doi:10.1016/j.vetpar.2012.04.015
- Anuracpreeda, P., Chawengkirttikul, R. and Sobhon, P. 2016. Surface histology, topography, and ultrastructure of the tegument of adult *Orthocoelium parvipapillatum* (Stiles & Goldberger, 1910). *Parasitol. Res.*, 115(7), 2757-2769.
- Anuracpreeda, P., Panyarachun, B., Ngamniyom, A., Tinikul, Y., Chotwiwatthanakun, C., Poljaroen, J. and Sobhon, P. 2012. *Fischoederius cobboldi*: a scanning electron microscopy investigation of surface morphology of adult rumen fluke. *Exp. Parasitol.*, 130(4), 400-407.
- Anuracpreeda, P., Phutong, S., Ngamniyom, A., Panyarachun, B. and Sobhon, P. 2015. Surface topography and ultrastructural architecture of the tegument of adult *Camyerius spatiosus* Brandes, 1898. *Acta. Tropica.*, 143, 18-28.
- Apinhasmit, W., Sobhon, P., Saitongdee, P. and Upatham, E.S. 1993. *Opisthorchis viverrini*: changes of the tegumental surface in newly excysted juvenile, first-week and adult flukes. *Int. J. Parasitol.*, 23(7), 829-839. doi:10.1016/0020-7519(93)90046-2
- Apinhasmit, W., Sobhon, P., Saitongdee, P., Menayotin, S. and Upatham, E.S. 1994. *Opisthorchis viverrini*: Ultrastructure of the tegument of the first-week juveniles and adult flukes. *Int. J. Parasitol.*, 24(5), 613-621. doi:https://doi.org/10.1016/0020-7519(94)90113-9
- Aunpromma, S., Kanjampa, P., Papirom, P., Tangkawattana, S., Tangkawattana, P., Tesana, S. and Sukon, P. 2016. Prevalence and risk factors for *Opisthorchis viverrini* infection among cats and dogs in six districts surrounding the Ubolratana dam, an endemic area for human Opisthorchiasis in Northeastern Thailand. *Southeast Asian J. Trop. Med. Pub. Heal.*, 47(6), 1153-1159.
- Basu, A.K. and Charles, R.A. 2014. A review of the cat liver fluke *Platynosomum fastosum* Kossack, 1910 (Trematoda: Dicrocoeliidae). *Vet. Parasitol.*, 200(1-2), 1-7. doi:10.1016/j.vetpar.2013.12.016

- Bennett, C.E. and Threadgold, L.T. 1975. *Fasciola hepatica*: development of tegument during migration in mouse. *Exp. Parasitol.*, 38(1), 38-55. doi:10.1016/0014-4894(75)90036-3
- Bowman, D.D., Hendrix, C.M., Lindsay, D.S. and Barr, S.C. 2002. *Feline Clin. Parasitol.* (Vol. 206): Wiley Online Library.
- Burden, D., Bland, A., Hammet, N. and Hughes, D. 1983. *Fasciola hepatica*: migration of newly excysted juveniles in resistant rats. *Exp. Parasitol.*, 56(2): 277-288.
- Cançado, J.R., da Cunha, A.S., de Carvalho, D.G. and Cambraia, J.S. 1965. Evaluation of the treatment of human *Schistosoma mansoni* infection by the quantitative oogram technique. *Bulletin of the World Health Organization*, 33(4), 557.
- Cifrian, B. and Garcia-Corrales, P. 1988. Scanning electron microscopy of adult *Dicrocoelium dendriticum*. *Parasitol. Res.*, 74(3), 235-242.
- Culioli, J.L., Foata, J., Mori, C. and Marchand, B. 2006. Spermiogenesis and sperm in *Mesostoma viaregginum* (Plathelminthes, Rhabdocoela): an ultrastructural study to infer sperm orientation. *Zoomorphology.*, 125(1), 47-56.
- Dangprasert, T., Khawsuk, W., Meepool, A., Wanichanon, C., Viyanant, V., Upatham, S. and Sobhon, P. 2001. *Fasciola gigantica*: Surface topography of the adult tegument. *J. Helminthol.*, 75, 43-50. doi:10.1079/JOH200041
- Eduardo, S. 1982. The taxonomy of the family Paramphistomidae Fiscoeder, 1901 with special reference to the morphology of species occurring in ruminants. I. General considerations. *Sys. Parasitol.*, 4(1), 7-57.
- Enes, J.E., Wages, A.J., Malone, J.B. and Tesana, S. 2010. Prevalence of *Opisthorchis viverrini* infection in the canine and feline hosts in three villages, Khon Kaen Province, northeastern Thailand. *The Southeast Asian J. Trop. Med. Pub. Heal.*, 41(1): 36.
- Filippi, J.J., Quilichini, Y., Foata, J. and Marchand, B. 2012. Topography and ultrastructure of the tegument of *Lecithochirium musculus* (Digenea: Hemiuridae), a parasite of the European eel *Anguilla anguilla* (Osteichthyes: Anguillidae). *J. Morphol.*, 273(4), 361-370.
- Filippi, J.J., Quilichini, Y. and Marchand, B. 2013. Topography and ultrastructure of the tegument of *Deropristis inflata* Molin, 1859 (Digenea: Deropristidae), a parasite

- of the European eel *Anguilla anguilla* (Osteichthyes: Anguillidae). *Parasitol. Res.*, 112(2), 517-528.
- Filippi, J.J., Quilichini, Y., Foata, J. and Marchand, B. 2010. Topography and ultrastructure of the tegument of *Bucephalus anguillae* (Digenea: Bucephalidae), a parasite of the European eel *Anguilla anguilla* (Osteichthyes: Anguillidae). *J. Parasitol.*, 96(6), 1102-1111.
- Fried, B. and Takahiro, F. 1984. Scanning electron microscopy of *Echinostoma revolutum* (Trematoda) during development in the chick embryo and the domestic chick. *Intern. J. Parasitol.*, 14(1), 75-81.
- Fujino, T., Ishii, Y. and Choi, D.W. 1979. Surface ultrastructure of the tegument of *Clonorchis sinensis* newly excysted juveniles and adult worms. *The J. Parasitol.*, 579-590.
- González, C.E., Hamann, M.I. and Salgad, C. 2012. Study of helminth parasites of amphibians by Scanning Electron Microscopy. In: Scanning Electron Microscopy. InTechOpen.
- Hanna, R.E.B. 1980. *Fasciola hepatica*: An immunofluorescent study of antigenic changes in the tegument during development in the rat and the sheep. *Exp. Parasitol.*, 50(2), 155-170. doi:[https://doi.org/10.1016/0014-4894\(80\)90017-X](https://doi.org/10.1016/0014-4894(80)90017-X)
- Hanna, R. and Trudgett, A. 1983. *Fasciola hepatica*: development of monoclonal antibodies and their use to characterize a glycolyx antigen in migrating flukes. *Parasite Immunol.*, 5(4), 409-425.
- Hoole, D. and Mitchell, J. 1981. Ultrastructural observations on the sensory papillae of juvenile and adult *Gorgoderina vitelliloba* (Trematoda: Gorgoderidae). *Intern. J. Parasitol.*, 11(5), 411-417.
- JC, F.I.B. 1999. Mechanisms of fasciolicide action and drug resistance in *Fasciola hepatica*. In J. P. Dalton (Ed.), *Fasciolosis* (pp. 225-276). CAB Intern.
- Jitsamai, W., Khrutkham, N., Hunprasit, V., Chandrashekar, R., Bowman, D. and Sukhumavasi, W. 2021. Prevalence of endoparasitic and viral infections in client-owned cats in metropolitan Bangkok, Thailand, and the risk factors associated with feline hookworm infections. *Vet. Parasitol., Regional Studies and Reports*, 100584.

- Jurberg, A.D., Gonçalves, T., Costa, T.A., de Mattos, A.C.A., Pascarelli, B.M., de Manso, P.P.A. and Coelho, P.M.Z. 2009. The embryonic development of *Schistosoma mansoni* eggs: proposal for a new staging system. *Development Gen. Evol.*, 219(5), 219.
- Krupenko, D. 2019. Oral sucker in Digenea: structure and muscular arrangement. *Zoomorphology.*, 138(1), 29-37.
- Lathroum, C.N., Shell, L., Neuville, K. and Ketzis, J.K. 2018. Efficacy of Praziquantel in the Treatment of *Platynosomum fastosum* in Cats with Natural Infections. *Vet. Sci.*, 5(2), 35.
- Lee, J.J., Jung, B.K., Lim, H., Lee, M.Y., Choi, S.Y., Shin, E.H. and Chai, J.Y. 2012. Comparative morphology of minute intestinal fluke eggs that can occur in human stools in the republic of Korea. *The Korean J. Parasitol.*, 50(3), 207.
- Leite, K., Lopes-Torres, E., Souza, J., Neves, R., Gomes, D. and Machado-Silva, J. 2020. *Eurytrema coelomaticum*: updated morphology of adult worms using advanced microscopy experiments. *J. Helminthol.*, 94.
- Loukas, A., Tran, M. and Pearson, M.S. 2007. *Schistosome* membrane proteins as vaccines. *Inter. J. Parasitol.*, 37(3-4): 257-263.
- Lucio-Forster, A. and Bowman, D.D. 2011. Prevalence of fecal-borne parasites detected by centrifugal flotation in feline samples from two shelters in upstate New York. *J. Feline Med. Surg.*, 13(4), 300-303.
- Marhaba, Z. and Haniloo, A. 2018. Staining of Parasitic Helminths by Extracts of *Allium cepa*, *Juglans regia*, and *Rubia tinctorum*: An Approach to Herbal Dyes. *Iranian J. Parasitol.*, 13(2), 293.
- Mata-López, R. and León-Règagnon, V. 2006. Comparative study of the tegumental surface of several species of *Gorgoderina* Looss, 1902 (Digenea: Gorgoderidae), as revealed by scanning electron microscopy. *Comp. Parasitol.*, 73(1), 24-34.
- Morris, G.P. and Threadgold, L.T. 1967. A presumed sensory structure associated with the tegument of *Schistosoma mansoni*. *J Parasitol.*, 53(3), 537-539.
- Nadakavukaren, M.J. and Nollen, P.M. 1975. A scanning electron microscopic investigation of the outer surfaces of *Gorgoderina attenuata*. *Inter. J. Parasitol.*, 5(6), 591-595.

- Otubanjo, O.A. 1985. Scanning electron microscopic studies of the body surface and external genitalia of a dicrocoeliid trematode, *Concinnum epomopis* Sandground 1973. Zeitschrift für Parasitenkunde, 71(4), 495-504.
- Palumbo, N., Taylor, D. and Perri, S. 1976. Evaluation of fecal technics for the diagnosis of cat liver fluke infection. Lab. Ani. Sci. 26(3), 490-493.
- Panyarachun, B., Ngamniyom, A., Sobhon, P. and Anuracpreeda, P. 2013. Morphology and histology of the adult *Paramphistomum gracile* Fiscoeder, 1901. J. Vet. Sci., 14(4), 425.
- Panyarachun, B., Sobhon, P., Tinikul, Y., Chotwiwatthanakun, C., Anupunpisit, V. and Anuracpreeda, P. 2010. *Paramphistomum cervi*: Surface Topography of the tegument of adult fluke. Exp. Parasitol., 125, 95-99. doi:10.1016/j.exppara.2009.12.020
- Pinheiro, J., Franco-Acuña, D., Oliveira-Menezes, A., Brandolini, S., Adnet, F., Torres, E.L. and Damatta, R. 2015. Additional study of the morphology of eggs and miracidia of *Eurytrema coelomaticum* (Trematoda). Helminthologia., 52(3), 244.
- Pinheiro, J., Franco-Acuña, D., Oliveira-Menezes, A., Brandolini, S., DaMatta, R. and Souza, W. 2012. New insight into the morphology of *Eurytrema coelomaticum* (Trematoda, Dicrocoeliidae) cercariae by light, scanning, and transmission electron microscopies. Parasitol. Res., 111, 1437-1445. doi:10.1007/s00436-012-2977-8
- Pinto, H., Mati, V. and De Melo, A. 2014. New insights into the life cycle of *Platynosomum* (Trematoda: Dicrocoeliidae). Parasitol. Res., 113. doi:10.1007/s00436-014-3926-5
- Ramos, R.A., Lima, V.F., Monteiro, M.F., Santana Mde, A., Lepold, R., Faustino, M.A. and Alves, L.C. 2016. New insights into diagnosis of *Platynosomum fastosum* (Trematoda: Dicrocoeliidae) in cats. Parasitol. Res, 115(2), 479-482. doi:10.1007/s00436-015-4763-x
- Ramos, R.A., Lima, V.F., Monteiro, M., Andrade - Santana, M., Lepold, R., Da Gloria Faustino, M. and Cringoli, G. 2015. New insights into diagnosis of

- Platynosomum fastosum* (Trematoda: Dicrocoeliidae) in cats. Parasitol. Res., 115. doi:10.1007/s00436-015-4763-x
- Sapp, S.G., Yabsley, M.J. and Bradbury, R.S. 2018. Abnormal helminth egg development, strange morphology, and the identification of intestinal helminth infections. Emerging infectious diseases, 24(8), 1407.
- Scholz, T., Ditrich, O. and Giboda, M. 1992. Study on the surface morphology of the developmental stages of the liver fluke, *Opisthorchis viverrini* (Trematoda: Opisthorchiidae). Annales de parasitologie humaine et comparée, 67(3), 82-90.
- Shell, L., Ketzis, J., Hall, R., Rawlins, G. and du Plessis, W. 2015. Praziquantel treatment for *Platynosomum* species infection of a domestic cat on St Kitts, West Indies. J. Feline Med. Surg. 1(1), 2055116915589834.
- Shin, D.H., Lim, D.S., Choi, K.J., Oh, C.S., Kim, M.J., Lee, I.S. and Chai, J. Y. 2009. Scanning electron microscope study of ancient parasite eggs recovered from Korean mummies of the Joseon Dynasty. J. Parasitol., 95(1), 137-145.
- Silva, K.S., Silva, R.J. and Pereira, W.L. 2012. Occurrence of infection by *Platynosomum illiciens* (Braun, 1901) in captive neotropical primates. Primates., 53(1), 79-82.
- Sobhon, P. and Upatham, E. S. 1990. Snail hosts, life-cycle, and tegumental structure of oriental schistosomes. Snail hosts, life-cycle, and tegumental structure of oriental schistosomes.
- Sobhon, P., Dangprasert, T., Chuanchaiyakul, S., Meepool, A., Khawsuk, W., Wanichanon, C. and Upatham, E. 2000. *Fasciola gigantica*: ultrastructure of the adult tegument. Sci. Asia., 26, 137-148.
- Świdorski, Z., Conn, D. B., Miquel, J. and Młocicki, D. 2004. Fertilization in the cestode *Gallegoides arfaai* (Mobedi et Ghadirian, 1977) Tenora et Mas-Coma, 1978 (Cyclophyllidea, Anoplocephalidae). Acta. Parasitol., 49, 108-115.
- Threadgold, L. 1976. *Fasciola hepatica*: ultrastructure and histochemistry of the glycocalyx of the tegument. Exp. Parasitol., 39(1), 119-134.
- Yun-liang Shi, X.L. W., Zhi-hua Jiang, Xiao-jing Cheng and Yi-chao Yang. 2018. Scanning electron microscopic and transmission electron microscopic observations of



the tegument structure of adult *Clonorchis sinensis*. Chinese J. Parasitol. Dis., 36(2): 184-186.



## Chapter 4

Antigenic profile and candidate antigen characterization of crude extract of

*Platynosomum fastosum* using mass spectrometry

Babi Kyi Soe<sup>a</sup>, Poom Adisakwattana<sup>b</sup>, Onrapak Reamtong<sup>c</sup>, Panat Anuracpreeda<sup>d</sup>,  
Woraporn Sukhumavasi<sup>a/\*</sup>

<sup>a</sup>Parasitology Unit, The International Graduate Program of Veterinary Science and  
Technology, Faculty of Veterinary Science, Chulalongkorn University, Bangkok 10330,  
Thailand

<sup>b</sup>Department of Helminthology, Faculty of Tropical Medicine, Mahidol University,  
Bangkok 10400, Thailand

<sup>c</sup>Department of Molecular Tropical Medicine and Genetics, Mahidol University,  
Bangkok 10400, Thailand

<sup>d</sup>Institute of Molecular Biosciences, Mahidol University, Bangkok 73170, Thailand

<sup>a/\*</sup>Parasitology Unit, Department of Pathology, Faculty of Veterinary Science,  
Chulalongkorn University, Bangkok 10330, Thailand

\*Corresponding email: [vetkwan@hotmail.com](mailto:vetkwan@hotmail.com)

## Abstract

Feline platynosomiasis, called lizard poisoning, is a feline hepatic disease caused by parasitic trematode, *Platynosomum fastosum*. Felid serve as definitive hosts and infection acquired through consumption of lizard, that carried infective stage of this parasite. Since parasite resides in biliary ducts and gallbladder, failure of hepatobiliary system and may later succumb to cholangiocarcinoma. Diagnosis of this infection basically relied on conventional fecal microscopic techniques, since there was lack of knowledge for immunodiagnosis potential of parasite antigens related to *P. fastosum* infection. Herein, the crude worm antigens (CWAs) were separated using 15% SDS PAGE and transferred to nitrocellulose membrane to perform immunoblotting with *P. fastosum*-infected sera, healthy control sera and other endoparasites infected sera. Sensitivity, specificity, positive predictive values and negative predictive values in immunoblotting of each reacted band were calculated. Three immunogenic protein bands of molecular weight 72kDa, 53kDa and 13kDa with high sensitivity and specificity, were excised from Coomassie G satin gel and then analyzed by liquid chromatography tandem mass spectrometry (LC-MS/MS). As results, 70kDa heat shock protein (HSP70), hypothetical protein (CRM22\_002083) (ATP synthase subunit beta) and histone H2B were found as associated proteins of 72kDa, 53kDa and 13kDa, respectively. This study is the first attempt and showed three promising proteins that could assist for development of diagnosis tool in feline platynosomiasis.

Keywords: crude worm extracts, candidate antigens, immunoblotting, liquid chromatography tandem mass spectrometry, *Platynosomum fastosum*



## 1. Introduction

Feline platynosomiasis, “lizard poisoning” seemed to be neglected as most of the prevalence come from post-mortem findings. *Platynosomum fastosum* is a cat liver fluke resides in hepatobiliary system and prolonged infection can succumb to bile duct cancer (Andrade et al., 2012). Worldwide distribution between 15 and 85% of prevalence has been reported especially in area favor development of intermediate hosts (Basu and Charles, 2014). In Thailand, within the year 2005 and 2015, the prevalence was between 0.1% and 4.0% from different provinces (Jittapalapong et al., 2007; Rojekittikhun et al., 2008; Rojekittikhun, 2015). Recently, prevalence rate raised to 8.9% in Bangkok and vicinities within year 2019 and 2020, by increasing sampling number that made higher sensitivity of parasite eggs detection (manuscript in prep.). As the cats are known as prey animals, they become infected by hunting lizards, geckos and isopods which carried infective stage metacercaria. The snail *Subulina octona* served as first intermediate host. Terrestrial lizards and isopods are the second intermediate host that harbored infective stage metacercaria (Pinto et al., 2014). As disease is mostly asymptomatic, clinical symptoms are occasionally occurred in case of chronic and/or heavy infection (Taylor and Perri, 1977; Ramos et al., 2016). Histopathological lesions showed cholangitis, cholangiohepatitis, cholecystitis, periductal fibrosis, biliary cirrhosis and may induce cholangiocarcinoma (Andrade et al., 2012). Despite praziquantel is recommended, the efficacy is still

uncleared, and accurate dosage is still unknown (Shell et al., 2015; Lathroum et al., 2018).

Though conventional microscopic examination is basic diagnosis tool to detect parasite eggs in the feces, the sensitivity of detection by this method is low, in case of light infection and possibly intermittent egg shedding (Carreira et al., 2008). In addition to this, these techniques could also favor to detect only in the stage of parasite matured, so false negative result would come out during prepatent period and also no fecal eggs was detected in complete biliary obstruction cases. On regards of this, serological tests become the method of choice to detect presence of parasites even in non-productive stage. Although the reliability of these tests could be challenged whereas common antigens were reported from different parasite helminths (Chen et al., 2011; Ngoc et al., 2015). To overcome this issue, investigation of immunodominant antigens from parasite secreted products could be beneficial. In the process of representing serodiagnosis, the antigens that secreted from the parasite especially crude worm extracts, excretory secretory extracts and parasite tegument extractions were mentioned as high immunogenic and might be beneficial to develop early serodiagnosis tool (Wongratanacheewin et al., 1988). To identify this fact, specific novel antigen from this liver fluke play crucial part. Understanding the fundamental antigenic components of parasite itself and investigating the potential candidate antigen/s, that could involve in host immune response, therefore, of great importance to develop early diagnosis tool. Up to present, there was no

comprehensive report investigating antigenic components and characterizing potential antigen/s of *P. fastosum*. Therefore, we extracted crude worm antigens to consider antigenic components and investigate potential antigen/s specific to *P. fastosum* infection in current study.

On behalf of new technologies, mass spectrometry-based proteomics become the preferable approach to analyze complex protein mixtures, since it can provide massive information with high reproducibility and high resolution (Aebersold and Mann, 2003; Reamtong, 2008). Recently, mass spectrometry based parasitic proteomics studies were done to enhance disease diagnosis (Ndao et al., 2010; Khoontawad et al., 2012; Thezenas et al., 2013; Zhang et al., 2019), drug targets and vaccine intervention (Dea-Ayuela et al., 2006; Chemale et al., 2010; Wongkamchai et al., 2011; Boamah et al., 2012; Urbaniak et al., 2012; Nuamtanong et al., 2019), it was also used to elucidate the host-parasite interaction (Zhou et al., 2011, Gonzalez-Miguel et al., 2012; Victor et al., 2012). Hence, mass spectrometry is suggested as indispensable tool to identify protein of interest, the candidate antigen/s revealed by immunoblotting technique was further pursued to characterize by mass spectrometry.

## 2. Materials and methods

### 2.1 Sample collection and identification

Adult *P. fastosum* were collected from liver, bile duct and gallbladder of infected cats during necropsy. The physiological saline (0.85% NaCl) was used to rinse the dissected liver tissue sample and biliary tracts thoroughly to let the

parasites out. After that, the fluke sample were quickly washed with distilled water and prepared for crude worm extraction as described previously (Adisakwattana et al., 2007). For parasite identification, the flukes were fixed in 10% formalin and stained overnight with Semichon' acetic carmine, then dehydration was done in graded series of ethanol (30%, 50%, 70%, 95% and 100%) for 10 min each. After that, the specimen was cleared in xylene for 5 min and mounted using permanent mounting medium (Permount, Sigma-Aldrich Co.). Subsequently, the specimen was identified according to their morphology as described by (Pinto et al., 2014).

## 2.2 Preparation of crude worm antigens

The soluble crude worm antigens (CWAs) were prepared according to (Adisakwattana et al., 2007). Briefly, the parasite specimen was homogenized with lysis buffer containing 0.01M PBS, 10mM Tris-HCl, 150 mM NaCl, 0.5% Triton X-100, pH 7.2, 10 mM EDTA and 1mM PMSF (P-7626, Sigma-Aldrich Co.) using tissue homogenizer. After that, the mixture was sonicated at 20% amplitude for 5 min in an ice bath with 15-s pulse on and 15-s pulse off (SONICS, USA). Subsequently, the suspension was centrifuged at 5000g for 20 min at 4°C to get rid of insoluble materials. Finally, the supernatant was collected and measured protein concentration by Bradford protein assay (Bradford, 1976) using Bio-Rad protein assay reagent kit (Bio-Rad, USA), in case bovine serum albumin as a standard.

## 2.3 Sera sample

Total of 46 sera sample were involved in this study (Table. 9). For *P. fastosum*-infected sera, positive sample were screened by both conventional



microscopic technique (Jitsamai et al., 2021) using PBS-ethyl acetate centrifugal sedimentation and conventional PCR technique (Nguyen et al., 2017). At least three times sampling of each sample was done for fecal examination to ascertain the positive results. On behalf of healthy control sera, 8 sera sample from normal cat whose liver biochemical profile was in normal ranges, also showed no fecal parasite eggs at blood collection time, regular deworming practice, and exclusively indoor cats were collected. In order to identify specificity, sensitivity and cross-reactivity, 22 sera sample from cats with other parasites infected cases containing nematodes (*Ancylostoma* spp., *Toxocara* spp., *Trichuris* spp., *Strongyloides* spp.), cestodes (*Dipylidium caninum*, *Taenia taeniaeformis*), and protozoa (*Cystoisospora* spp.) were also collected since numbers of reports on cats with these endoparasites in Bangkok and vicinities. To consider as significant results, individual sera sample were used for immunoblotting.

Table 9. Number of sera sample and diagnosis methods

Species infected	No. of sera	Types of sample	Diagnosis methods
<b>Trematode</b>			
<i>Platynosomum fastosum</i>	16	Feces	PBS-ethyl acetate centrifugal sedimentation
		Feces	Conventional PCR
<b>Nematodes</b>			
<i>Ancylostoma</i> spp.	5	Feces	PBS-ethyl acetate centrifugal sedimentation
<i>Toxocara</i> spp.	5	Feces	PBS-ethyl acetate centrifugal sedimentation
<i>Trichuris</i> spp.	2	Feces	PBS-ethyl acetate centrifugal sedimentation
<i>Strongyloides</i> spp.	2	Feces	PBS-ethyl acetate centrifugal sedimentation
<b>Cestodes</b>			
<i>Dipylidium caninum</i>	2	Feces	PBS-ethyl acetate centrifugal sedimentation
<i>Taenia taeniaeformis</i>	2	Feces	PBS-ethyl acetate centrifugal sedimentation
<b>Protozoa</b>			
<i>Cystoisospora</i> spp.	4	Feces	PBS-ethyl acetate centrifugal sedimentation
<b>Control</b>			
Healthy	8	Feces	PBS-ethyl acetate centrifugal sedimentation
		Blood	Liver biochemical profile
			Tumor markers (CEA and AFP)
<b>Total</b>	<b>46</b>		

Note: CEA, carcinoembryonic antigen and AFP, alpha-fetoprotein.

#### 2.4 SDS-PAGE and immunoblotting

SDS-PAGE of CWAs was performed using the Hoefer apparatus (Mini-Vertical Gel, USA). Two major parts of SDS polyacrylamide gel (15% separating and 4% stacking gel) was prepared and 15 $\mu$ g of protein sample was used to run the gel with running buffer as described previously (Laemmli, 1970). The prestained standard protein marker (Bio-Rad, USA) at range of 10kDa to 170kDa was loaded to calibrate and run the gel at a constant current of 40mA for approximately 2 hr at room temperature until the dye front reached to the bottom of gel plate. After

electrophoresis, the protein patterns were visualized using Coomassie Brilliant Blue (CBB) staining overnight or silver staining (SIGMA, USA).

Immunoblotting was performed according to the procedures described previously (Towbin et al., 1979; Adisakwattana et al., 2007). Briefly, the protein from the gel was electrophoretically transferred to nitrocellulose membrane (Bio-Rad, USA) using semi-dry blotting apparatus (HorizeBlot, Japan) for 100 min at 140 mA. The whole blotting process was done in the transfer buffer containing 25mM Tris, 192mM glycine, 0.2% SDS and 20% methanol. After transfer process, the nitrocellulose membrane was air dried and cut into strips (0.3cm), then nonspecific binding was blocked with blocking solution (5% skimmed milk in 1xPBST, pH 7.4 containing 0.05% Tween-20) for 1hr. Subsequently, the membrane strips were quickly washed with 1xPBST and incubated with *P. fastosum*-infected cat serum samples as primary antibody, diluted in 1: 100 with a diluent (5% skimmed milk in 1xPBST), for overnight. Afterwards, each strip was thoroughly washed four times with 1xPBST for 5 min each, and then reacted with horse-radish peroxidase (HRP)-conjugated goat anti-feline IgG (Southern Biotech, USA) at dilution of 1: 1000 with a diluent (5% skimmed milk in 1xPBST), for 1 hr. By then, the washing steps with 1xPBST for 4 times 5 min each was done with the same manner. Finally, the color reaction was developed by adding 6 mg 3,3'-diaminobenzidine (DAB) substrate (Sigma-Aldrich Inc). Distilled water was used to stop the enzymatic reaction. All the steps were carried out at room temperature using rocking platform shaker. To evaluate specificity and sensitivity of

these antigenic proteins, sera from healthy control cat and other parasites infected cat sera (*Ancylostoma* spp., *Toxocara* spp., *Cystoisospora* spp., *Dipylidium caninum*, *Taenia taeniaeformis*, *Trichuris* spp. and *Strongyloides* spp.) were also tested. The immunoblot strips were scanned using Bio-Rad Image Scanner (Bio-Rad, USA).

## 2.5 LC-MS/MS analysis

The immunogenic bands were cut and subjected to gel tryptic digestion according to in-gel digestion method following the previous study (Chienwichai et al., 2020). Briefly, the gel was destained in 50% acetonitrile (ACN) until colorless and then removed all solution. The 10mM dithiothreitol (DTT) was added to reduce disulfide bonds. After that, the gel pieces were alkylated in 10mM iodoacetamide (IAA) in dark place for 1 hr and the solution was discarded. Then, these gel fragments were added in acetonitrile (ACN) and stored at room temperature for 5 min. After that, proteins in gel plug was immersed in 10ng/ $\mu$ l trypsin and incubated in 30% ACN, at 37°C overnight. Subsequently, the peptide products were extracted from gel fragments using 50% ACN, 0.1% formic acid and kept in -80°C before used. Tryptic peptide sample was then analyzed for amino acid sequences using tandem mass spectrometer coupled with a nano-liquid chromatography system (Thermo Fisher Scientific). Data from mass spectrometry analysis was used to search the sequence against the platyhelminth NCBI database of the MASCOT search engine (Matrix Science, London, UK, <http://www.matrixscience.com/>). The search parameters were accounted for trypsin digest, monoisotopic mass, and allowing a maximum of one missed

cleavage. Peptide and fragment mass tolerance were set as 0.8Da and 0.8Da, respectively. Variable modifications were set to carbamidomethylation of cysteine and oxidation of methionine. According to the data, proteins matched with significant ( $p < 0.05$ ) was reported. Finally, proteins were verified with protein ID scores, peptide matches and percentage of sequence coverage.

## 2.6 Statistical analyses

Sensitivity, specificity, positive predictive value and negative predictive value of each immunogenic band was calculated as described by (Galen, 1980). For further clinical and field practice, cumulative probability of diagnostic potential between immunogenic proteins were also tested.

## 3. Results

### 3.1 Immunopattern specific to platynosomiasis in cats

Regarding to SDS-PAGE and staining results, *P. fastosum* crude worm extracts showed the protein bands with molecular weight ranging from 120 to 13kDa. The distinct bands were appeared at 75kDa, 60kDa, 45kDa, 36kDa, 30kDa, 25kDa, 19kDa, 16kDa and 13kDa (Figure. 24A and 24B). Immunoblotting was performed to determine specific immunogenic pattern to *P. fastosum*-infected cats. As immunoblotting results, 7 major proteins that recognized by sera of *Platynosomum fastosum*-infected cats were determined. Their molecular weights ranging from 72kDa to 13kDa, briefly 72kDa, 60kDa, 53kDa, 43kDa, 37kDa, 30kDa and 13kDa. The immunoreactivity percentage of each antigenic components against sera of *P. fastosum*-infected cats, healthy control cats and other parasites infected cats were shown in (Table. 10). Out

of these 7 major bands, 72kDa, 53kDa and 13kDa were found as immunogenic proteins since their reactivities percentage recognized by infected sera were 81.25% (13/16), 81.25% (13/16) and 62.5% (10/16), respectively. Immunoblotting results for all tested sera sample were shown in (Figure. 25A-C).

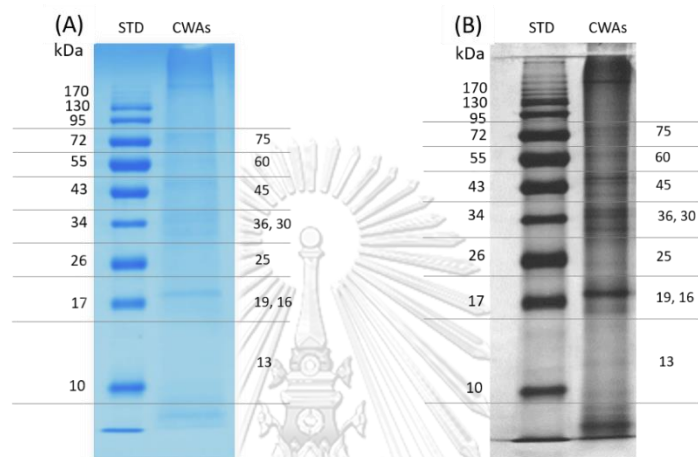


*Figure 24.* SDS-PAGE protein patterns of crude worm antigens of *P. fastosum*.

Crude worm antigens (15 $\mu$ g) were separated by 15% sodium dodecyl sulfate-polyacrylamide gel electrophoresis.

Numbers in right margins revealed different ranges of protein patterns using (A). Coomassie stain; (B). Silver stain.

Note: STD (standard molecular weight marker) and CWAs (crude worm antigens).

Table 10. Reactivities percentage of antigenic components against *P. fastosum*-infected sera, healthy control sera and other parasites infected sera

	72kDa (%)	60kDa (%)	53kDa (%)	43kDa (%)	37kDa (%)	30kDa (%)	13kDa (%)
<i>P. fastosum</i> -infected cases	81.25 (13/16)	31.25 (5/16)	81.25 (13/16)	18.75 (3/16)	25 (4/16)	31.25 (5/16)	62.5 (10/16)
Healthy control	50.00 (4/8)	-	-	-	-	-	-
Other parasites- infected cases	18.18 (4/22)	13.63 (3/22)	-	9.09 (2/22)	-	-	-

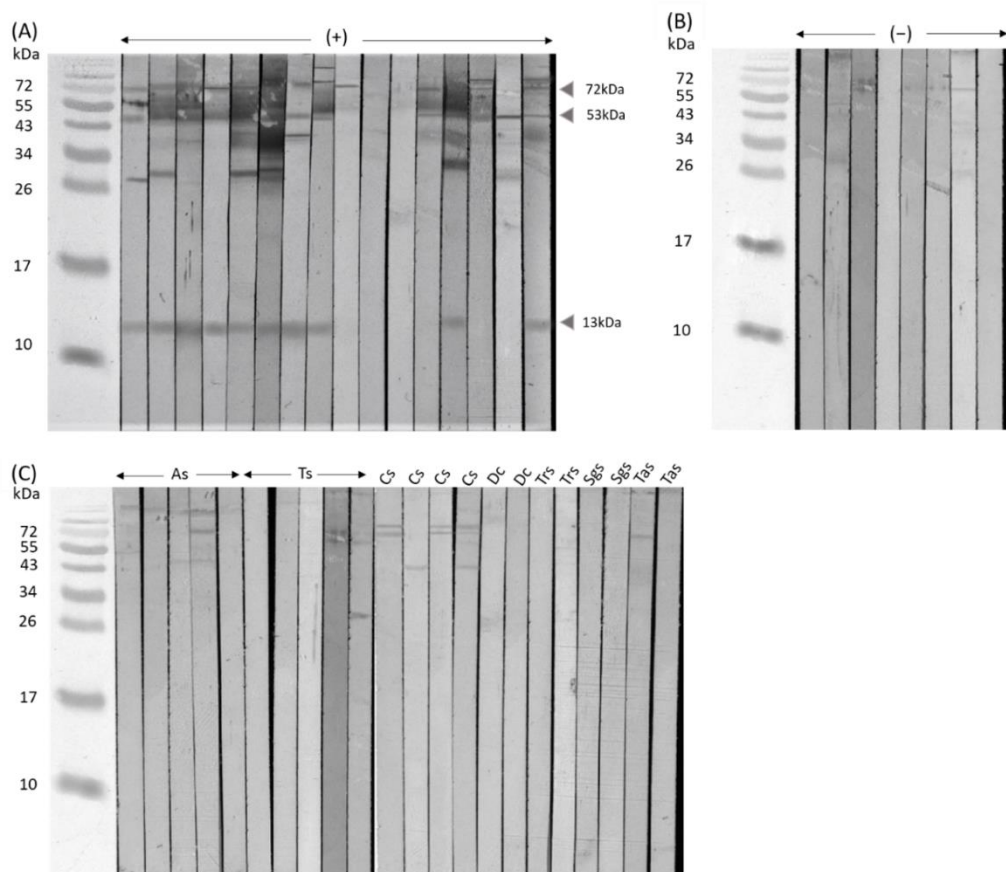


Figure 25. Western blot analyses of *P. fastosum* crude worm antigens using *P. fastosum*-infected cat sera, healthy control sera and other endoparasites infected sera as probes. (A) The bands at 72kDa, 53kDa and 13kDa (arrow head) were detected using sera from *P. fastosum*-infected cats (n, 16) with high percentage of reactivities. (B) The weak band at 72kDa was detected 50% (4 out of 8 cats) using sera from healthy control cats (n, 8). (C) Western blot analyses using sera from other endoparasites infected cats (n, 22)

Note: As, *Ancylostoma* spp.; Ts, *Toxocara* spp.; Cs, *Cystoisospora* spp.; Dc, *Dipylidium caninum*; Trs, *Trichuris* spp.; Sgs, *Strongyloides* spp. and Tas, *Taenia taeniaeformis*.

### 3.2 Analysis of sensitivity, specificity and predictive values

The calculated individual and cumulative sensitivity, specificity, positive predictive values and negative predictive values between these three immunogenic bands were shown in (Table. 11). Of these three bands, 53kDa and 13kDa showed 100% specificity whereas 72kDa with 78.94%. The sensitivity of 84.21% was shown in 72kDa and 53kDa while 72.72% in 13kDa. Cumulative sensitivity and specificity between these three immunogenic bands was calculated with the option either/or and both/and. With the option either/or, the sensitivity percentage was shifted, in case specificity was slightly decreased. However, when we analyzed either 53kDa or 13kDa, both sensitivity and specificity became higher, 88.88% and 100%, respectively. With regard to both/and condition, specificity was shifted to 100% in all cases, but sensitivity was lessened.



Table 11. Cumulative sensitivity, specificity, positive predictive value and negative predictive value of potential antigenic bands

	Sensitivity (%)	Specificity (%)	Predictive values (%)	
			Positive	Negative
72 kDa	84.21	78.94	66.66	90.90
53 kDa	84.21	100	100	90.90
13 kDa	72.72	100	100	83.33
72 or 53 kDa	94.11	78.94	66.66	96.77
72 or 13 kDa	88.88	78.94	66.66	93.75
53 or 13 kDa	<b>88.88</b>	<b>100</b>	100	93.75
72 and 53 kDa	<b>84.21</b>	<b>100</b>	100	90.90
72 and 13 kDa	69.56	100	100	81.08
53 and 13 kDa	69.56	100	100	81.08
72, 53 and 13 kDa	69.56	100	100	81.08

Note: High percentage of sensitivities and specificities (in bold) were occurred in two conditions i.e., using either 53kDa or 13kDa and using both 72kDa and 53kDa.

### 3.3 Mass spectrometry analysis

After immunoblot analysis, identification of potential candidate proteins was done using a nano LC-MS/MS. Briefly, bands of interest were excised and digested with trypsin. The resulted peptide digests were then identified using a nano LC-MS/MS. According to Mascot results, 70kDa heat shock protein (HSP70) of *Paragonimus westermani*, hypothetical protein (CRM22\_002083) (ATP synthase subunit beta) of *Opisthorchis felinus* and histone H2B proteins of *Trichobilharzia regenti* were exhibited highest MS score and number of peptides matches for 72kDa, 53kDa and 13kDa bands, respectively. The identified protein accession no. in database, protein scores, theoretical molecular weight and peptide matches were shown in (Table. 12).

Table 12. Identification of candidate proteins from crude worm extracts of *P. fastosum* using a nano LC-MS/MS

Protein (MW)	Protein (helminths)	Accession no.	Theoretical MW	Protein score	No. of matched peptides
72kDa	70kDa Heat shock protein ( <i>Paragonimus westermani</i> )	KAA3675093.1	70	658	34
53kDa	Hypothetical protein CRM22_002083 (ATP synthase subunit $\beta$ ) ( <i>Opisthorchis felineus</i> )	TGZ72442.1	55	236	15
13kDa	Histone H2B ( <i>Trichobilharzia regenti</i> )	VDQ05944.1	13	82	4

Note: MW, molecular weight.

#### 4 Discussion

Nowadays, large number of *P. fastosum*-infected cats were diagnosed at the necropsy table, stated that the disease is still overlooked and mostly asymptomatic (Basu and Charles, 2014). Since neoplastic changes in biliary epithelium has been reported, *P. fastosum* was considered as etiologic agent for cholangiocarcinoma (Andrade et al., 2012). Despite of its significance, the genomics dataset of cat liver fluke *P. fastosum* still poorly understood. Serodiagnosis approach become great interest since it could detect presence of parasite even in prepatent period (Revilla-Nuin et al., 2005). For PCR-based techniques, extraction of DNA from the fecal egg sample could be difficult due to presence of PCR inhibitors (Nunes et al., 2006) and it has not been applied onsite clinics since it required expensive equipment and trained personnel (Chan et al., 2016). Considering these scenarios, early serodiagnosis tool intervention become crucial. Up to present, there was no information about *P. fastosum* antigen/s that might be useful to devise serodiagnosis tool. Herein, crude worm antigens (CWAs) of *P. fastosum* was investigated. Three proteins were

considered as immunogenic and further analyzed by liquid chromatography tandem mass spectrometry.

According to SDS PAGE, the protein patterns from CWAs of *P. fastosum* ranged between 120kDa to 13kDa. After immunoblotting, there were 7 major proteins of molecular weights ranging from 72kDa to 13kDa were tested against sera of *P. fastosum*-infected cat. Briefly, 72kDa, 60kDa, 53kDa, 43kDa, 37kDa, 30kDa and 13kDa. With regard to immunoreactivity percentage, 72kDa, 53kDa and 13kDa showed high percentage of immunoreactivities 81.25%, 81.25% and 62.5%, respectively. Although 72kDa showed 81.25% immunoreactivity with *P. fastosum* infected sera, this protein was found to be reacted with sera from healthy control cats. It could probably be due to presence of previous infection, resulting in remaining antibodies whereas sera sample in current study were collected at a particular time point.

To validate serodiagnosis potential for further clinical usage, cumulative sensitivity and specificity percentage of these three immunogenic proteins were analyzed. With regard to sensitivity, 72kDa and 53kDa showed 84.21% whereas 72.72% for 13kDa. However, sensitivity was shifted, if choosing either/or condition of three proteins. Thus, the option either/or should be used to address *P. fastosum* infected cat with impress sensitivity values within three proteins. However, 100% specificity was shown for 53kDa and 13kDa, while 78.94% only for 72kDa. Interestingly, if we tested 72kDa combined with 53kDa protein, specificity reached to 100% with remain unchanged sensitivity value. Within three immunogenic proteins,

100% specificity occurred in two conditions, i.e., using either 53kDa or 13kDa and using both 72kDa and 53kDa to rule out non-infected cases. Considering these facts, we suggested that either 53kDa or 13kDa might be allowed for definite diagnosis in feline platynosomiasis with high sensitivity and specificity value 88.88% and 100%, respectively.

Quite a few studies have been investigated for diagnostic potential of antigen/s from parasite crude worm extracts. For instance, 37kDa and 28kDa antigens from CWAs of *C. sinensis*, in which recombinant cathepsin L protease (35kDa) was revealed as reliable diagnostic antigen with high sensitivity and specificity, 96% and 96.2%, respectively (Nagano et al., 2004). Besides, diagnostic value of recombinant 70kDa heat shock protein has been analyzed out of six immunodominant proteins (120kDa, 110kDa, 95kDa, 80kDa, 70kDa and 65kDa) in schistosomiasis (Kanamura et al., 2002; Sulahian et al., 2005). Moreover, 100kDa, 70kDa, 43kDa and 37kDa were considered as major immunoreactive bands for *O. viverrini* infection, followed by evaluating diagnostic potential of recombinant cathepsin B1 (44kDa) (Choi et al., 2003; Sripa et al., 2012). Compared to these helminths, *P. fastosum* revealed specific immunodominant antigens of 72kDa, 53kDa and 13kDa. It has been noted, recombinant antigens are reliable and more practical to use in serodiagnosis since it avoid cross reactivities and can be reproducible (Makarova et al., 2005). So, it might be beneficial if we could pursue further recombinant protein production. However,

the recombinant technique is solely relied on the existing database while very limited sequences were available for *P. fastosum*.

Recently, 70kDa protein was reported as immunogenic in trematode species, such as *D. dendriticum*, *O. viverrini* and *C. sinensis* (Choi et al., 2003; Meshgi and Khodaveisi, 2014). Furthermore, serodiagnosis potential of 52kDa protein for fasciolosis (Itagaki et al., 1995) and diagnostic value of this protein in paramphistomiasis (Anuracpreeda et al., 2008) have been reported previously. So, it was interesting to see 72kDa and 53kDa proteins as immunogenic in current study in case of more or less difference in percentage of separating gel.

Previously, number of low molecular weight proteins were considered as immunodiagnostic potential. In brief, 12-14kDa in fasciolosis (Sobhon et al., 1998), 16kDa in paramphistomiasis (Anuracpreeda et al., 2016), 12.8kDa in schistosomiasis (Carvalho et al., 2011) and 8kDa in clonorchiasis (Chung et al., 2002). Thus, low molecular weight proteins of 13kDa in our study might be critical and supports further development for serodiagnosis.

The identified sequences of these candidate protein bands might not be able to compare with same species, however we have been able to check with other closely related helminths. On the aspect of LC-MS/MS analysis, 70kDa heat shock protein (HSP70), hypothetical protein (CRM22\_002083) (ATP synthase subunit beta) and histone H2B proteins were determined as most significant proteins for resulted three immunogenic protein bands.

To our knowledge, heat shock proteins were considered as molecular chaperones and classified into different families according to their molecular weights. It has been noted that, their main function involved in protein synthesis, modifying processes and several immune responses (Abaza, 2014). Since HSPs are capable of eliciting pro and anti-inflammatory cytokines, these proteins also play pivotal role in innate immune response. Due to multi-host life cycle of parasite, they have to overcome dissimilar growth throughout their biological cycle. Then, parasite heat shock proteins plays an integral part to settle down in hostile environment by mediating environmental stresses and cellular homeostasis (Mayer and Bukau, 2005). Because of wide expression of 70 kDa heat shock protein (HSP70) in different organisms, the role of HSP70 become critical with various purposes such as biomarker validation and molecular phylogenetic studies (Polla, 1991; Borchiellini et al., 1998; Smith et al., 2008). Moreover, heat shock proteins have been considered as parasite' major immunogens by analyzing humoral immune response (Sotillo et al., 2008) and immunohistochemistry studies as well (Higon et al., 2008). As previously described, the fusion of bovine heat shock proteins and DNA vaccines encoded with triose phosphate isomerase (SjCTPI) or the tetraspanin membrane protein (SjC23) of *S. japonicum* was shown to reduce fecal miracidial hatching, which in turn reduced in worm burden and transmission of schistosomiasis (Da dara et al., 2008). Despite of their role in vaccine intervention for infectious disease (Tascon et al., 1996) and cancer related diseases (Colaco, 2013), HSP70 was also considered as diagnostic

candidate for helminth infections such as schistosomiasis, echinococcosis and trichinellosis (Kanamura et al., 2002; Sotillo et al., 2008; Liu et al., 2009; Wang et al., 2009). Besides, recombinant major egg antigen (heat shock proteins) of *P. westermani* is shown to be target antigen for serodiagnosis of paragonimiasis (Lee et al., 2007). So, we suggested that HSP70 proteins could be major constituents of crude worm extracts of *P. fastosum* and could be useful as candidate antigen for immunodiagnosis.

Herein, 53kDa protein appear to be involved in ATP synthesis as ATP synthase  $\beta$  subunit. The mitochondrial ATP synthase is a complex enzyme with multi-subunit that essential for oxidative phosphorylation under physiological condition. Beside this, ATP synthase plays critical role in number of mitochondrial functions. Briefly, reactive oxygen species (ROS) formation,  $\text{Ca}^{2+}$  homeostasis and participate on different aspects of tumor growth as well. Moreover, desensitization of permeability transition pore (PTP) by ATP synthase was found to promote apoptosis in primary phase of cancer development. Since abnormal regulation of ATP synthase subunits has been occurred in different cancer cell lines, thus this enzyme was considered as novel target for cancer treatment regime (Galber et al., 2020). As previously described, ATPase play vital role in nematodes biochemical metabolism and located mainly in mitochondria, intracellular fluid and also microsomes. So, ATPase might be potential enzyme that can carry acquired facts about parasite behavior and infections (Dhaka et al., 2016). Interestingly, ATP synthase was described as one of

the most abundant protein from *S. mekongi* eggs (Thiangtrongjit et al., 2018) and *O. viverrini* adult fluke (Mulvenna et al., 2010). Considering transmission and protective measures of malaria via mosquitoes, ATP synthase subunit gene was disrupted by ablating the protein that converts ADP to ATP (Strum et al., 2015). Up to present, very limited studies have been done to investigate involvement of this enzyme in helminth infection. Since parasite mitochondria plays pivotal role in parasite survival and host environmental adaptation (Kita et al., 2001), it still need to validate their prospective roles in diagnosis of *P. fastosum* infection.

So far, 13 H2B isoforms were informed relating to their role in post translational modifications such as acetylation, methylation and phosphorylation (Peterson and Lanier, 2004). Considering, histones were involved in immune response via producing antimicrobial protein from their N-terminus end (Li et al., 2007). Recently, histones was shown to be targeted proteins against parasitic infection associating with their activities for new therapies (Nawaz et al., 2020). With regard to parasite complex life cycle, histone proteins play pivotal role in epigenetic mechanism especially parasite development and environmental cues through post translational modifications mediated by chromatin linked proteins (Vilcinskas, 2016). Despite their unclear role, upregulation of histones in transcript level could provoke chromatin modifications, and thus result in misfolding or packaging chromatin which may lead to DNA damage (Molden et al., 2015). Therefore, targeting of parasite chromatin proteins become great interest. It has been established that



histones was involved in chromatin remodeling, which is important for regulating transcription level of *T. brucei* (Lowell et al., 2005). As previously described, histone was shown to be secreted copiously in secretory products of *F. hepatica* sporocysts, *S. japonicum* and *O. viverrini* (Gourbal et al., 2008; Mulvenna et al., 2010; Liu et al., 2015). Moreover, *P. falciparum* histones were recently demonstrated as causal agent that involved in pathogenesis of cerebral malaria (Moxon et al., 2020). So, it was interesting to see this protein as immunogenic in current study. However, diagnostic potential of histone in helminth infection have not been identified yet. So, this study addressed histone protein as neglected novel antigen and thus the possibility of recombinant histone protein should be further pursued for diagnosis of feline platynosomiasis.

Up to present, limited sequences of *P. fastosum* were deposited in gene bank whereas whole genome map has not been available. So, it could not be able to perform further recombinant studies for these three immunogenic proteins. To solve this, construction of genome database need to be done promptly. Nonetheless of database, we have investigated three immunogenic proteins with their diagnostic potential for further clinical application.

This study has been focused on potential protein that could involve in *P. fastosum* infection. However, study limitations are still existing. Firstly, lack of database has been made comparison of resulted peptide sequences with closely related helminths. Secondly, we did not compare the results using other cat liver

fluke, *O. felineus* infected cat sera since only *P. fastosum*-infected cat sera was available in current study. But, as far as authors' knowledge, there was no previous study about antigenic components and possible candidate antigen/s of *P. fastosum*. Our results indicated the potential utility of three immunogenic proteins in clinical and field studies with high diagnostic value.

## 5. Conclusion

This study is the first attempt to address the specific antigens that should be further used for serodiagnosis of *P. fastosum* infection. Since most of the infected cats were later diagnosed at necropsy table, serodiagnosis would be helpful to determine presence of infection whether light infection or biliary obstruction case. We have investigated diagnostic potential of three immunogenic proteins. As early diagnosis could favor proper care and treatment in time, it might be able to use appropriate drugs to rescue. Although genome database unavailable, further utility of three immunogenic proteins for serodiagnosis tool intervention were discussed. In veterinary practice, it should be applied for both clinical diagnosis and field studies with large sample size.

## Acknowledgements

This research was financially supported to WS by the grant of Faculty of Veterinary Science, Feline Health and Infectious Disease Research Unit, Animal Vector-Borne Disease Research Unit, Chulalongkorn University. In addition, this research was financially supported to Babi Kyi Soe by the 90<sup>th</sup> Anniversary of

Chulalongkorn University Scholarships (Rachadaphiseksomphot Endowment Fund), Grant of Faculty of Veterinary Science, Chulalongkorn University. Authors would like to gratefully thank Prof. Dr. Chollada Buranakarl and the Department of Livestock Development for the opportunity to join the public veterinary services. Authors would like to gratitude undergraduate students and Ms. Shin Moe Aoke for participating sample collection to do this research. Moreover, authors would like to thank the staff from Department of Helminthology, Faculty of Tropical Medicine, Mahidol University for their kind support.



## References

- Abaza, S. 2014. Heat shock proteins and parasitic diseases: Part 1: Helminths. 7(2), 93-103. doi:10.4103/1687-7942.149556
- Adisakwattana, P., Viyanant, V., Chaicumpa, W., Vichasri-Grams, S., Hofmann, A., Korge, G. and Grams, R. 2007. Comparative molecular analysis of two asparaginyl endopeptidases and encoding genes from *Fasciola gigantica*. Mol. Biochem. Parasitol., 156(2), 102-116.
- Aebersold, R. and Mann, M. 2003. Mass spectrometry-based proteomics. Nature, 422(6928), 198-207.
- Andrade, R.L., Dantas, A.F., Pimentel, L.A., Galiza, G.J., Carvalho, F.K., Costa, V.M. and Riet-Correa, F. 2012. *Platynosomum fastosum*-induced cholangiocarcinomas in cats. Vet. Parasitol., 190(1-2), 277-280. doi:10.1016/j.vetpar.2012.04.015
- Anuracpreeda, P., Chawengkirttikul, R. and Sobhon, P. 2016. Antigenic profile, isolation and characterization of whole body extract of *Paramphistomum gracile*. Parasite Immunol., 38(7), 431-438. doi:10.1111/pim.12330
- Anuracpreeda, P., Wanichanon, C. and Sobhon, P. 2008. *Paramphistomum cervi*: Antigenic profile of adults as recognized by infected cattle sera. Exp. Parasitol., 118(2), 203-207.
- Basu, A.K. and Charles, R.A. 2014. A review of the cat liver fluke *Platynosomum fastosum* Kossack, 1910 (Trematoda: Dicrocoeliidae). Vet. Parasitol., 200(1-2), 1-7. doi:10.1016/j.vetpar.2013.12.016
- Boamah, D., Kikuchi, M., Huy, N.T., Okamoto, K., Chen, H., Ayi, I. and Hirayama, K. 2012. Immunoproteomics identification of major IgE and IgG4 reactive *Schistosoma japonicum* adult worm antigens using chronically infected human plasma. Tropical medicine and health.
- Borchiellini, C., Boury-Esnault, N., Vacelet, J. and Le Parco, Y. 1998. Phylogenetic analysis of the Hsp70 sequences reveals the monophyly of Metazoa and specific phylogenetic relationships between animals and fungi. Mol. Bio. Evol., 15(6), 647-655.

- Bradford, N. 1976. A rapid and sensitive method for the quantitation microgram quantities of a protein isolated from red cell membranes. *Anal. Biochem.*, 72(248), e254.
- Carreira, V.S., Vieira, R.F., Machado, G.F. and Luvizotto, M.C. 2008. Feline cholangitis/cholangiohepatitis complex secondary to *Platynosomum fastosum* infection in a cat. *Revista Brasileira de Parasitologia Veterinária*, 17(1), 184-187.
- Carvalho, G.B., Silva-Pereira, R.A., Pacifico, L.G. and Fonseca, C.T. 2011. Identification of *Schistosoma mansoni* candidate antigens for diagnosis of schistosomiasis. *Mem Inst Oswaldo Cruz*, 106(7), 837-843. doi:10.1590/s0074-02762011000700009
- Chan, K., Wong, P.Y., Yu, P., Hardick, J., Wong, K.Y., Wilson, S.A. and Wong, S.S. 2016. A rapid and low-cost PCR thermal cycler for infectious disease diagnostics. *PloS one*, 11(2), e0149150.
- Chemale, G., Perally, S., LaCourse, E.J., Prescott, M.C., Jones, L.M., Ward, D. and Brophy, P.M. 2010. Comparative proteomic analysis of triclabendazole response in the liver fluke *Fasciola hepatica*. *J. Proteome Res.*, 9(10), 4940-4951. doi:10.1021/pr1000785
- Chen, J., Xu, H., Zhang, Z., Zeng, S., Gan, W., Yu, X. and Hu, X. 2011. Cloning and expression of 21.1-kDa tegumental protein of *Clonorchis sinensis* and human antibody response to it as a trematode–nematode pan-specific serodiagnosis antigen. *Parasitol. Res.*, 108(1), 161-168.
- Chienwichai, P., Ampawong, S., Adisakwattana, P., Thiangtrongjit, T., Limpanont, Y., Chusongsang, P. and Reamtong, O. 2020. Effect of Praziquantel on *Schistosoma mekongi* Proteome and Phosphoproteome. *Pathogens*, 9(6), 417.
- Choi, M.H., Ryu, J.S., Lee, M., Li, S., Chung, B.S., Chai, J.Y. and Hong, S.T. 2003. Specific and common antigens of *Clonorchis sinensis* and *Opisthorchis viverrini* (Opisthorchidae, Trematoda). *The Korean J. Parasitol.*, 41(3), 155.
- Chung, Y.B., Lee, M., Yang, H.J., Chung, B.S., Lee, S.Y., Choi, M.H. and Hong, S.T. 2002. Characterization of partially purified 8 kDa antigenic protein of *Clonorchis sinensis*. *The Korean J. Parasitol.*, 40(2), 83.

- Colaco, C. 2013. Autologous heat-shock protein vaccines. *Human vaccines & immunotherapeutics*, 9(2), 275-276.
- Da'dara, A.A., Li, Y.S., Xiong, T., Zhou, J., Williams, G.M., McManus, D.P. and Harn, D.A. 2008. DNA-based vaccines protect against zoonotic schistosomiasis in water buffalo. *Vaccine*, 26(29-30), 3617-3625. doi:10.1016/j.vaccine.2008.04.080
- Dar, J., Ganai, B., Shahardar, R. and Zargar, U. 2019. Molecular characterization and Immunodiagnostic potential of various antigenic proteins of *Fasciola gigantica* species isolated from sheep of North-West Himalayan Region. *Helminth.*, 56(2), 93-107.
- Dea-Ayuela, M.A., Rama-Iñiguez, S. and Bolás-Fernández, F. 2006. Proteomic analysis of antigens from *Leishmania infantum* promastigotes. *Proteomics*, 6(14), 4187-4194.
- Dhaka, M.S., Srivastava, S. and Bhattacharya, S.M. 2016. Role and Significance of Various ATPases of Nematode Parasites. In *Regulation of Ca<sup>2+</sup>-ATPases, V-ATPases and F-ATPases* (pp. 567-576): Springer.
- Galber, C., Acosta, M.J., Minervini, G. and Giorgio, V. 2020. The role of mitochondrial ATP synthase in cancer. *Bio. Chem.*, 401(11), 1199-1214.
- Galen, R.S. 1980. Predictive value and efficiency of laboratory testing. *Pediatric Clinics of North America*, 27(4), 861-869.
- González-Miguel, J., Morchón, R., Mellado, I., Carretón, E., Montoya-Alonso, J.A. and Simón, F. 2012. Excretory/secretory antigens from *Dirofilaria immitis* adult worms interact with the host fibrinolytic system involving the vascular endothelium. *Mol. Biochem. Parasitol.*, 181(2), 134-140.
- Gourbal, B.E., Guillou, F., Mitta, G., Sibille, P., Thèron, A., Pointier, J.P. and Coustau, C. 2008. Excretory–secretory products of larval *Fasciola hepatica* investigated using a two-dimensional proteomic approach. *Mol. Biochem. Parasitol.*, 161(1), 63-66.
- Higón, M., Monteagudo, C., Fried, B., Esteban, J., Toledo, R. and Marcilla, A. 2008. Molecular cloning and characterization of *Echinostoma caproni* heat shock protein-70 and differential expression in the parasite derived from low-and high-compatible hosts. *Parasitol.*, 135(12), 1469.

- Itagaki, T., Sakamoto, T. and Itagaki, H. 1995. Analysis of *Fasciola* spp. antigen by enzyme-linked immunotransfer blot using sera from experimentally and naturally infected cattle. *J. Vet. Med. Sci.*, 57(3), 511-513. doi:10.1292/jvms.57.511
- Jitsamai, W., Khrutkham, N., Hunprasit, V., Chandrashekar, R., Bowman, D. and Sukhumavasi, W. 2021. Prevalence of endoparasitic and viral infections in client-owned cats in metropolitan Bangkok, Thailand, and the risk factors associated with feline hookworm infections. *Vet. Parasitol., Regional Studies and Reports*, 100584.
- Kanamura, H.Y., Hancock, K., Rodrigues, V. and Damian, R.T. 2002. *Schistosoma mansoni* heat shock protein 70 elicits an early humoral immune response in *S. mansoni* infected baboons. *Memorias do Instituto Oswaldo Cruz*, 97(5), 711-716.
- Khoontawad, J., Laothong, U., Roytrakul, S., Pinlaor, P., Mulvenna, J., Wongkham, C. and Sithithaworn, P. 2012. Proteomic identification of plasma protein tyrosine phosphatase alpha and fibronectin associated with liver fluke, *Opisthorchis viverrini*, infection. *PloS one*, 7(9), e45460.
- Kita, K., Miyadera, H., Saruta, F., & Miyoshi, H. 2001. Parasite mitochondria as a target for chemotherapy. *J. Heal. Sci.*, 47(3), 219-239.
- Knaus, M., Rapti, D., Shukullari, E., Kusi, I., Postoli, R., Xhaxhiu, D. and Winter, R. 2014. Characterisation of ecto-and endoparasites in domestic cats from Tirana, Albania. *Parasitol. Res.*, 113(9), 3361-3371.
- Laemmli, U.K. 1970. Cleavage of structural proteins during the assembly of the head of bacteriophage T4. *Nature*, 227(5259), 680-685. doi:10.1038/227680a0
- Lathroum, C.N., Shell, L., Neuville, K. and Ketzis, J.K. 2018. Efficacy of Praziquantel in the Treatment of *Platynosomum fastosum* in Cats with Natural Infections. *Vet. Sci.*, 5(2), 35.
- Lee, J.S., Lee, J., Kim, S.H. and Yong, T.S. 2007. Molecular cloning and characterization of a major egg antigen in *Paragonimus westermani* and its use in ELISA for the immunodiagnosis of paragonimiasis. *Parasitol. Res.*, 100(4), 677-681. doi:10.1007/s00436-006-0324-7

- Li, C., Song, L., Zhao, J., Zhu, L., Zou, H., Zhang, H. and Cai, Z. 2007. Preliminary study on a potential antibacterial peptide derived from histone H2A in hemocytes of scallop *Chlamys farreri*. *Fish & shellfish Immunol.*, 22(6), 663-672.
- Makarova, E., Goes, T., Leite, M. and Goes, A. 2005. Detection of IgG binding to *Schistosoma mansoni* recombinant protein RP26 is a sensitive and specific method for acute schistosomiasis diagnosis. *Parasitol. Intern.*, 54(1), 69-74.
- Mayer, M. and Bukau, B. 2005. Hsp70 chaperones: cellular functions and molecular mechanism. *Cell. Mol. Life Sci.*, 62(6), 670-684.
- Meshgi, B. and Khodaveisi, M. 2014. Determination of immunodominant antigens of *Dicrocoelium dendriticum* by hyperimmune sera. *Immunol. Infect. Dis.*, 2(1), 4-8.
- Molden, R.C., Bhanu, N.V., LeRoy, G., Arnaudo, A.M. and Garcia, B.A. 2015. Multifaceted quantitative proteomics analysis of histone H2B isoforms and their modifications. *Epigenetics & chromatin*, 8(1), 1-17.
- Moxon, C.A., Alhamdi, Y., Storm, J., Toh, J.M., McGuinness, D., Ko, J.Y. and Seydel, K.B. 2020. Parasite histones are toxic to brain endothelium and link blood barrier breakdown and thrombosis in cerebral malaria. *Blood Adv.*, 4(13), 2851-2864.
- Mulvenna, J., Sripa, B., Brindley, P.J., Gorman, J., Jones, M.K., Colgrave, M.L., Suttiaprapa, S. 2010. The secreted and surface proteomes of the adult stage of the carcinogenic human liver fluke *Opisthorchis viverrini*. *Proteomics.*, 10(5), 1063-1078.
- Nagano, I., Pei, F., Wu, Z., Wu, J., Cui, H., Boonmars, T. and Takahashi, Y. 2004. Molecular expression of a cysteine proteinase of *Clonorchis sinensis* and its application to an enzyme-linked immunosorbent assay for immunodiagnosis of clonorchiasis. *Clin. Dia. lab. Immunol.*, 11(2), 411.
- Nawaz, M., Malik, I., Hameed, M., Kuthu, Z.H. and Zhou, J. 2020. Modifications of histones in parasites as drug targets. *Vet. Parasitol.*, 278: 109029.
- Ndao, M., Spithill, T.W., Caffrey, R., Li, H., Podust, V.N., Perichon, R. and Powell, M.R. 2010. Identification of novel diagnostic serum biomarkers for Chagas' disease in asymptomatic subjects by mass spectrometric profiling. *J. Clin. Microbiol.*, 48(4), 1139.



- Ngoc, D.P., Arimatsu, Y., Kaewkes, S. and Sripa, B. 2015. Characterization of immunogenic *Clonorchis sinensis* protein fractions by gel filtration chromatography. *Asian Pacific J. Trop. Dis.*, 5(4), 284-288.
- Nguyen, H.M., Van Hoang, H. and Ho, L.T. 2017. *Platynosomum fastosum* (Trematoda: Dicrocoeliidae) from cats in Vietnam: morphological redescription and molecular phylogenetics. *The Korean J. Parasitol.*, 55(1), 39.
- Nuamtanong, S., Reamtong, O., Phuphisut, O., Chotsiri, P., Malaithong, P., Dekumyoy, P. and Adisakwattana, P. 2019. Transcriptome and excretory–secretory proteome of infective-stage larvae of the nematode *Gnathostoma spinigerum* reveal potential immunodiagnostic targets for development. *Parasite.*, 26.
- Peterson, C.L. and Laniel, M.A. 2004. Histones and histone modifications. *Current Biol.*, 14(14), R546-R551.
- Pinto, H.A., Mati, V.L. and de Melo, A.L. 2014. New insights into the life cycle of *Platynosomum* (Trematoda: Dicrocoeliidae). *Parasitol. Res.*, 113(7), 2701-2707. doi:10.1007/s00436-014-3926-5
- Pinto, H.A., Pulido-Murillo, E.A., Braga, R.R., Mati, V.L., Melo, A.L. and Tkach, V.V. 2018. DNA sequences confirm low specificity to definitive host and wide distribution of the cat pathogen *Platynosomum illiciens* (= *P. fastosum*)(Trematoda: Dicrocoeliidae). *Parasitol. Res.*, 117(6), 1975-1978.
- Polla, B.S. 1991. Heat shock proteins in host-parasite interactions. *Immunol. today*, 12(3), A38-A41.
- Ramos, R.A., Lima, V.F., Monteiro, M., Andrade - Santana, M., Lepold, R., Da Gloria Faustino, M. and Cringoli, G. 2015. New insights into diagnosis of *Platynosomum fastosum* (Trematoda: Dicrocoeliidae) in cats. *Parasitol. Res.*, 115. doi:10.1007/s00436-015-4763-x
- Reamtong, O. 2008. Mass spectrometry-based parasitic proteomics.
- Revilla-Nuín, B., Manga-González, M.Y., Miñambres, B. and González-Lanza, C. 2005. Partial characterization and isolation of 130 kDa antigenic protein of *Dicrocoelium dendriticum* adults. *Vet. Parasitol.*, 134(3-4), 229-240.
- Rojekittikhun, W., Prummongkol, S., Puangsa-art, S., Chaisiri, K. and Kusolsuk, T. 2013. Prevalence of Gastrointestinal Parasitic Infections in Refuge Dogs and Cats and

- Evaluation of Two Conventional Examination Techniques. *J. Trop. Med. Parasitol.*, 36, 58-67.
- Rojekittikhun, W., Mahittikorn, A., Prummongkol, S., Puangsa-art, S., Chaisiri, K. and Kusolsuk, T. 2015. Evaluation of Sugar Flotation and Formalin-Ether Concentration Techniques in the Examination of GI Parasites of Refuge Dogs and Cats in Kanchanaburi Province, Thailand. *The Journal.*, 38(1), 18.
- Shell, L., Ketzis, J., Hall, R., Rawlins, G. and du Plessis, W. 2015. Praziquantel treatment for *Platynosomum* species infection of a domestic cat on St Kitts, West Indies. *J. Feline. Med. Surg.*, 1(1), 2055116915589834.
- Smith, R.E., Spithill, T.W., Pike, R.N., Meeusen, E.N. and Piedrafita, D. 2008. *Fasciola hepatica* and *Fasciola gigantica*: Cloning and characterization of 70 kDa heat-shock proteins reveals variation in HSP70 gene expression between parasite species recovered from sheep. *Exp. Parasitol.*, 118(4), 536-542.
- Sotillo, J., Valero, L., Sanchez Del Pino, M., Fried, B., Esteban, J., Marcilla, A. and Toledo, R. 2008. Identification of antigenic proteins from *Echinostoma caproni* (Trematoda) recognized by mouse immunoglobulins M, A and G using an immunoproteomic approach. *Parasite Immunol.*, 30(5), 271-279.
- Sripa, J., Brindley, P.J., Sripa, B., Loukas, A., Kaewkes, S. and Laha, T. 2012. Evaluation of liver fluke recombinant cathepsin B-1 protease as a serodiagnostic antigen for human opisthorchiasis. *Parasitol. Int.*, 61(1), 191-195. doi:10.1016/j.parint.2011.05.009
- Sturm, A., Mollard, V., Cozijnsen, A., Goodman, C.D. and McFadden, G.I. 2015. Mitochondrial ATP synthase is dispensable in blood-stage *Plasmodium berghei* rodent malaria but essential in the mosquito phase. *Proceedings of the National Academy of Sciences*, 112(33), 10216-10223.
- Sulahian, A., Garin, Y.J.F., Izri, A., Verret, C., Delaunay, P., van Gool, T. and Derouin, F. 2005. Development and evaluation of a Western blot kit for diagnosis of schistosomiasis. *Clin. Dia. Lab. Immunol.*, 12(4), 548.
- Tascon, R.E., Colston, M.J., Ragno, S., Stavropoulos, E., Gregory, D. and LowRIE, D.B. 1996. Vaccination against tuberculosis by DNA injection. *Nature Med.*, 2(8), 888-892.

- Taylor, D. and Perri, S. 1977. Experimental infection of cats with the liver fluke *Platynosomum concinnum*. Am. J. Vet. Res., 38(1), 51-54.
- Thézénas, M.L., Huang, H., Njie, M., Ramaprasad, A., Nwakanma, D.C., Fischer, R. and Kessler, B.M. 2013. PfHPRT: a new biomarker candidate of acute *Plasmodium falciparum* infection. J. Proteome Res., 12(3), 1211-1222.
- Thiangtrongjit, T., Adisakwattana, P., Limpanont, Y., Dekumyoy, P., Nuamtanong, S., Chusongsang, P. and Reamtong, O. 2018. Proteomic and immunomic analysis of *Schistosoma mekongi* egg proteins. Exp. Parasitol., 191, 88-96.
- Towbin, H., Staehelin, T. and Gordon, J. 1979. Electrophoretic transfer of proteins from polyacrylamide gels to nitrocellulose sheets: procedure and some applications. Proc. Natl. Aca. Sci., 76(9), 4350-4354. doi:10.1073/pnas.76.9.4350
- Urbaniak, M.D., Mathieson, T., Bantscheff, M., Eberhard, D., Grimaldi, R., Miranda-Saavedra, D. Wyatt P, Ferguson, M.A., Frearson, J. and Drewes, G. 2012. Chemical proteomic analysis reveals the drug ability of the kinome of *Trypanosoma brucei*. ACS Chem. Biol., 7(11): 1858-1865.
- Victor, B., Kanobana, K., Gabriël, S., Polman, K., Deckers, N., Dorny, P. and Palmblad, M. 2012. Proteomic analysis of *Taenia solium* metacestode excretion–secretion proteins. Proteomics., 12(11), 1860-1869.
- Vilcinskas, A. 2016. The role of epigenetics in host–parasite coevolution: lessons from the model host insects *Galleria mellonella* and *Tribolium castaneum*. Zool., 119(4), 273-280.
- Wang, S., Zhu, X., Yang, Y., Yang, J., Gu, Y., Wei, J. and Cui, S. 2009. Molecular cloning and characterization of heat shock protein 70 from *Trichinella spiralis*. Acta Tropica., 110(1), 46-51.
- Wongkamchai, S., Chiangjong, W., Sinchaikul, S., Chen, S.T., Choochote, W. and Thongboonkerd, V. 2011. Identification of *Brugia malayi* immunogens by an immunoproteomics approach. J. Proteomics., 74(9), 1607-1613.
- Wongratanacheewin, S., Bunnag, D., Vaeusorn, N. and Sirisinha, S. 1988. Characterization of humoral immune response in the serum and bile of patients with opisthorchiasis and its application in immunodiagnosis. Am. J. Trop. Med. Hyg., 38(2), 356-362.

- Xavier, M.A., Tirloni, L., Pinto, A.F., Diedrich, J.K., Yates, J.R., Mulenga, A. and Termignoni, C. 2018. A proteomic insight into vitellogenesis during tick ovary maturation. *Sci. Rep.*, 8(1), 1-14.
- Zhang, F.K., Hu, R.S., Elsheikha, H.M., Sheng, Z.A., Zhang, W.Y., Zheng, W.B. and He, J.J. 2019. Global serum proteomic changes in water buffaloes infected with *Fasciola gigantica*. *Parasite & Vectors.*, 12(1), 1-11.
- Zhou, D., Yuan, Z., Zhao, F., Li, H., Zhou, Y., Lin, R. and Zhu, X. 2011. Modulation of mouse macrophage proteome induced by *Toxoplasma gondii* tachyzoites in vivo. *Parasitol. Res.*, 109(6), 1637-1646.



## Chapter 5

### General discussion, conclusion and further recommendations

This study provided the clinical parameters that could be useful to diagnose for feline platynosomiasis. Hence the recommended dosage for praziquantel is still overlooked, evaluating the efficacy any rational drug become interest. On regards of this, the basic morphological characteristics of *P. fastosum*, both adult worm and eggs were investigated in our study. Since fecal microscopic examination and conventional PCR techniques were not readily available on-site clinics, serodiagnosis is another way to approach for early diagnosis. However, there were no previous reports for potential antigen of *P. fastosum*, that could be used to devise serodiagnosis tool.

First of all, the sample cats in current study did not show noticeable clinical symptoms and thus they were subclinically infected. According to our results, previous strayed cats could be able to carry infection for their lifetime. Blood eosinophilia was occurred in two out of fourteen cats (14.3%), in which these two cats were also infected with *Ancylostoma* spp. and *Toxocara* spp. as helminth infections have been considered as one of the causes for blood eosinophilia (Mehta and Furuta, 2015). As results, ALT, GGT and ALP level were elevated in 57.1%, 57.1% and 21.4%, respectively. Interestingly, a half of *P. fastosum* infected cats showed elevated AFP level without having association with parasite egg count in current study. Two types of tumor markers were used in our study whereas CEA showed

normal ranges. On the aspect of bacterial culture, we found the bacterial growth in four out of fourteen cats, in which these cats showed high number of fluke eggs (625-7800 eggs/ml) in bile. Despite of histopathological findings have performed in current study, the severity of lesions that could lead to sonographic changes still need to discuss. Since bile egg number was significantly different from fecal egg number ( $P=0.001$ ), then PUC technique could more sensitive than fecal microscopy. We have investigated that *P. fastosum* shed the eggs inconsistently by subsequent findings of fluke eggs in the fecal sample. Therefore, routine fecal examination should be performed for the cats with outdoor accessed.

According to morphology, we have investigated morphology of *P. fastosum* adult worms and eggs using stereo and light microscope, scanning electron microscope and transmission electron microscope. Due to presence of strong muscular suckers, the worm could be able to firmly attach biliary epithelial wall and may eventually lead to epithelial cell damage (Krupenko, 2019). The tegument of *P. fastosum* shows corrugating surface with slender villous-like projections structures that might be helpful to enhance ionic exchange and osmolarity (Fujino et al., 1979). Presence of typical and atypical structures of *P. fastosum* eggs were found so, the microscopic examiner should be aware to interpret false negative results. We have investigated that tegumental granules ( $TG_1$  and  $TG_2$ ) can be produced by only one type of tegument cell. Due to presence of microtubules within cytoplasmic process, the granules might be easily transported to the surface tegument (Sobhon and

Upatham, 1990). However, ultrastructural characteristics of parasite developmental stages still need to be discussed.

Three proteins from CWAs of *P. fastosum* were considered as immunogenic and further analyzed by liquid chromatography tandem mass spectrometry. After that, cumulative sensitivity and specificity percentage of these three immunogenic proteins were analyzed. On the aspect of LC-MS/MS analysis, 70kDa heat shock protein (HSP70), hypothetical protein (CRM22\_002083) (ATP synthase subunit beta) and histone H2B proteins were determined as most significant proteins with highest protein scores. Heat shock proteins have been considered as parasite' major immunogens (Sotillo et al., 2008; Higon et al., 2008). ATPase play vital role in nematodes biochemical metabolism and located mainly in mitochondria. Thus, this enzyme could carry acquired information about parasite behavior (Dhaka et al., 2016). Since histones involved in transcriptional modification by DNA methylation, DNA acetylation and chromatin remodeling (Molden et al., 2015). Then, parasite chromatin-linked proteins become great interest. Presence of common antigens with helminths, recombinant protein expression is highly recommended. However, only limited sequences were available for *P. fastosum* while recombinant technique was solely relied on genome database. Nonetheless of database, we have investigated three immunogenic proteins with their diagnostic potential for further clinical application. However, construction of genome database need to be done promptly in case of further recombinant studies.

## Appendix

Table 13. Fecal egg number, bile egg number, blood biochemistry and imaging parameters of *P. fastosum*-infected cats

Cat No.	Fecal egg number (eggs/g)	Bile egg number (eggs/ml)	Blood chemistry						Imaging results			
			ALT	GGT	ALP	BUN	Protein	Liver	Gallbladder	Biliary dilatation		
1.	NF	NF	129	1	85	30.3	6	Enlargement	Normal	Normal		
2.	40	55	114	10	18	25	8	Enlargement	Bile sediment	Dilated		
3.	NF	2750	70	-	35	35.2	7	Enlargement	Bile sediment	Dilated		
4.	33	350	759	10	137	22.3	8.2	Enlargement	Bile sediment	Dilated		
5.	40	178	147	7	26	34.2	7.4	Enlargement	Bile sediment	Dilated		
6.	40	150	48	1	59	19.4	8.1	Normal	Bile sediment	Normal		
7.	40	3300	33	3	38	22.2	10	Normal	Bile sediment	Normal		
8.	NF	NF	46	1	17	35.6	7.1	Enlargement	Normal	Normal		
9.	14	1025	23	2.5	24	20.6	7	Normal	Bile sediment	Dilated		
10.	NF	625	57	4.8	22	19.5	6.5	Enlargement	Bile sediment	Normal		
11.	NF	NF	100	1.3	67	35.3	7.4	Enlargement	Bile sediment	Normal		
12.	201	7800	80	0.9	45	24.7	9	Enlargement	Bile sediment	Dilated		
13.	NF	280	109	6	30	23.3	8.3	Normal	Bile sediment	Dilated		
14.	137	1050	117	2.2	26	29.1	8	Normal	Bile sediment	Normal		



## REFERENCES



จุฬาลงกรณ์มหาวิทยาลัย  
**CHULALONGKORN UNIVERSITY**

## REFERENCES

- Abaza, S. 2014. Heat shock proteins and parasitic diseases: Part 1: Helminths. 7(2), 93-103. doi:10.4103/1687-7942.149556
- Adisakwattana, P., Viyanant, V., Chaicumpa, W., Vichasri-Grams, S., Hofmann, A., Korge, G. and Grams, R. 2007. Comparative molecular analysis of two asparaginyl endopeptidases and encoding genes from *Fasciola gigantica*. Mol. Biochem. Parasitol., 156(2), 102-116.
- Aebersold, R. and Mann, M. 2003. Mass spectrometry-based proteomics. Nature, 422(6928), 198-207.
- Andrade, R.L., Dantas, A.F., Pimentel, L.A., Galiza, G.J., Carvalho, F.K., Costa, V.M. and Riet-Correa, F. 2012. *Platynosomum fastosum*-induced cholangiocarcinomas in cats. Vet. Parasitol., 190(1-2), 277-280. doi:10.1016/j.vetpar.2012.04.015
- Anuracpreeda, P., Chawengkirttikul, R. and Sobhon, P. 2016. Antigenic profile, isolation and characterization of whole body extract of *Paramphistomum gracile*. Parasite Immunol., 38(7), 431-438. doi:10.1111/pim.12330
- Anuracpreeda, P., Wanichanon, C. and Sobhon, P. 2008. *Paramphistomum cervi*: Antigenic profile of adults as recognized by infected cattle sera. Exp. Parasitol., 118(2), 203-207.
- Basu, A.K. and Charles, R.A. 2014. A review of the cat liver fluke *Platynosomum fastosum* Kossack, 1910 (Trematoda: Dicrocoeliidae). Vet. Parasitol., 200(1-2), 1-7. doi:10.1016/j.vetpar.2013.12.016
- Boamah, D., Kikuchi, M., Huy, N.T., Okamoto, K., Chen, H., Ayi, I. and Hirayama, K. 2012. Immunoproteomics identification of major IgE and IgG4 reactive *Schistosoma japonicum* adult worm antigens using chronically infected human plasma. Tropical medicine and health.
- Borchiellini, C., Boury-Esnault, N., Vacelet, J. and Le Parco, Y. 1998. Phylogenetic analysis of the Hsp70 sequences reveals the monophyly of Metazoa and specific phylogenetic relationships between animals and fungi. Mol. Bio. Evol., 15(6), 647-655.

- Bradford, N. 1976. A rapid and sensitive method for the quantitation microgram quantities of a protein isolated from red cell membranes. *Anal. Biochem.*, 72(248), e254.
- Carreira, V.S., Vieira, R.F., Machado, G.F. and Luvizotto, M.C. 2008. Feline cholangitis/cholangiohepatitis complex secondary to *Platynosomum fastosum* infection in a cat. *Revista Brasileira de Parasitologia Veterinária*, 17(1), 184-187.
- Carvalho, G.B., Silva-Pereira, R.A., Pacifico, L.G. and Fonseca, C.T. 2011. Identification of *Schistosoma mansoni* candidate antigens for diagnosis of schistosomiasis. *Mem Inst Oswaldo Cruz*, 106(7), 837-843. doi:10.1590/s0074-02762011000700009
- Chan, K., Wong, P.Y., Yu, P., Hardick, J., Wong, K.Y., Wilson, S.A. and Wong, S.S. 2016. A rapid and low-cost PCR thermal cycler for infectious disease diagnostics. *PloS one*, 11(2), e0149150.
- Chemale, G., Perally, S., LaCourse, E.J., Prescott, M.C., Jones, L.M., Ward, D. and Brophy, P.M. 2010. Comparative proteomic analysis of triclabendazole response in the liver fluke *Fasciola hepatica*. *J. Proteome Res.*, 9(10), 4940-4951. doi:10.1021/pr1000785
- Chen, J., Xu, H., Zhang, Z., Zeng, S., Gan, W., Yu, X. and Hu, X. 2011. Cloning and expression of 21.1-kDa tegumental protein of *Clonorchis sinensis* and human antibody response to it as a trematode–nematode pan-specific serodiagnosis antigen. *Parasitol. Res.*, 108(1), 161-168.
- Chienwichai, P., Ampawong, S., Adisakwattana, P., Thiangtrongjit, T., Limpanont, Y., Chusongsang, P. and Reamtong, O. 2020. Effect of Praziquantel on *Schistosoma mekongi* Proteome and Phosphoproteome. *Pathogens*, 9(6), 417.
- Choi, M.H., Ryu, J.S., Lee, M., Li, S., Chung, B.S., Chai, J.Y. and Hong, S.T. 2003. Specific and common antigens of *Clonorchis sinensis* and *Opisthorchis viverrini* (Opisthorchidae, Trematoda). *The Korean J. Parasitol.*, 41(3), 155.
- Chung, Y.B., Lee, M., Yang, H.J., Chung, B.S., Lee, S.Y., Choi, M.H. and Hong, S.T. 2002. Characterization of partially purified 8 kDa antigenic protein of *Clonorchis sinensis*. *The Korean J. Parasitol.*, 40(2), 83.

- Colaco, C. 2013. Autologous heat-shock protein vaccines. *Human vaccines & immunotherapeutics*, 9(2), 275-276.
- Da'dara, A.A., Li, Y.S., Xiong, T., Zhou, J., Williams, G.M., McManus, D.P. and Harn, D.A. 2008. DNA-based vaccines protect against zoonotic schistosomiasis in water buffalo. *Vaccine*, 26(29-30), 3617-3625. doi:10.1016/j.vaccine.2008.04.080
- Dar, J., Ganai, B., Shahardar, R. and Zargar, U. 2019. Molecular characterization and Immunodiagnostic potential of various antigenic proteins of *Fasciola gigantica* species isolated from sheep of North-West Himalayan Region. *Helminth.*, 56(2), 93-107.
- Dea-Ayuela, M.A., Rama-Iñiguez, S. and Bolás-Fernández, F. 2006. Proteomic analysis of antigens from *Leishmania infantum* promastigotes. *Proteomics*, 6(14), 4187-4194.
- Dhaka, M.S., Srivastava, S. and Bhattacharya, S.M. 2016. Role and Significance of Various ATPases of Nematode Parasites. In *Regulation of Ca<sup>2+</sup>-ATPases, V-ATPases and F-ATPases* (pp. 567-576): Springer.
- Galber, C., Acosta, M.J., Minervini, G. and Giorgio, V. 2020. The role of mitochondrial ATP synthase in cancer. *Bio. Chem.*, 401(11), 1199-1214.
- Galen, R.S. 1980. Predictive value and efficiency of laboratory testing. *Pediatric Clinics of North America*, 27(4), 861-869.
- González-Miguel, J., Morchón, R., Mellado, I., Carretón, E., Montoya-Alonso, J.A. and Simón, F. 2012. Excretory/secretory antigens from *Dirofilaria immitis* adult worms interact with the host fibrinolytic system involving the vascular endothelium. *Mol. Biochem. Parasitol.*, 181(2), 134-140.
- Gourbal, B.E., Guillou, F., Mitta, G., Sibille, P., Thèron, A., Pointier, J.P. and Coustau, C. 2008. Excretory–secretory products of larval *Fasciola hepatica* investigated using a two-dimensional proteomic approach. *Mol. Biochem. Parasitol.*, 161(1), 63-66.
- Higón, M., Monteagudo, C., Fried, B., Esteban, J., Toledo, R. and Marcilla, A. 2008. Molecular cloning and characterization of *Echinostoma caproni* heat shock protein-70 and differential expression in the parasite derived from low-and high-compatible hosts. *Parasitol.*, 135(12), 1469.

- Itagaki, T., Sakamoto, T. and Itagaki, H. 1995. Analysis of *Fasciola* spp. antigen by enzyme-linked immunotransfer blot using sera from experimentally and naturally infected cattle. *J. Vet. Med. Sci.*, 57(3), 511-513. doi:10.1292/jvms.57.511
- Jitsamai, W., Khrutkham, N., Hunprasit, V., Chandrashekar, R., Bowman, D. and Sukhumavasi, W. 2021. Prevalence of endoparasitic and viral infections in client-owned cats in metropolitan Bangkok, Thailand, and the risk factors associated with feline hookworm infections. *Vet. Parasitol., Regional Studies and Reports*, 100584.
- Kanamura, H.Y., Hancock, K., Rodrigues, V. and Damian, R.T. 2002. *Schistosoma mansoni* heat shock protein 70 elicits an early humoral immune response in *S. mansoni* infected baboons. *Memorias do Instituto Oswaldo Cruz*, 97(5), 711-716.
- Khoontawad, J., Laothong, U., Roytrakul, S., Pinlaor, P., Mulvenna, J., Wongkham, C. and Sithithaworn, P. 2012. Proteomic identification of plasma protein tyrosine phosphatase alpha and fibronectin associated with liver fluke, *Opisthorchis viverrini*, infection. *PloS one*, 7(9), e45460.
- Kita, K., Miyadera, H., Saruta, F., & Miyoshi, H. 2001. Parasite mitochondria as a target for chemotherapy. *J. Heal. Sci.*, 47(3), 219-239.
- Knaus, M., Rapti, D., Shukullari, E., Kusi, I., Postoli, R., Xhaxhiu, D. and Winter, R. 2014. Characterisation of ecto-and endoparasites in domestic cats from Tirana, Albania. *Parasitol. Res.*, 113(9), 3361-3371.
- Laemmli, U.K. 1970. Cleavage of structural proteins during the assembly of the head of bacteriophage T4. *Nature*, 227(5259), 680-685. doi:10.1038/227680a0
- Lathroum, C.N., Shell, L., Neuville, K. and Ketzis, J.K. 2018. Efficacy of Praziquantel in the Treatment of *Platynosomum fastosum* in Cats with Natural Infections. *Vet. Sci.*, 5(2), 35.
- Lee, J.S., Lee, J., Kim, S.H. and Yong, T.S. 2007. Molecular cloning and characterization of a major egg antigen in *Paragonimus westermani* and its use in ELISA for the immunodiagnosis of paragonimiasis. *Parasitol. Res.*, 100(4), 677-681. doi:10.1007/s00436-006-0324-7

- Li, C., Song, L., Zhao, J., Zhu, L., Zou, H., Zhang, H. and Cai, Z. 2007. Preliminary study on a potential antibacterial peptide derived from histone H2A in hemocytes of scallop *Chlamys farreri*. *Fish & shellfish Immunol.*, 22(6), 663-672.
- Makarova, E., Goes, T., Leite, M. and Goes, A. 2005. Detection of IgG binding to *Schistosoma mansoni* recombinant protein RP26 is a sensitive and specific method for acute schistosomiasis diagnosis. *Parasitol. Intern.*, 54(1), 69-74.
- Mayer, M. and Bukau, B. 2005. Hsp70 chaperones: cellular functions and molecular mechanism. *Cell. Mol. Life Sci.*, 62(6), 670-684.
- Meshgi, B. and Khodaveisi, M. 2014. Determination of immunodominant antigens of *Dicrocoelium dendriticum* by hyperimmune sera. *Immunol. Infect. Dis.*, 2(1), 4-8.
- Molden, R.C., Bhanu, N.V., LeRoy, G., Arnaudo, A.M. and Garcia, B.A. 2015. Multifaceted quantitative proteomics analysis of histone H2B isoforms and their modifications. *Epigenetics & chromatin*, 8(1), 1-17.
- Moxon, C.A., Alhamdi, Y., Storm, J., Toh, J.M., McGuinness, D., Ko, J.Y. and Seydel, K.B. 2020. Parasite histones are toxic to brain endothelium and link blood barrier breakdown and thrombosis in cerebral malaria. *Blood Adv.*, 4(13), 2851-2864.
- Mulvenna, J., Sripa, B., Brindley, P.J., Gorman, J., Jones, M.K., Colgrave, M.L., Suttiaprapa, S. 2010. The secreted and surface proteomes of the adult stage of the carcinogenic human liver fluke *Opisthorchis viverrini*. *Proteomics.*, 10(5), 1063-1078.
- Nagano, I., Pei, F., Wu, Z., Wu, J., Cui, H., Boonmars, T. and Takahashi, Y. 2004. Molecular expression of a cysteine proteinase of *Clonorchis sinensis* and its application to an enzyme-linked immunosorbent assay for immunodiagnosis of clonorchiasis. *Clin. Dia. lab. Immunol.*, 11(2), 411.
- Nawaz, M., Malik, I., Hameed, M., Kuthu, Z.H. and Zhou, J. 2020. Modifications of histones in parasites as drug targets. *Vet. Parasitol.*, 278: 109029.
- Ndao, M., Spithill, T.W., Caffrey, R., Li, H., Podust, V.N., Perichon, R. and Powell, M.R. 2010. Identification of novel diagnostic serum biomarkers for Chagas' disease in asymptomatic subjects by mass spectrometric profiling. *J. Clin. Microbiol.*, 48(4), 1139.

- Ngoc, D.P., Arimatsu, Y., Kaewkes, S. and Sripa, B. 2015. Characterization of immunogenic *Clonorchis sinensis* protein fractions by gel filtration chromatography. *Asian Pacific J. Trop. Dis.*, 5(4), 284-288.
- Nguyen, H.M., Van Hoang, H. and Ho, L.T. 2017. *Platynosomum fastosum* (Trematoda: Dicrocoeliidae) from cats in Vietnam: morphological redescription and molecular phylogenetics. *The Korean J. Parasitol.*, 55(1), 39.
- Nuamtanong, S., Reamtong, O., Phuphisut, O., Chotsiri, P., Malaithong, P., Dekumyoy, P. and Adisakwattana, P. 2019. Transcriptome and excretory–secretory proteome of infective-stage larvae of the nematode *Gnathostoma spinigerum* reveal potential immunodiagnostic targets for development. *Parasite.*, 26.
- Peterson, C.L. and Laniel, M.A. 2004. Histones and histone modifications. *Current Biol.*, 14(14), R546-R551.
- Pinto, H.A., Mati, V.L. and de Melo, A.L. 2014. New insights into the life cycle of *Platynosomum* (Trematoda: Dicrocoeliidae). *Parasitol. Res.*, 113(7), 2701-2707. doi:10.1007/s00436-014-3926-5
- Pinto, H.A., Pulido-Murillo, E.A., Braga, R.R., Mati, V.L., Melo, A.L. and Tkach, V.V. 2018. DNA sequences confirm low specificity to definitive host and wide distribution of the cat pathogen *Platynosomum illiciens* (= *P. fastosum*)(Trematoda: Dicrocoeliidae). *Parasitol. Res.*, 117(6), 1975-1978.
- Polla, B.S. 1991. Heat shock proteins in host-parasite interactions. *Immunol. today*, 12(3), A38-A41.
- Ramos, R.A., Lima, V.F., Monteiro, M., Andrade - Santana, M., Lepold, R., Da Gloria Faustino, M. and Cringoli, G. 2015. New insights into diagnosis of *Platynosomum fastosum* (Trematoda: Dicrocoeliidae) in cats. *Parasitol. Res.*, 115. doi:10.1007/s00436-015-4763-x
- Reamtong, O. 2008. Mass spectrometry-based parasitic proteomics.
- Revilla-Nuín, B., Manga-González, M.Y., Miñambres, B. and González-Lanza, C. 2005. Partial characterization and isolation of 130 kDa antigenic protein of *Dicrocoelium dendriticum* adults. *Vet. Parasitol.*, 134(3-4), 229-240.
- Rojekittikhun, W., Prummongkol, S., Puangsa-art, S., Chaisiri, K. and Kusolsuk, T. 2013. Prevalence of Gastrointestinal Parasitic Infections in Refuge Dogs and Cats and

- Evaluation of Two Conventional Examination Techniques. *J. Trop. Med. Parasitol.*, 36, 58-67.
- Rojekittikhun, W., Mahittikorn, A., Prummongkol, S., Puangsa-art, S., Chaisiri, K. and Kusolsuk, T. 2015. Evaluation of Sugar Flotation and Formalin-Ether Concentration Techniques in the Examination of GI Parasites of Refuge Dogs and Cats in Kanchanaburi Province, Thailand. *The Journal.*, 38(1), 18.
- Shell, L., Ketzis, J., Hall, R., Rawlins, G. and du Plessis, W. 2015. Praziquantel treatment for *Platynosomum* species infection of a domestic cat on St Kitts, West Indies. *J. Feline. Med. Surg.*, 1(1), 2055116915589834.
- Smith, R.E., Spithill, T.W., Pike, R.N., Meeusen, E.N. and Piedrafita, D. 2008. *Fasciola hepatica* and *Fasciola gigantica*: Cloning and characterization of 70 kDa heat-shock proteins reveals variation in HSP70 gene expression between parasite species recovered from sheep. *Exp. Parasitol.*, 118(4), 536-542.
- Sotillo, J., Valero, L., Sanchez Del Pino, M., Fried, B., Esteban, J., Marcilla, A. and Toledo, R. 2008. Identification of antigenic proteins from *Echinostoma caproni* (Trematoda) recognized by mouse immunoglobulins M, A and G using an immunoproteomic approach. *Parasite Immunol.*, 30(5), 271-279.
- Sripa, J., Brindley, P.J., Sripa, B., Loukas, A., Kaewkes, S. and Laha, T. 2012. Evaluation of liver fluke recombinant cathepsin B-1 protease as a serodiagnostic antigen for human opisthorchiasis. *Parasitol. Int.*, 61(1), 191-195. doi:10.1016/j.parint.2011.05.009
- Sturm, A., Mollard, V., Cozijnsen, A., Goodman, C.D. and McFadden, G.I. 2015. Mitochondrial ATP synthase is dispensable in blood-stage *Plasmodium berghei* rodent malaria but essential in the mosquito phase. *Proceedings of the National Academy of Sciences*, 112(33), 10216-10223.
- Sulahian, A., Garin, Y.J.F., Izri, A., Verret, C., Delaunay, P., van Gool, T. and Derouin, F. 2005. Development and evaluation of a Western blot kit for diagnosis of schistosomiasis. *Clin. Dia. Lab. Immunol.*, 12(4), 548.
- Tascon, R.E., Colston, M.J., Ragno, S., Stavropoulos, E., Gregory, D. and LowRIE, D.B. 1996. Vaccination against tuberculosis by DNA injection. *Nature Med.*, 2(8), 888-892.



- Taylor, D. and Perri, S. 1977. Experimental infection of cats with the liver fluke *Platynosomum concinnum*. *Am. J. Vet. Res.*, 38(1), 51-54.
- Thézénas, M.L., Huang, H., Njie, M., Ramaprasad, A., Nwakanma, D.C., Fischer, R. and Kessler, B.M. 2013. PfHPRT: a new biomarker candidate of acute *Plasmodium falciparum* infection. *J. Proteome Res.*, 12(3), 1211-1222.
- Thiangtrongjit, T., Adisakwattana, P., Limpanont, Y., Dekumyoy, P., Nuamtanong, S., Chusongsang, P. and Reamtong, O. 2018. Proteomic and immunomic analysis of *Schistosoma mekongi* egg proteins. *Exp. Parasitol.*, 191, 88-96.
- Towbin, H., Staehelin, T. and Gordon, J. 1979. Electrophoretic transfer of proteins from polyacrylamide gels to nitrocellulose sheets: procedure and some applications. *Proc. Natl. Aca. Sci.*, 76(9), 4350-4354. doi:10.1073/pnas.76.9.4350
- Urbaniak, M.D., Mathieson, T., Bantscheff, M., Eberhard, D., Grimaldi, R., Miranda-Saavedra, D. Wyatt P, Ferguson, M.A., Frearson, J. and Drewes, G. 2012. Chemical proteomic analysis reveals the drug ability of the kinome of *Trypanosoma brucei*. *ACS Chem. Biol.*, 7(11): 1858-1865.
- Victor, B., Kanobana, K., Gabriël, S., Polman, K., Deckers, N., Dorny, P. and Palmblad, M. 2012. Proteomic analysis of *Taenia solium* metacestode excretion–secretion proteins. *Proteomics.*, 12(11), 1860-1869.
- Vilcinskas, A. 2016. The role of epigenetics in host–parasite coevolution: lessons from the model host insects *Galleria mellonella* and *Tribolium castaneum*. *Zool.*, 119(4), 273-280.
- Wang, S., Zhu, X., Yang, Y., Yang, J., Gu, Y., Wei, J. and Cui, S. 2009. Molecular cloning and characterization of heat shock protein 70 from *Trichinella spiralis*. *Acta Tropica.*, 110(1), 46-51.
- Wongkamchai, S., Chiangjong, W., Sinchaikul, S., Chen, S.T., Choochote, W. and Thongboonkerd, V. 2011. Identification of *Brugia malayi* immunogens by an immunoproteomics approach. *J. Proteomics.*, 74(9), 1607-1613.
- Wongratanacheewin, S., Bunnag, D., Vaeusorn, N. and Sirisinha, S. 1988. Characterization of humoral immune response in the serum and bile of patients with opisthorchiasis and its application in immunodiagnosis. *Am. J. Trop. Med. Hyg.*, 38(2), 356-362.

- Xavier, M.A., Tirloni, L., Pinto, A.F., Diedrich, J.K., Yates, J.R., Mulenga, A. and Termignoni, C. 2018. A proteomic insight into vitellogenesis during tick ovary maturation. *Sci. Rep.*, 8(1), 1-14.
- Zhang, F.K., Hu, R.S., Elsheikha, H.M., Sheng, Z.A., Zhang, W.Y., Zheng, W.B. and He, J.J. 2019. Global serum proteomic changes in water buffaloes infected with *Fasciola gigantica*. *Parasite & Vectors.*, 12(1), 1-11.
- Zhou, D., Yuan, Z., Zhao, F., Li, H., Zhou, Y., Lin, R. and Zhu, X. 2011. Modulation of mouse macrophage proteome induced by *Toxoplasma gondii* tachyzoites in vivo. *Parasitol. Res.*, 109(6), 1637-1646.



## Appendix

Table 14. Fecal egg number, bile egg number, blood biochemistry and imaging parameters of *P. fastosum*-infected cats

Cat No.	Fecal egg number (eggs/g)	Bile egg number (eggs/ml)	Blood chemistry					Imaging results			
			ALT	GGT	ALP	BUN	Protein	Liver	Gallbladder	Biliary dilatation	
1.	NF	NF	129	1	85	30.3	6	Enlargement	Normal	Normal	
2.	40	55	114	10	18	25	8	Enlargement	Bile sediment	Dilated	
3.	NF	2750	70	-	35	35.2	7	Enlargement	Bile sediment	Dilated	
4.	33	350	759	10	137	22.3	8.2	Enlargement	Bile sediment	Dilated	
5.	40	178	147	7	26	34.2	7.4	Enlargement	Bile sediment	Dilated	
6.	40	150	48	1	59	19.4	8.1	Normal	Bile sediment	Normal	
7.	40	3300	33	3	38	22.2	10	Normal	Bile sediment	Normal	
8.	NF	NF	46	1	17	35.6	7.1	Enlargement	Normal	Normal	
9.	14	1025	23	2.5	24	20.6	7	Normal	Bile sediment	Dilated	
10.	NF	625	57	4.8	22	19.5	6.5	Enlargement	Bile sediment	Normal	
11.	NF	NF	100	1.3	67	35.3	7.4	Enlargement	Bile sediment	Normal	
12.	201	7800	80	0.9	45	24.7	9	Enlargement	Bile sediment	Dilated	
13.	NF	280	109	6	30	23.3	8.3	Normal	Bile sediment	Dilated	
14.	137	1050	117	2.2	26	29.1	8	Normal	Bile sediment	Normal	

## VITA

NAME Babi Kyi Soe  
DATE OF BIRTH 30 July 1986  
PLACE OF BIRTH Yenangyaung  
INSTITUTIONS ATTENDED University of Veterinary Science  
HOME ADDRESS Yangon



จุฬาลงกรณ์มหาวิทยาลัย  
CHULALONGKORN UNIVERSITY